Studies on molecular biological interactions between bovine viral diarrhea virus and innate immune system

（牛ウイルス性下痢ウイルスと先天性免疫機構との分子生物学的相互作用に関する研究）

山根　大典

March 2009

CONTENTS

PAGE

PREFACE: Aims and scope of the thesis 6

GENERAL INTRODUCTION: Host-virus interactions of BVDV 9

Introduction 10

Genetic structure of BVDV 11

Viral interaction with innate immune responses 12

Viral mechanisms to regulate cellular signaling 13

Conclusive remarks 15

Figure legends 16

Figures 17

CHAPTER 1: Enhancement of apoptosis via an extrinsic factor, TNFα, in cells infected with cytopathogenic bovine viral diarrhea virus 19

Abstract 20

Introduction 21

Materials and methods 23

Results 27

Discussion 31

Figure legends 35

Figures 38

CHAPTER 2: The double-stranded RNA-induced apoptosis pathway is involved in the cytopathogenicity of bovine viral diarrhea virus 44

Abstract 45

Introduction 46

Materials and methods 48

Results 52

Discussion 57

Figure legends 61

Figures 65

CHAPTER 3: The relationship between the viral RNA level and up-regulation of innate immunity in spleen of cattle persistently infected with bovine viral diarrhea virus 70

Abstract 71

Introduction 72

Materials and methods 73

Results 76

Discussion 79

Figure legends 82

Figures 84

CHAPTER 4: Oxidative stress induced by bovine viral diarrhea virus infection mediates activation of extracellular signal-regulated kinase in MDBK cells 91

Abstract 92

Introduction 93

Materials and methods 94

Results and discussion 96

Figure legends 101

Figures 103

CHAPTER 5: Microarray analysis reveals distinct signaling pathways transcriptionally activated by infection with bovine viral diarrhea virus in different cell types 106

Abstract 107

Introduction 108

Materials and methods 109

Results and Discussion 112

Conclusions 124

Figure legends 126

Figures 128

CHAPTER 6: Inhibition of sphingosine kinase by bovine viral diarrhea virus NS3 is crucial for efficient viral replication and cytopathogenesis 141

Abstract 142

Introduction 143

Materials and methods 145

Results 154

Discussion 163

Figure legends 167

Figures 173

GENERAL CONCLUSION 181

ACKNOWLEDGEMENTS 186

REFERENCES 188

LIST OF PUBLICATION 214

SUMMARY IN JAPANESE 216

PREFACE

Aims and scope of the thesis

Bovine viral diarrhea virus (BVDV) causes an array of clinical syndromes including growth retardation, respiratory and enteric diseases, and lethal mucosal disease (MD) with worldwide distribution. BVDV is also an important pathogen as a surrogate model for hepatitis C virus (HCV), since BVDV and HCV share virological and molecular properties and generally cause chronic long-term infections in their respective hosts.

BVDV is divided into cytopathogenic (cp) and noncytopathogenic (ncp) strains, based on their effects on cell culture. Infection with cp strain induces innate immune responses such as apoptosis and IFN responses, whereas ncp strain does not. Since the high prevalence of BVDV in cattle populations can be attributed to the ability of ncp BVDV to establish persistent infection, evasion of innate immune responses by ncp BVDV seems to be crucial for the viral persistence. In contrast, cp BVDV is isolated almost exclusively from cattle diagnosed with MD and does not establish persistent infection in fetuses. The strong induction of innate immune responses by cp BVDV is thus likely to be correlated to its inability to establish persistent infection in the fetus as well as the pathogenic effects of MD.

However, cellular responses to cp BVDV infection *in vitro* as well as *in vivo* have not been fully studied in detail. Unraveling the BVDV interaction with host will be a clue to better understand the mechanisms involved in an establishment of persistent infection as well as the viral pathogenesis.

In the thesis, the author described molecular biological interactions of BVDV on cellular signaling pathways, primarily focusing on innate immune responses. In the GENERAL INTRODUCTION, known functions of the BVDV proteins and the BVDV interactions with innate immunity were overviewed for the background of the thesis.

In CHAPTER 1, the author described novel apoptosis pathway mediated by extrinsic

factor, TNFα, in cp BVDV-infected cells.

The author further described the involvement of viral double-stranded RNA, resulting from efficient viral RNA replication, in the induction of BVDV-induced apoptosis and the IFN and proinflammatory responses *in vitro* (CHAPTER 2) and *in vivo* (CHAPTER 3).

In CHAPTER 4, the author described and discussed the role of the activation of a cellular protein kinase, extracellular signal-regulated kinase, following cp BVDV infection.

In CHAPTER 5, the author performed microarray analysis and analyzed the comprehensive profiles of gene transcription following BVDV infection in different cell types and discussed the possible implications of the obtained array data.

In CHAPTER 6, the author described a novel protein-protein interaction between BVDV and host that are involved in efficient BVDV replication and apoptosis induction.

In GENERAL CONCLUSION, the author discussed the data in the thesis collectively.

GENERAL INTRODUCTION

Host-virus interactions of BVDV

Introduction

BVDV is classified in the genus *Pestivirus* within the family *Flaviviridae* that includes two additional genera, the classical flaviviruses like *yellow fever virus*, *dengue virus*, *West Nile virus* etc., and the *hepacivirus* of which *hepatitis C virus* (HCV) is the sole member. Pestiviruses consisting of BVDV-1, BVDV-2, *classical swine fever virus*, and *border disease virus* are economically important pathogens of domestic livestock that also infect wild ruminants (Moennig & Plagemann, 1992; Thiel *et al.*, 1996). The members of this family are enveloped positive-stranded RNA viruses that share similarities in genome organization, protein processing, and RNA replication. Given its close resemblance to HCV in terms of translation strategy and processing scheme, BVDV is being studied, not only to unravel details of RNA replication that are of intrinsic interest but also to inform future studies of HCV. In addition, since both HCV and BVDV generally cause chronic long-term infections in their respective hosts, BVDV infection is regarded as surrogate model of persistent infection with HCV (Buckwold *et al.*, 2003).

BVDV isolates are divided into two biotypes that are distinguished by their effect on cultured cells; noncytopathogenic (ncp) isolates infect permissive host cells without causing cell death, whereas cytopathogenic (cp) isolates cause cytopathic effects (CPE) and kill cells via apoptosis (Hoff & Donis, 1997; Zhang *et al.*, 1996). BVDV causes a wide variety of clinical symptoms that range from asymptomatic infections to a fatal disease called mucosal disease (MD), and remarkable clinical correlations exist between these biotypes. In pregnant animals, ncp BVDV can be efficiently transmitted across the placenta, where it can infect the fetus and cause fetal death or congenital abnormalities. In addition, infection during the first 4 months of pregnancy results in the birth of persistently infected BVDV-immunotolerant

animals that are a major reservoir for the virus. Such animals sporadically develop mucosal disease and a virus pair of both ncp and cp biotypes can be isolated from these animals (Moennig & Plagemann, 1992; Thiel *et al.*, 1996). In contrast to ncp BVDV, experimental infection of a fetus with cp BVDV does not establish persistent BVDV infection (Brownlie *et al.*, 1989). Mucosal disease is therefore considered to be triggered by the superinfection with cp BVDV in immunotolerant animals (Brownlie *et al.*, 1984).

Genetic structure of BVDV

The genome of BVDV is about 12.5 kb in length and consists of a single long open reading frame flanked by 5' and 3' nontranslated regions (Collett *et al.*, 1988b). Translation is cap independent and mediated by a type III internal ribosome entry site (Chon *et al.*, 1998; Pestova & Hellen, 1999; Yu *et al.*, 2000). The resulting polyprotein is processed co- and posttranslationally by host- and virus-encoded proteases to give rise to at least 12 individual proteins (Collett *et al.*, 1988a; Collett *et al.*, 1991; Elbers *et al.*, 1996) (Fig. 1). N^{pro} is a nonstructural autoprotease that cleaves at its C terminus to liberate the capsid (C) protein (Wiskerchen *et al.*, 1991). C protein is followed by three virion glycoproteins E^{rns}, E1, and E2, with E^{rns} encoding an RNase of unknown function that is also secreted in nonvirion forms (Rumenapf *et al.*, 1993; Schneider *et al.*, 1993). NS3 through NS5B, but not the structural proteins p7 and NS2, are required for pestivirus RNA replication (Behrens *et al.*, 1998; Tautz *et al.*, 1999). The N terminal one-third of NS3 encodes a serine protease that functions in concert with NS4A to mediate processing at all downstream cleavage sites (Tautz *et al.*, 1997; Xu *et al.*, 1997). The C-terminal NS3 domain encodes an RNA helicase that is required for viral RNA replication (Grassmann *et al.*, 1999; Gu *et al.*, 2000; Warrener & Collett, 1995).

NS5B, the viral RNA-dependent RNA polymerase, has been expressed, purified, and extensively compared to the corresponding enzyme of HCV (Baginski *et al.*, 2000; Lai *et al.*, 1999; Zhong *et al.*, 1998). NS5A is a serine phosphoprotein that is tightly associated with one or more cellular kinases (Reed *et al.*, 1998) and reported to directly interact with a subunit of eukaryotic translation elongation factor-1 (Johnson *et al.*, 2001). Although NS4B and NS5A, together with NS3/4A and NS5B are each essential component of viral RNA replication complex, specific functions of p7, NS2, NS4B and NS5A remain unknown.

The productive expression of a discrete NS3 protein is the molecular feature that distinguishes cp from ncp biotypes (Meyers & Thiel, 1996). Both uncleaved NS2-NS3 (NS2-3) and NS3 are present in cp BVDV-infected cells, whereas only uncleaved NS2-3 is found in ncp BVDV-infected cells at later time points (9 h ~) after infection (Lackner *et al.*, 2004). By sequence analysis of multiple pairs of ncp/cp isolates, it has become apparent that deletions, genome duplications and rearrangements, insertions of cellular sequences, and even point mutations in NS2 (Kummerer & Meyers, 2000; Kummerer *et al.*, 1998) correlate with NS3 production and cytopathogenesis (Lackner *et al.*, 2005; Lackner *et al.*, 2004). The fact that distinct molecular events in independent cp BVDV isolates all lead to NS3 production implicates a central role for this protein in cytopathogenesis, yet how the expression of NS3 lead to the viral cytopathogenicity remains unclear.

Viral interactions with innate immune responses

Apart from the induction of cell death in virus-infected cells, there is an additional difference between ncp and cp BVDV, in their interactions with the innate immune response: cp BVDV has been shown to induce interferon (IFN) in macrophages and various cell

cultures, whereas ncp BVDV lacks this ability (Adler *et al.*, 1997; Baigent *et al.*, 2004; Baigent *et al.*, 2002; Schweizer & Peterhans, 2001). Infection with ncp BVDV to cultured cells has been shown to enhance the replication of other viruses. In the case of Newcastle disease virus (NDV), a paramyxovirus which induces IFN and is sensitive to IFN, the enhancement has been associated with a reduction in the titer of IFN induced in BVDV-coinfected cultures (Diderholm & Dinter, 1966). This enhancement is referred to as the END (enhancement/exaltation of NDV) effect (Inaba *et al.*, 1968) and has also been observed for an orbivirus (Nakamura *et al.*, 1995). Furthermore, the activity of poly(IC), a synthetic double-stranded RNA (dsRNA), against vesicular stomatitis virus can be inhibited in BVDV-infected cells (Rossi & Kiesel, 1983), and it has recently been shown that BVDV blocks the IFN induction by dsRNA in bovine monocyte-derived macrophages (Schweizer & Peterhans, 2001).

While *in vivo*, infection with cp BVDV to a bovine fetus induces a significant IFN response that is not observed following infection with ncp BVDV (Charleston *et al.*, 2001). Inability of cp BVDV to establish persistent infection is therefore considered to be due to induction of IFN response. As IFN signaling is also a crucial mediator of apoptosis in virally infected cells (Tanaka *et al.*, 1998), strong IFN responses following cp BVDV-infection appear to be a crucial step in the induction of apoptosis.

Viral mechanisms to regulate IFN signaling

Several lines of evidence have indicated that ncp BVDV interferes with antiviral signaling, but the underlying molecular basis for the suppression of IFN signaling remains unknown. As dsRNA is a key element for cells that sensors viral infection, many viruses have

evolved strategy to “mask” dsRNA recognition by hosts (Saunders & Barber, 2003). In most cases, viral proteins prevent cellular factors from binding to dsRNA as well as the downstream effectors of the antiviral protein. There are many viral dsRNA-binding proteins (DRBPs) encoded by many viruses, but functions of the majority are still largely unknown (Saunders & Barber, 2003). Fig. 2 depicted the dsRNA-activated IFN regulatory pathways. Intracellular RNA helicases, RIG-I and MDA-5, are activated upon binding to dsRNA and then mediates the signal to a downstream factor, interferon β-promoter stimulator 1 (IPS-1) (Kawai *et al.*, 2005). IPS-1 activates two IκB kinase (IKK)-related kinases, IKKε and TANK-binding kinase-1 (TBK-1), which phosphorylate interferon regulatory factor 3 (IRF-3). Phosphorylated IRF-3 forms homodimer and translocate to nucleus to activate IFN-β promoter. BVDV is known to interfere with IFN signaling induced by dsRNA. Prior studies have shown that apoptosis and IFN synthesis induced by polyIC, a synthetic dsRNA, is efficiently inhibited by the dsRNase activity encoded by envelope glycoprotein E^{rns} (Iqbal *et al.*, 2004). Since E^{rns} is secreted into medium, but not existed in the cytoplasm, E^{rns} is considered to antagonize extracellular, but not intracellular dsRNA-mediated signaling (Magkouras *et al.*, 2008). As dsRNA itself is known to trigger apoptosis signaling, efficient degradation of dsRNA by E^{rns} seems important for prevention of apoptosis (Schweizer & Peterhans, 2001). Alternatively, intracellular dsRNA signaling is suppressed by the viral N-terminal protease fragment, N^{pro}, which is known to target IRF-3 to proteasome-dependent degradation independently of its autoprotease activity (Hilton *et al.*, 2006). But it was not sufficient to explain the suppression of IFN signaling by ncp BVDV since cp BVDV also encodes same N^{pro}, but still induces strong IFN induction. Indeed, cp BVDV similarly suppresses IRF-3 signaling in N^{pro} -dependent manner (Chen *et al.*, 2007). As cp BVDV does

not prevent NFκB signaling, strong IFN responses may be triggered via NFκB-mediated pathway (Hilton *et al.*, 2006), although further detailed studies are required.

Conclusive remarks

As described above, only a limited aspect of virus-host interaction of BVDV has been revealed to date. To probe virus-host interactions that lead to efficient viral replication as well as pathogenesis, the author focuses on the analyses of cellular signaling pathways and the direct interaction between cellular and viral proteins. Although cellular stress responses triggered by cp BVDV infection such as mitochondrial, oxidative stress- as well as ER stress-mediated and dsRNA-activated signaling pathways (Bendfeldt *et al.*, 2003; Grummer *et al.*, 2002b; Jordan *et al.*, 2002; Schweizer & Peterhans, 1999; Vassilev & Donis, 2000) have been reported previously, the viral factors triggering innate immune responses remain unclear. As the transmission to a fetus is correlated with the biotype (ncp versus cp) rather than the virulence, the apparently distinguishable behavior observed in cell cultures possibly reflects the mechanisms of successful transplacental transmission or establishment of persistent infection *in vivo*. Unraveling the difference in intracellular behavior between two biotypes *in vitro* may lead to an understanding of how MD is developed by cp BVDV, as well as why only ncp BVDV is transmitted to a fetus and establishes immunotolerance.

Figure legends

Figure 1. Genomic organization of BVDV. A schematic representation of the BVDV genome with the 5'- and 3'-nontranslated regions (NTRs) is shown in the top, the translation products in the middle and the processed proteins with their known functions below.

Figure 2. Type I IFN gene expression. dsRNA, a characteristic by-product of viral replication, leads to activation of the transcription factor IRF-3. IRF-3 is phosphorylated by the kinases IKKε and TBK-1 which in turn are activated by the intracellular RNA-sensor proteins RIG-I and MDA-5. IPS-1 serves as an adaptor protein connecting dsRNA sensing and IRF-3 phosphorylation. A second dsRNA signaling pathway involves extracellular/endosomal TLR-3 and the adaptor protein TRIF. As indicated, BVDV E^{rns} protein degrades extracellular dsRNA depending on its dsRNase activity, while N^{pro} protein targets IRF-3 to proteasome-dependent degradation.

GENERAL INTRODUCTION Fig.1

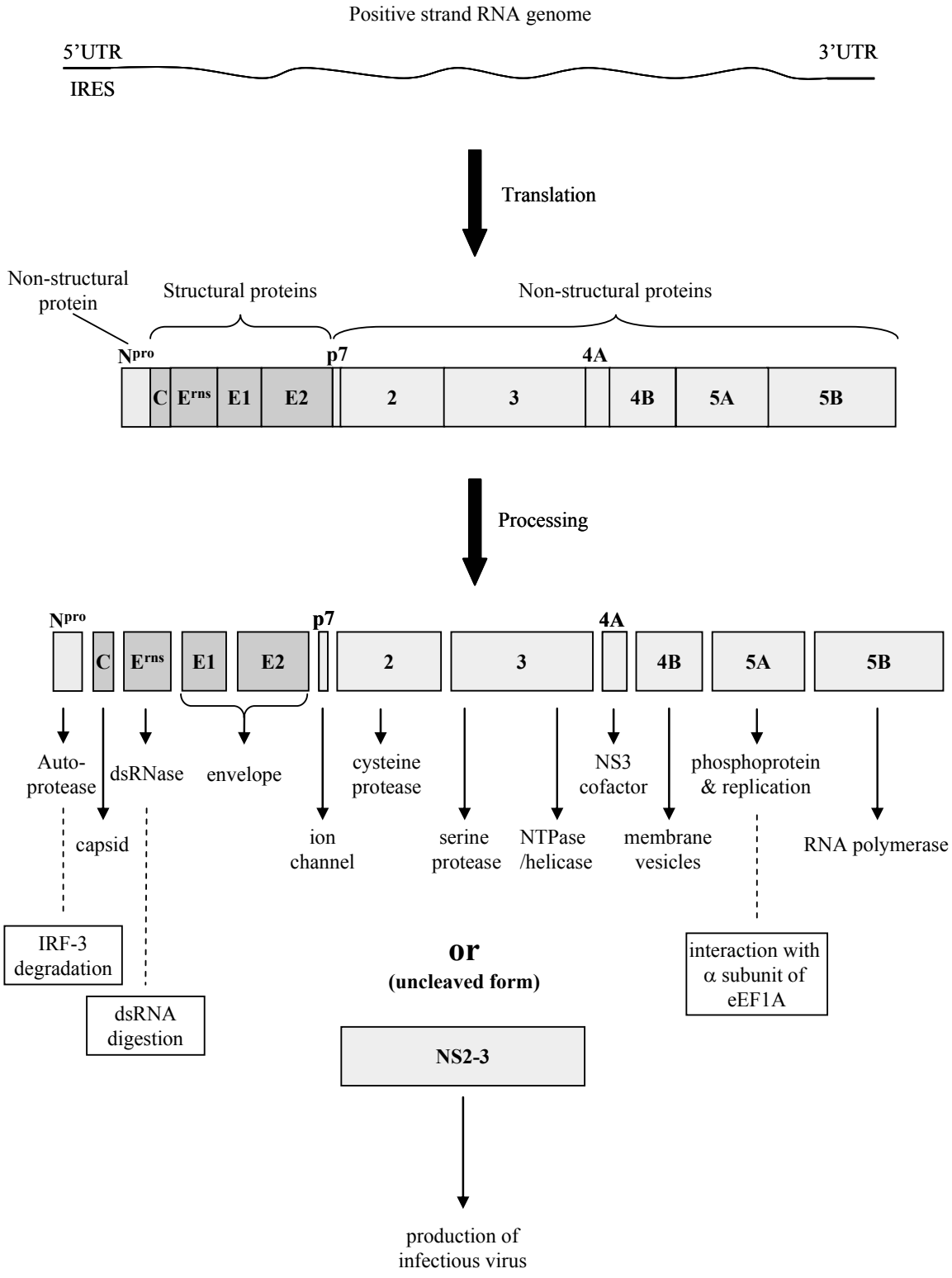

GENERAL INTRODUCTION Fig.2

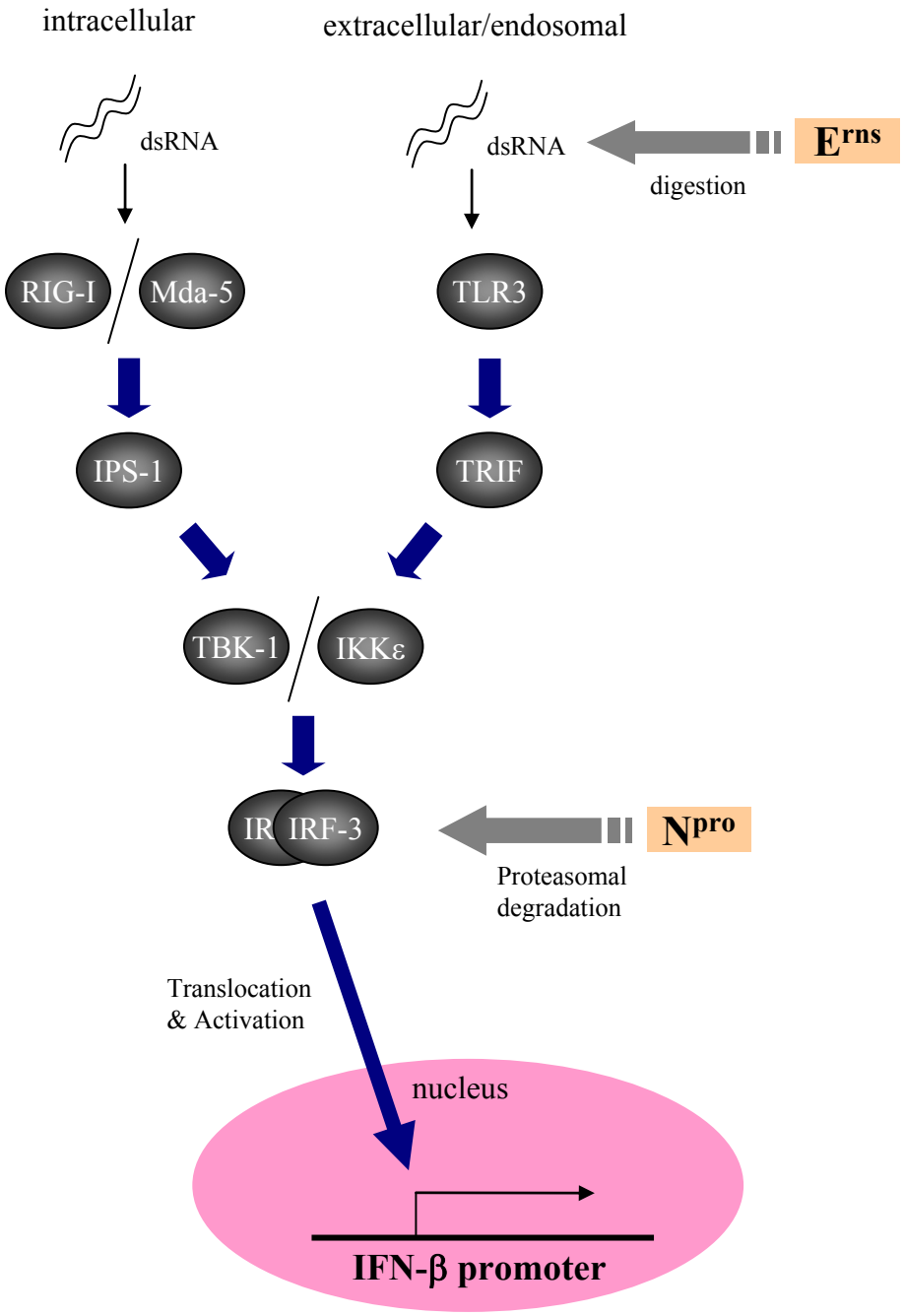

CHAPTER 1

Enhancement of apoptosis via an extrinsic factor, TNFα, in cells infected with cytopathogenic bovine viral diarrhea virus

Microbes and Infection (2005) 7:1482-91

Abstract

In search of cellular factors that mediate apoptosis in cytopathogenic (cp) BVDV-infected cells, up-regulation of tumor necrosis factor alpha (TNFα) and inducible nitric oxide synthase (iNOS) mRNAs was detected specifically in cp BVDV-infected primary bovine fetal muscle (BFM) cells. Suppression of TNFα via antisense oligonucleotide transfection or incubation with a polyclonal antibody against TNFα resulted in attenuation of apoptosis induced by cp BVDV, suggesting that TNFα participates in apoptosis induction. Although iNOS expression is known to be stimulated by TNFα, cp BVDV-induced iNOS expression was not regulated by TNFα. Furthermore, iNOS was revealed to serve as anti-apoptotic factor. Importantly, the expression level of both TNFα and iNOS mRNAs in the noncytopathogenic (ncp) BVDV-infected cells was kept lower than that in the mock-infected cells, suggesting that ncp BVDV reduced or interfered with the factor triggering the expression of both mRNAs. These characteristic mRNA transcriptions would help to explain why BVDV acts differently in cells as well as *in vivo* depending on its biotype.

Introduction

The cp BVDV-infected cells have been shown to induce apoptosis via an intrinsic pathway and oxidative stress-related mechanisms (Grummer *et al.*, 2002b; Jordan *et al.*, 2002; Schweizer & Peterhans, 1999). The intrinsic pathway is regulated by the release of cytochrome c from mitochondria and the subsequent ATP-dependent activation of the death regulator apoptotic protease-activating factor 1 (apaf-1) (Mignotte & Vayssiere, 1998).

One of the extrinsic factors of apoptosis, tumor necrosis factor alpha (TNFα) is a proinflammatory cytokine known to exert various effects on different cell types. TNFα is known to enhance CPE of cp BVDV when exogenously added (Bielefeldt Ohmann & Babiuk, 1988), however, no report has indicated that BVDV-infected cells produce TNFα or other extrinsic factors of apoptosis. Ligand binding to TNF receptor-1 (TNFR-1) is generally thought to activate two main signaling pathways, one leading to cell death through apoptosis (Yeh *et al.*, 1999), which is initiated by recruitment of the proximal regulator caspase-8 (Budihardjo *et al.*, 1999), and the other NFκB-mediated pathway leading to apoptosis-related gene transcriptions, such as inducible nitric oxide synthase (iNOS) (Neu *et al.*, 2003).

Activation of iNOS results in generation of a NO-radical from L-arginine. Although iNOS and NO-radicals have been shown to exert a pro-apoptotic function, mostly they have been reported to mediate anti-apoptotic effects (Liu & Stamler, 1999; Monteiro *et al.*, 2004; Zhao *et al.*, 1998). It seems that the effect of NO-radicals is concentration-dependent and may be influenced by the presence of other reactive oxygen species (ROS). The functions of iNOS on apoptotic effects are still uncertain.

In this study, the author found that mRNAs of TNFα and iNOS were induced specifically in cp BVDV-infected cells. By inhibiting each factor of the cells infected with cp

BVDV, the effect of each factor on apoptosis induction was evaluated. Each function was revealed to be an inversion; TNFα functioned as a pro-apoptotic factor, while iNOS was anti-apoptotic. However, the pro-apoptotic effect of TNFα seemed to exceed the anti-apoptotic effect of iNOS. Although what stimulates TNFα induction still need to be elucidated, the author showed that apoptosis of cp BVDV-infected cells was caused via not only an intrinsic, but also an extrinsic pathway.

Materials and methods

Cells and viruses. Primary bovine fetal muscle (BFM) cells were maintained in Dulbecco's modified Eagle's medium (DMEM) supplemented with 10% fetal calf serum (FCS), penicillin and streptomycin at 37 °C in a humidified 5% CO_2 atmosphere. The cells were confirmed to be free of BVDV by reverse transcriptase-polymerase chain reaction (RT-PCR). BVDV strains KS86-1cp, KS86-1ncp, IS5cp, IS4ncp (genotype 1), and KZ91cp, KZ91ncp (genotype 2) were used (Nagai *et al.*, 2004; Nagai *et al.*, 2001).

Virus infection. BFM cells were infected with the appropriate BVDV strain at a multiplicity of infection (MOI) of 1 for 1 h at 37 °C. After adsorption of the virus, the inoculum was removed by washing the cells in DMEM without FCS prior to the addition of medium with 5% FCS.

TUNEL assay. Apoptotic cells were detected with an Apoptosis Screening Kit wako (Wako Osaka, Japan). Cells were seeded onto 96-well plates (Corning NY, USA). After the virus was inoculated at an MOI of 5, cells were incubated for 72 h. Thereafter, the apoptotic index of infected cells was assayed according to the manufacturer's protocol. Apoptotic cells were detected by reading the absorbance wavelength at 490 nm using a microplate reader (model 3550 EIA reader, Bio-Rad, Hercules, CA, USA).

Fractionation of soluble proteins. BFM cells were mock-infected or infected with the KS86-1ncp or KS86-1cp strain and incubated for 72 h at 37 °C. First, 15 ml of supernatants were fractionated to more than 10 kDa with a centrifugal filter device (Centricon, Millipore

Billerica, MA, USA). The filtered fraction was used as an under 10 kDa sample. Thereafter, DMEM was added to concentrated supernatants over 10 kDa up to 15 ml, and diluted samples were applied to a 30 kDa filter device. The filtered fraction was used as a sample of a 10-30 kDa fraction. DMEM was added again to the concentrated fraction up to 15 ml, and the diluted samples were fractionated with a 100 kDa filter device. Then, filtered fractions were used as a sample of 30-100 kDa. Ten microliters of each sample were added to BFM cells in a 96-well plate at a total volume of 50 μl, and incubated for 72 h. Then, apoptotic cells were measured with ELISA-based TUNEL staining as described above.

RT-PCR. Total RNA from either mock treated or virus-infected cells was extracted using Trizol LS Reagent (Invitrogen, CA, USA) according to the manufacturer's protocol. RT-PCR was performed using a SuperScript One-step RT-PCR with Platinum Taq (Invitrogen California, USA) according to the manufacturer's instructions. Complementary DNA (cDNA) synthesis was performed for 30 min at 50 °C, and PCR with each cycle consisting of 45 s at 94 °C, 30 s at 57 °C, and 45 s at 70 °C, followed by 10 min at 72 °C. The primers used to amplify bovine TNFα mRNA (467-bp product) were 5'-AGCACCAAAAGCATGATCCG-3' (sense) and 5'-ATGGTGTGGGTGAGGAACAA-3' (antisense); the primers used for bovine TNFR-1 mRNA (370-bp product) were 5'-AGCTCTGTTGGCAGATGTGT-3' (sense) and 5'-AGTTTCACCCCAGTATTCCC-3' (antisense); the primers used for bovine TNFR-2 mRNA (236-bp product) were 5'-TCGACCAGCAGCACGGACAA-3' (sense) and 5'-GTGCTGGCGTCTGTGTCCCT-3' (antisense); the primers used for glyceraldehyde-3-phosphate dehydrogenase (GAPDH) mRNA (487-bp product) were 5'-GTCACCAGGGCTGCTTTTAA-3' (sense) and 5'-CGTGGACAGTGGTCATAAGT-3'

(antisense); the primers used for bovine Mx1 mRNA (469-bp product) were 5'-CAGCCAATATGAAGAGAAGG-3' (sense) and 5'-CCGACATTGAATATCAGATC-3' (antisense); the primers used for bovine iNOS mRNA (520-bp product) were 5'-ATCTGCAGACACGTGCGTTA-3' (sense) and 5'-TGAGGCCACCTTGTGCGTTT-3' (antisense).

TNFα ELISA. Recombinant bovine TNFα (rboTNFα) was purchased from Endogen. Mouse anti-rboTNFα monoclonal antibody and rabbit anti-rboTNFα polyclonal serum were kindly provided from Dr. Paape (Immunology and Disease Resistance Laboratory, USA). ELISA was performed as previously described (Paape *et al.*, 2002). Horseradish peroxidase activity was detected with a TMB Microwell Peroxidase Substrate System (Kirlegaard & Perry Laboratories, Guildford, UK), following the manufacturer's instructions. After substrate color was developed at ambient temperature for 10 min, absorbance was measured at 450 nm using the microplate reader.

Antisense transfections. At 24 h post inoculation (p.i.) at an MOI of 5, the cells were transfected with the TNFα antisense oligonucleotide 5'-CCAACGGTGTGAAGCTGGAAG-3', or with control oligonucleotide containing the same base composition in a random order, 5'-CGAGAGTCGAGAGTACCTGAG-3', at a final concentration of 100 nM using Trans-IT LT1 (Mirus, WI, USA) in serum-free medium.

Caspase assay. Activity of caspase-3 or caspase-8 was detected by ApoProbe-3 or ApoProbe-8 kit (BioDynamics Laboratory, Tokyo, Japan). Apoptosis-induced or

mock-infected cells were scraped into the medium and centrifuged. After washing the cell pellet with PBS, it was resuspended in lysis buffer and incubated on ice for 10 min. Then, cell lysates were centrifuged in a microcentrifuge at 12,000 rpm for 3 min at 4 °C and the supernatants were used to detect caspase activity. The supernatants were incubated with substrates for 30 min at 37 °C, and the fluorescence liberated from caspase-treated substrates was detected by reading samples in a fluorometer equipped with 360 nm excitation and 460 nm emission filters.

Quantitative real-time PCR. Transcribed mRNAs of iNOS and TNFα were quantified by means of a real-time PCR assay using the SmartCycler (Cepheid, CA, USA). The primer pairs were the same as described above in the RT-PCR section. cDNA synthesis was performed with SuperScript III RNaseH$^-$ Reverse Transcriptase (Invitrogen) as per manufacturer's protocol. In addition, PCR amplification of GAPDH mRNA was performed as an internal control for the quality of extracted cellular RNA. PCR amplifications were performed with SYBR Premix Ex Taq (TaKaRa, Tokyo, Japan) using 1 μl of cDNA as described in the manufacturer's protocol**.** PCR consisted of an initial denaturation step of 5 s at 95 °C, followed by 45 cycles, with 1 cycle consisting of 3 s at 95 °C, 10 s at 55 °C, and 20 s at 72 °C. All the samples were analyzed in triplicate. At the end of each run, a DNA melting step was performed, and the fusion curve was recorded to control for the homogeneity and quality of amplified DNA. The measured amounts of RNA were normalized to the amount of GAPDH mRNA in each sample.

Results

Apoptosis induced by cp BVDV in BFM cells.

Cell death via apoptosis in cp BVDV-infected BFM cells (Fig. 1A) was confirmed by an ELISA-based TUNEL staining method (Fig. 1B). To investigate the apoptotic pathway, activities of caspase-3 and caspase-8 were measured by a substrate-specific colorimetric assay. Caspase-3 is induced through activation of both intrinsic and extrinsic pathway, while caspase-8 activity is the indicator of an activated extrinsic apoptotic pathway, finally activating caspase-3 (Budihardjo *et al.*, 1999). Although the level of caspase-8 activity was relatively low in contrast to that of caspase-3 activity (Fig. 1C), the caspase-8 activity of the cp BVDV-infected cells was relatively higher than that of the ncp BVDV-infected cells (Fig. 1C). In addition, when the UV-irradiated supernatant obtained from the cp BVDV-infected cell culture was added, caspase-8 was activated at a level approximately 2 times higher than the mock-infected case (Fig. 2A), which suggests that slight caspase-8 activation occurs via factors in the supernatant of the cp BVDV-infected cells.

To investigate what activates caspase-8, the death ligand in the cell supernatant was investigated. Both virus- and mock-infected cell supernatants were fractionated by centrifugal filter devices and the soluble proteins were fractionated to <10 kDa, 10-30 kDa, and 30-100 kDa. After BFM cells were incubated with the fractionated supernatant, the apoptotic state was analyzed by ELISA-based TUNEL staining. The level of the apoptotic state was higher after the cp BVDV-infected cell supernatant of the 10-30 kDa fraction was added (Fig. 2B). These results suggested that 10-30 kDa proteins in the supernatant of the cell cultures infected with cp BVDV triggered an extrinsic apoptotic pathway.

Identification of 10-30 kDa apoptosis-inducing factors.

Although there has been no report of death ligand overexpression in cells infected with cp BVDV, there are many potential induced extrinsic factors within interferon (IFN) stimulated genes such as Fas/FasL or TNF-related apoptosis-inducing ligand because cp BVDV infection is known to induce type I IFNs (Baigent *et al.*, 2002; Schweizer & Peterhans, 2001). The author first examined transcription of Mx1 mRNA, which is known to be induced by viral infection or virus-induced IFN-α/β. As expected, Mx1 mRNA was detected only in the cp BVDV-infected cells, indicating that IFNs or antiviral responses were activated in BFM cells only by the cp BVDV infection (Fig. 3A). The author next examined the mRNA expression of potential death ligand proteins using RT-PCR. Fas/FasL was not detected even when PCR was performed at 40 cycles (data not shown), but overexpression of TNFα (17 kDa) was detected when performed at 25 cycles (Fig. 3A). TNFα or Mx1 mRNA expression in the cp BVDV-infected cells was detected independent of the virus strain and the genotype used. Subsequently, expressed TNFα protein was quantitated using ELISA. As shown in Table 1, approximately 1.3-1.8 ng/ml of TNFα was detected in the cp BVDV-infected cells, while less than 0.1 ng/ml was found in the mock or ncp BVDV-infected cells. To investigate whether TNFα is actually involved in the apoptotic effect of cp BVDV-infected cells, caspase-3 activity was measured after TNFα was suppressed through transfection of antisense oligonucleotides into the BFM cells infected with cp BVDV. As shown in Fig. 4A, antisense oligonucleotides against TNFα reduced caspase-3 activity induced by TNFα. In addition, the apoptotic potential of UV-inactivated supernatant of the antisense-treated cells infected with cp BVDV was also reduced by approximately 15%, compared with control antisense-treated cells. These results also suggested that an apoptotic participation of TNFα was approximately

15% of total apoptotic effect induced by cp BVDV. Furthermore, when the cells infected with cp BVDV were incubated with a variety of dilutions of a bovine TNFα-specific polyclonal antibody, inhibition of apoptosis was detected in a dose-dependent manner (Fig. 4B). These results suggest that TNFα participates in cp BVDV-induced apoptosis as an extrinsic factor.

Inhibition of both TNFα and iNOS by ncp BVDV.

The author next examined the levels of TNFα and iNOS mRNA by quantitative real-time PCR to determine the relative amounts in the cells infected with BVDV. As shown in Fig. 3B, in the cp BVDV-infected cells, the transcription level of iNOS was increased approximately 740-fold higher, and that of TNFα was approximately 80-fold higher than those in mock-infected cells, respectively. On the other hand, in the ncp BVDV-infected cells, expression of TNFα mRNA was undetectable even after 50 PCR cycles were performed, and that of iNOS mRNA was 82% lower than the mock-infected cells. Thus, it appears that ncp BVDV might interfere with the factor(s) which induces iNOS or TNFα.

TNFR expressions.

To transduce a signal of an extrinsic factor into an intracellular death signal, the expressions of TNFR superfamily members, such as TNFR-1 and TNFR-2, are required. The TNFα death signal is believed to be mainly mediated by TNFR-1, while TNFR-2 is believed to enhance the cell death signal of TNFR-1 (Chan & Lenardo, 2000; Weiss *et al.*, 1997). As shown in Fig. 3C, only the cp BVDV-infected cells induced both TNFR-1 and TNFR-2. In contrast, the mock-infected cells expressed both receptors at extremely low levels (data not shown), and the ncp BVDV-infected cells showed relatively higher levels of TNFR-1,

suggesting that the ncp BVDV-infected cells could be also susceptible to exogenously added TNFα. These results suggested that cp BVDV infection might also stimulate cellular sensitivity to TNFα-related apoptosis by expressing TNFR-2 in addition to the expression of TNFR-1.

iNOS expression independent of TNFα.

In searches of apoptosis factors using RT-PCR, overexpression of iNOS mRNA was detected (Fig. 3A). Because iNOS is known to be induced by several factors, such as lipopolysaccharide (LPS), IFN-γ, and TNFα, this overexpression of iNOS was first presumed to be regulated by the TNFα overexpression. Unexpectedly, when cells were treated with rboTNFα of the same amount (2 ng/ml) as detected in the supernatant of BFM cells infected with cp BVDV, iNOS overexpression was not detected (Fig. 5A). Furthermore, the cells incubated with the UV-irradiated culture supernatant of the cp BVDV-infected cells did not express iNOS (data not shown). These results suggest that induction of iNOS is not TNFα-dependent, but seems to be triggered by other factors, possibly intracellular events.

To examine the function of iNOS, the mock or cp BVDV-infected BFM cells were treated with an NOS inhibitor, N^G-monomethyl-l-arginine acetate (L-NMMA). Suppression of NOS resulted in up-regulation of caspase-3 (Fig. 5B) and increased the apoptosis in the cp BVDV-infected cells (data not shown), suggesting that iNOS induced by cp BVDV infection plays an anti-apoptotic role in a direction opposite to TNFα. These results show that iNOS-mediated events interfere with the pro-apoptotic effects in cp BVDV-infected cells.

Discussion

In this study, the author showed that only cp strains of BVDV induced an extrinsic factor, TNFα, while ncp BVDV did not. Bielefeldt-Ohmann & Babiuk reported that cp BVDV-like CPE was induced in cells infected with ncp BVDV when the cells were exogenously added both TNFα and IFN-α simultaneously (Bielefeldt Ohmann & Babiuk, 1988). As IFN induction was suggested through detection of Mx1 mRNA overexpression (Goetschy *et al.*, 1989) in cp BVDV-infected cells, TNFα and IFN inductions detected in this study might correlate with CPE induced by cp BVDV. Grummer et al. previously reported that the involvement of an extrinsic pathway of cp BVDV-induced cell death seemed very unlikely, since UV-inactivated supernatants from cp BVDV-infected fetal bovine kidney cells did not induce apoptosis visibly (Grummer *et al.*, 2002b). On the contrary, the author found that the UV-irradiated supernatant from the cp BVDV-infected BFM cells boosted the number of apoptotic nuclei compared to those from the mock- or ncp BVDV-infected cells, although no clear cell death has been observed. These results also conflicted with a previous report that bovine bone marrow-derived macrophages decreased the level of TNFα production upon stimulation with heat-inactivated *Salmonella* Dublin or LPS when infected with ncp or cp BVDV (Brune *et al.*, 1999). Nevertheless, since overexpression of Mx1, TNFα and iNOS mRNA was similarly detected in primary bovine testicle cells, but not in a bovine kidney cell line, MDBK (data not shown), the property of inducing these mRNAs may be restricted to certain cell types such as fibroblast or primary cell cultures.

When the author investigated whether the susceptibility of cells to TNFα is altered by viral infection, the author found that the cp BVDV-infected cells expressed more TNFRs, which initiate the caspase-8 cascade and NFκB-mediated pathway, than the mock-infected

cells. Thus, the author concluded that the cells became more susceptible to the TNFα-mediated cell death signaling via receptor recruitment due to the cp BVDV infection. ncp BVDV infection also facilitated the TNFR-1 mRNA, however, because of an absence of the ligand, the extrinsic effect failed to occur in ncp BVDV-infected cells. Although what stimulates those receptor transcriptions remains unclear, the cp BVDV-infected cells might be enhanced via TNFR-2-mediated signaling pathway since it was detected only in the cp BVDV-infected cells.

In search of apoptosis-related factors, overexpression of iNOS was detected, as well as TNFα, in the cp BVDV-infected cells. The author first considered that detected iNOS was induced by TNFα, contributing to apoptosis by exerting a pro-apoptotic effect (Adler *et al.*, 1996; Neu *et al.*, 2003). On the contrary, iNOS expression of the cp BVDV-infected cells was demonstrated to be independent of TNFα. Furthermore, iNOS was revealed to act as an anti-apoptotic factor since incubation with an NOS inhibitor, L-NMMA, resulted in the potentiation of caspase-3 activity and apoptosis. There are several reports indicating that NO may inhibit the early stage in viral replication (Reiss & Komatsu, 1998; Tay & Welsh, 1997), including Japanese encephalitis virus, which is also classified in the family *Flaviviridae.* Thus, the author determined the amount of cp BVDV genome for each condition, with or without L-NMMA at multiple time points (24 h and 48 h p.i.), using real-time PCR to exclude the possibility that enhancement of caspase-3 by addition of L-NMMA was due to an increase in viral replication. The comparison showed no significant difference in viral genome levels between L-NMMA or mock-treated samples (data not shown), suggesting that iNOS does not largely affect BVDV genome replication. Therefore, one of the reasons for the anti-apoptotic effect of iNOS seemed to be that NO produced by iNOS served as an antioxidant (Monteiro *et*

al., 2004) against cp BVDV-induced oxidative stress, because cp BVDV infection is known to induce oxidative stress, like ROS (Jordan *et al.*, 2002; Schweizer & Peterhans, 1999). However, it is controversial as to why the anti-apoptotic pathway is up-regulated by only the cp strain, but not by the ncp strain. The fact that cp BVDV infection culminates in apoptotic cell death indicates that pro-apoptotic signaling exceeds anti-apoptotic effects by far. Nevertheless, the participation of extrinsic factor in cp BVDV-induced apoptosis seems to be a minor route since the addition of UV-irradiated supernatant did not have capacity to induce cell death clearly and the involvement of a key death ligand, TNFα, was revealed to be only 15% of the total apoptotic activity. Thus, major route for cp BVDV-induced apoptosis is thought to be via intrinsic pathway, which seems to correlate with the intracellular viral RNA accumulation (Vassilev & Donis, 2000), or caused by endoplasmic reticulum stress-mediated pathway as previously reported (Jordan *et al.*, 2002). Consequently, an extrinsic pathway seems to engage in enhancing the cell death induced by cp BVDV.

Although the cp BVDV-specific viral factor(s), which causes iNOS or TNFα induction, remains to be elucidated, it has been reported that transcription of both iNOS and TNFα is induced by polyIC, a synthetic dsRNA (Meusel *et al.*, 2002). Vassilev and Donis have also shown previously that an increased level of intracellular viral RNA accumulation was observed in cp BVDV-infected cells, suggesting that production of dsRNA in these cells was much higher than that in ncp BVDV-infected cells (Vassilev & Donis, 2000). Therefore, transcription of both TNFα and iNOS might be stimulated by dsRNA produced in cp BVDV-infected BFM cells. On the other hand, the inhibition of both iNOS and TNFα transcriptions by ncp BVDV might be occurred via the same mechanism as the interference of ncp BVDV with dsRNA-induced IFN synthesis (Baigent *et al.*, 2002; Schweizer & Peterhans,

2001).

The cp BVDV-specific mRNA expression found in this study seems to be an indicative of different intracellular behavior from that of ncp BVDV, although it is still uncertain whether the difference between cp and ncp BVDV is derived from the existence of dsRNA or type I IFN induction, or another mechanism. In addition, whether the extrinsic apoptotic pathway induced by viral actions in bovine primary cell cultures is identical to that *in vivo*, where lymphoid and epithelial cells undergo apoptosis (Teichmann *et al.*, 2000), is also a significant matter to be solved. Since TNFα has been shown to correlate with the mucosal inflammation in Crohn's diseases (van Deventer, 2001; van Deventer & Tytgat, 1998), which are associated with apoptosis inductions of monocytes and lymphocytes, the TNFα mediated cell death induced by cp BVDV observed in primary cell cultures might be involved in the pathology of MD.

Figure legends

Figure 1. Apoptosis induced by cp BVDV. (A) Cell death induced by cp BVDV. BFM cells were mock-infected or infected with the KS86-1ncp (ncp) or KS86-1cp (cp) strain and incubated for 72 h at 37 °C. (B) Apoptotic index shown by TUNEL staining. BFM cells in a 96-well plate were infected and incubated in the same way as above. The apoptotic cells were assayed by ELISA-based TUNEL staining. Apoptotic index was measured by reading absorbance at 490 nm as described in Materials and methods. (C) Caspase-3 and -8 activities induced by cp BVDV. BFM cells in a 6-well plate were inoculated and incubated in the same way as above. Both caspase-3 and caspase-8 activities were measured as described in Materials and methods. (**$P < 0.01$, *$P < 0.05$; determined by Student's t test)

Figure 2. Caspases induced by a supernatant of cp BVDV-infected BFM cells. (A) Caspase-3 and caspase-8 activities induced by the UV-irradiated supernatants of BFM cell cultures infected with cp BVDV. Cells were inoculated and incubated in the same way in Fig. 1. Thereafter, viruses in the supernatants were inactivated by UV-irradiation at a distance of 20 cm for 20 min. The UV-irradiated supernatants of mock, ncp or cp BVDV-infected cells (lanes of Mock, ncp and cp) were added to confluent BFM cells and incubated for 24 h at 37 °C. Then, caspase-3 and caspase-8 activities were measured as described in Materials and methods. The value for mock-infected cells was set at 1. (B) Apoptotic effects due to the 10-30 kDa fraction in the supernatants of cp or ncp BVDV-infected BFM cells. Cells were treated as described in Materials and methods. Apoptotic state was represented using ELISA-based TUNEL staining.

Figure 3. Various mRNA expressions observed in cp and ncp BVDV-infected BFM cells. (A) Induction of Mx1, TNFα and iNOS by cp BVDV. BFM cells were mock-infected or infected with ncp (KS86-1ncp; K–, IS4, KZ91ncp; KZ–) or cp (KS86-1cp; K+, IS5, KZ91cp; KZ+) BVDV. After 48 h post infection (p.i.), RNA was extracted from the cells, reverse transcribed, and amplified by PCR with primers specific for mRNA of bovine Mx1 (20 cycles) or TNFα (30 cycles) or iNOS (35 cycles) or GAPDH (20 cycles). (B) Inhibition of both TNFα and iNOS mRNA expressions by infection with ncp BVDV. The amount of mRNA expression was quantitated using real-time PCR on the basis of standard curve made by quantitating GAPDH mRNA of each sample as described in Materials and methods. The values for mock-infected cells in cases of TNFα and iNOS were set at 1. (C) Different expressions of TNFR mRNA depending on the BVDV biotype used. BFM cells were mock-infected or infected with ncp (IS4) or cp (IS5) BVDV. After 48 h p.i., RNA was extracted from the cells, and both expressions were detected by RT-PCR with primers specific for TNFR-1 and TNFR-2 simultaneously by 26 PCR cycles. The TNFR-1 and -2 expression of mock-infected cells was detected when PCR was performed for 31 cycles.

Figure 4. Apoptosis attenuated by inhibition of TNFα. (A) (i) The antisense oligonucleotide against TNFα reduced caspase-3 activity induced by cp BVDV infection. BFM cells were either mock-infected or infected with ncp (KS86-1ncp) or cp (KS86-1cp) BVDV at an MOI of 1 for 24 h, followed by transfection of either control or TNFα antisense oligonucleotide for the final 72 h of culture. (ii) Transfection with antisense oligonucleotide against TNFα reduced extrinsic factor of apoptosis in the supernatant of cp BVDV-infected cells. The supernatants of the antisense-treated cell cultures were UV-irradiated and incubated

in the same way in Fig. 2. Each cell culture was collected and activity of caspase-3 was measured as described in Materials and methods. The resulting level of TNFα of antisense-treated cells was reduced to approximately 20% than that of control treated cells, which was detected by ELISA (data not shown). The value for mock-infected cells treated with control oligonucleotide was set at 1. (B) Incubation with a bovine TNFα-specific polyclonal antibody reduced apoptosis. After KS86-1cp-infected cells were incubated for 24 h, the cell supernatants were removed and replaced with medium containing a variety of antibody dilutions × 1000-5000 (lanes of × 1000, × 3000, and × 5000) or antibody-free medium (lane of (–)), and incubated for the final 72 h p. i. Inhibition of apoptosis was observed in a dose-dependent manner. In the case of incubation with an antibody dilution of × 1000, CPE was inhibited visibly.

Figure 5. (A) iNOS mRNA expression induced by exogenously added rboTNFα. Cells were incubated with cell culture medium containing rboTNFα at a concentration of 0.2-200 ng/ml for 24 h. Then, intracellular RNA was extracted and iNOS mRNA was detected using RT-PCR for 35 PCR cycles. (B) Potentiation of caspase-3 activity by L-NMMA treatment in cells infected with cp BVDV. Cells were either mock-infected or infected with KS86-1cp strain at an MOI of 1 and incubated for 24 h, then L-NMMA (100μM) was added for the final 72 h of culture. Caspase-3 activity was measured as described in Materials and methods. The value for mock-infected cells was set at 1.

CHAPTER 1 Fig. 1

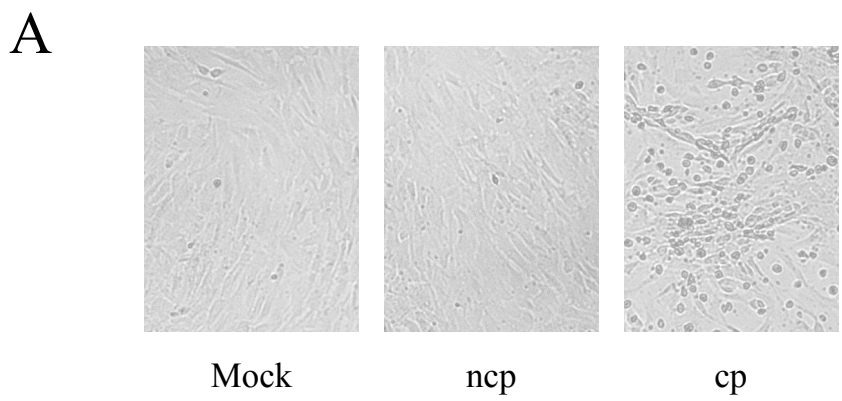

CHAPTER 1　Fig. 2

A

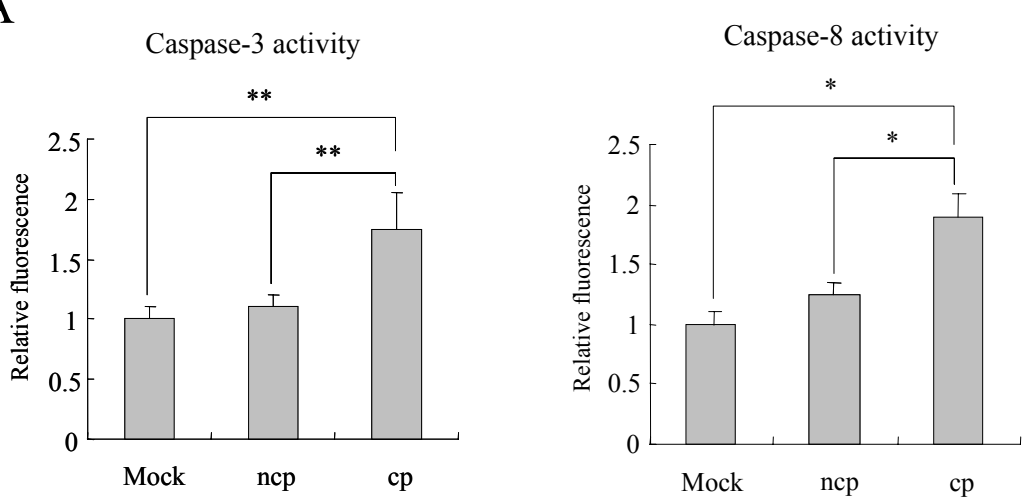

B

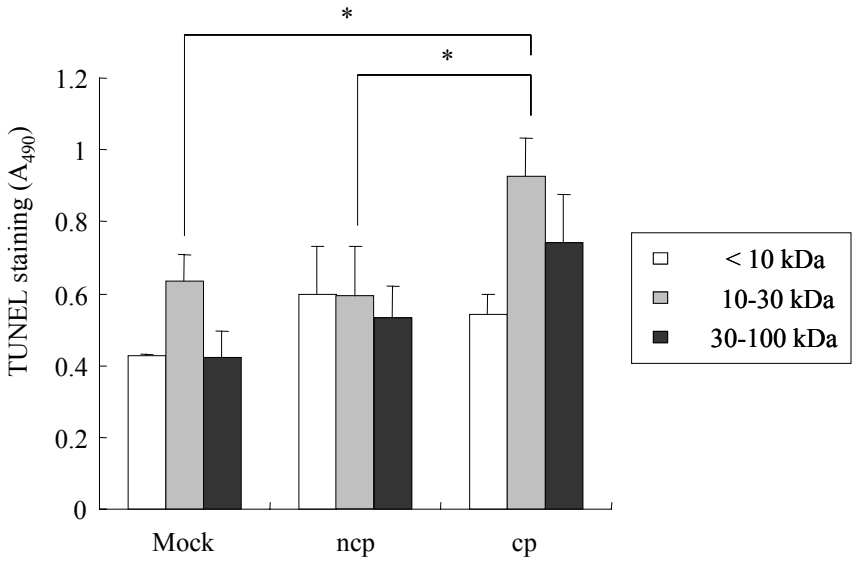

CHAPTER 1 Fig. 3

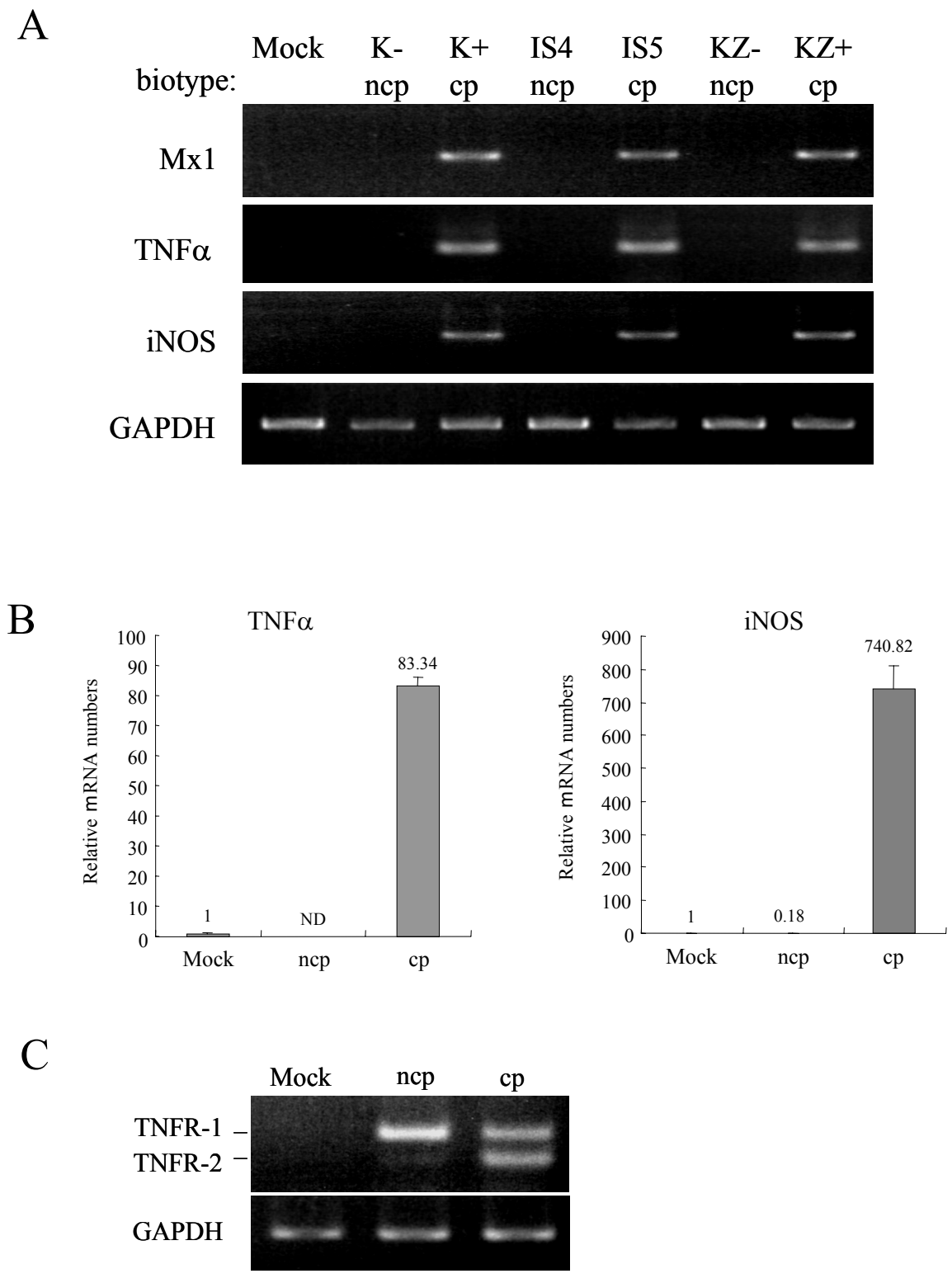

CHAPTER 1 Fig. 4

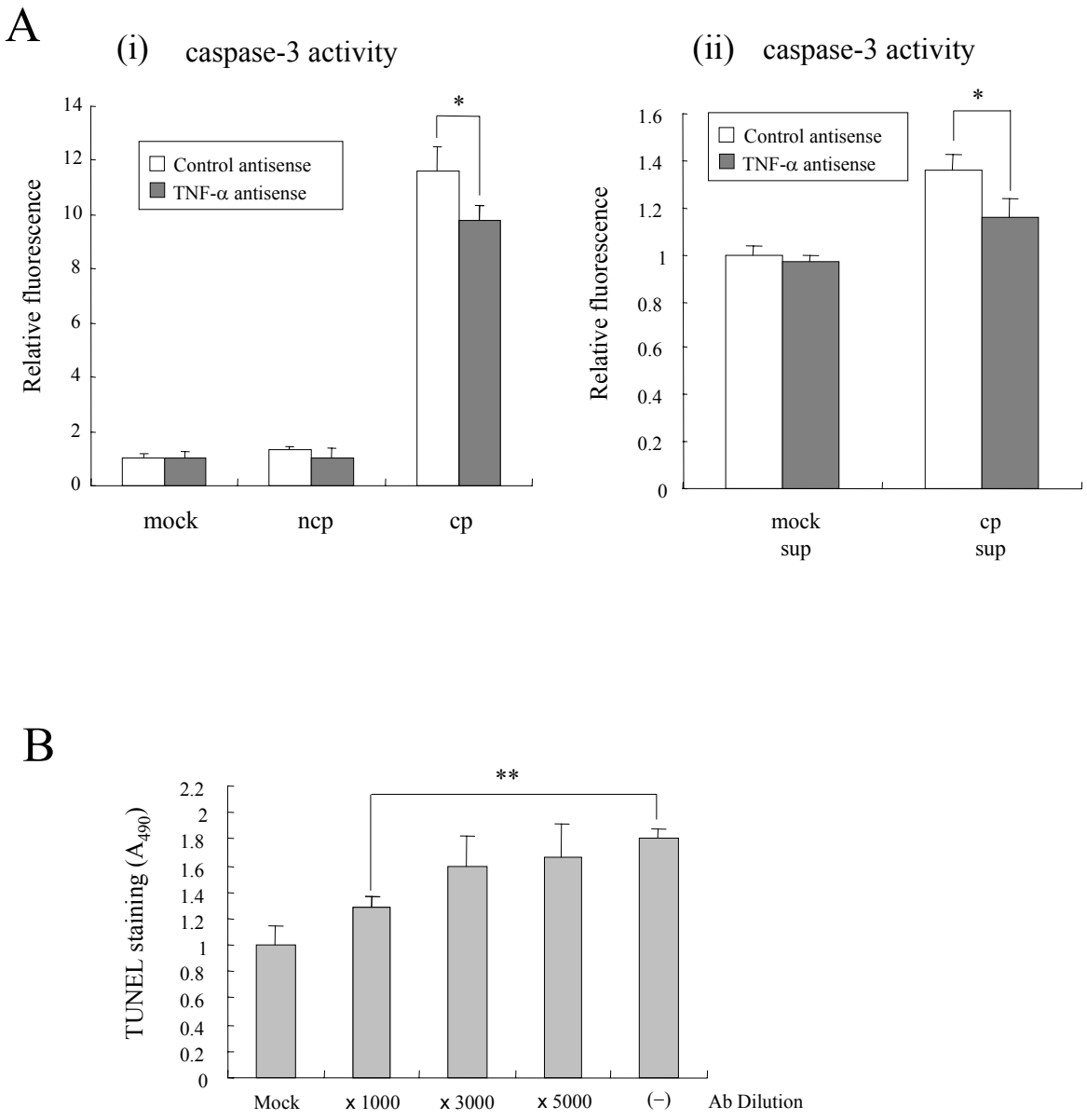

CHAPTER 1　Fig. 5

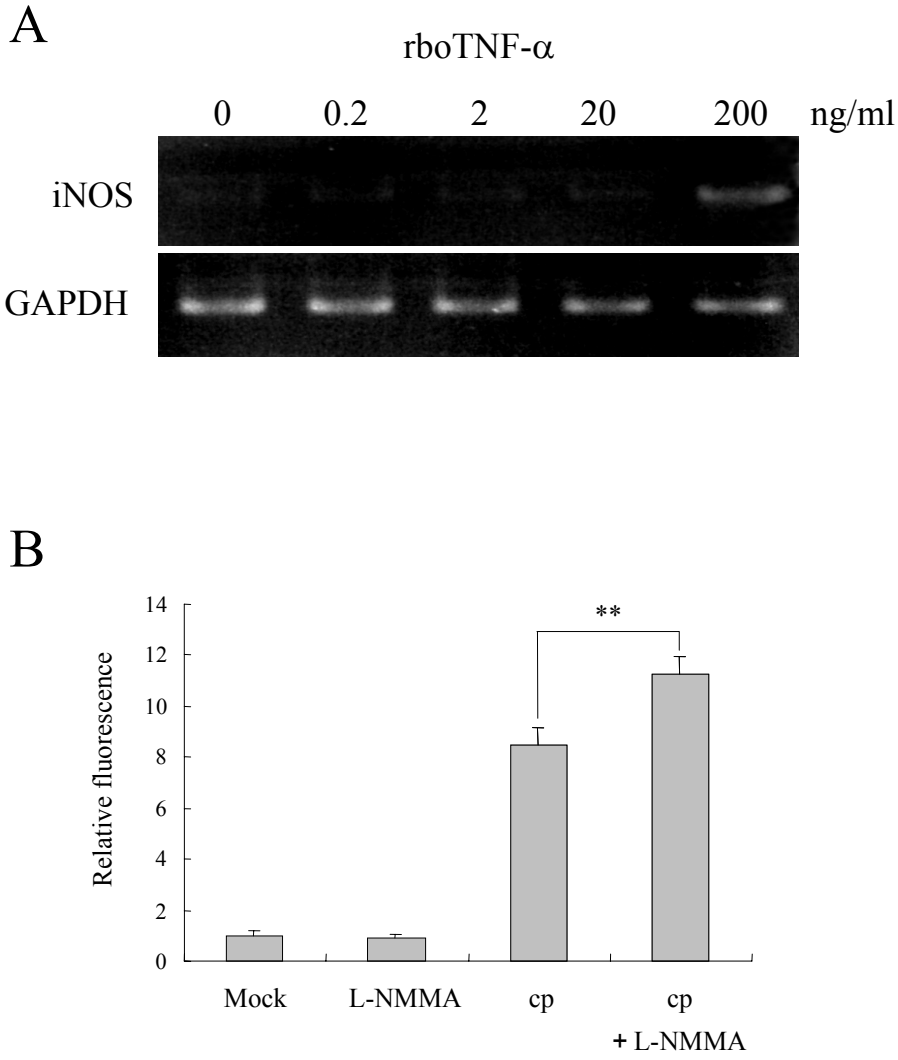

CHAPTER 1 Table 1

TNFα production in BFM cells infected with various BVDV strains[a]

Infection	TNFα (ng/ml)
Mock	0.071
ncp strains	
KS86-1ncp	0.105
IS4	0.078
KZ91ncp	0.069
cp strains	
KS86-1cp	1.838
IS5	1.440
KZ91cp	1.322

[a]The infection of BVDV at a MOI of 1 occurred 48 h before the cells were harvested for TNFα detection.

CHAPTER 2

The double-stranded RNA-induced apoptosis pathway is involved in the cytopathogenicity of bovine viral diarrhea virus

Journal of General Virology (2006) 87:2961-70

Abstract

The author found that overexpression of four apoptosis-related cellular mRNAs in cells infected with cytopathogenic (cp) BVDV was correspondingly caused by transfection with synthetic double-stranded RNA (dsRNA). Also, the amount of dsRNA produced by cp BVDV was found to exceed considerably the amount yielded by ncp BVDV. To evaluate the possible involvement of viral dsRNA in the induction of apoptosis, the author examined whether the RNAi-mediated depletion of two dsRNA-reactive cellular factors, dsRNA-dependent protein kinase (PKR) and 2′,5′-oligoadenylate synthetase 1 (OAS-1), results in preventing cp BVDV-induced apoptosis. Although the induction of apoptosis was reduced after the suppression of either factor alone, the simultaneous silencing of both factors resulted in an almost complete inhibition of apoptosis without affecting the viral titer. These results show that dsRNA is the main trigger of apoptosis in the cp BVDV-infected cells and that the cytopathogenicity of BVDV depends on the yield potential of dsRNA. In contrast, noncytopathogenic (ncp) BVDV yields minimal levels of dsRNA, thereby establishing a persistent infection without inducing apoptosis. This report supports the significance of viral dsRNA as a trigger of innate immune responses.

Introduction

A persistent viral infection causes profound disease in host animals. On the other hand, viruses must avoid or overcome the defensive mechanisms of the host to establish persistent infection. The innate immune responses of host cells, such as apoptosis and interferon (IFN) synthesis, provide a crucial first line of defense by eliminating virus-infected cells before the onset of a virus-specific immune response (Chawla-Sarkar *et al.*, 2003). As previous studies have suggested that the prevention of apoptosis could convert a lytic infection into a persistent infection (Gregory *et al.*, 1991; Levine *et al.*, 1993; Yeung *et al.*, 1999), evading apoptosis seems to be crucial for establishing persistent infection. Indeed, viruses have evolved various survival strategies by suppressing apoptosis and IFN responses (Cebulla *et al.*, 1999; Roulston *et al.*, 1999).

Double-stranded RNA (dsRNA) is formed mainly as a replicative intermediate during the viral replication of positive-strand RNA viruses and is an active component of the viral infection that stimulates host antiviral responses, including apoptosis (Clemens, 1997; Gil & Esteban, 2000; Williams, 1997) and cytokine productions, such as IFNs and nitric oxide (Auch *et al.*, 2004; Blair *et al.*, 2002; Heitmeier *et al.*, 1998). Two cellular factors, dsRNA-dependent protein kinase (PKR) and 2′,5′-oligoadenylate synthetase (OAS), is inducible by Type I IFNs and are activated by binding with dsRNA (Chawla-Sarkar *et al.*, 2003). Activated PKR phosphorylates the α subunit of eukaryotic translation initiation factor 2 (eIF2α), leading to the arrest of translation and cell death (Kaufman, 1999). On the other hand, activated OAS synthesizes 2′,5′-oligoadenylates and, in turn, activates RNase L, which causes apoptosis through the degradation of single-stranded RNA (ssRNA) including viral and cellular RNAs (Castelli *et al.*, 1998). Thus, the PKR and OAS systems induce apoptosis

by inhibiting the synthesis of both viral and host proteins through independent mechanisms.

Interestingly, several reports have demonstrated that increased viral RNA replication occurs in cells infected with cp BVDV (Becher *et al.*, 2001; Lackner *et al.*, 2004; Mendez *et al.*, 1998; Vassilev & Donis, 2000). However, the cp BVDV-derived factor(s) that induce cell death via apoptosis have not been determined. In this study, the author shows that cp BVDVs, but not ncp BVDVs, produce a large amount of dsRNA in host cells. Subsequently, to analyze the involvement of the interactions between cp BVDV-yielded dsRNA and dsRNA-binding cellular proteins in the execution of apoptosis, the author examined the potential of PKR and OAS-1-targeted RNAi to inhibit cp BVDV-induced apoptosis.

Materials and methods

Reagents. Synthetic polyribonucleotides, polyinosinic-polycytidylic acid, poly(IC), and polyinosinic acid, poly(I), and 2-aminopurine (2-AP) were purchased from Sigma (St. Louis, MO, USA).

Cells and viruses. Primary bovine fetal muscle (BFM) cells were maintained as described in CHAPTER 1. BVDV strains KS86-1cp and KS86-1ncp (genotype 1) were used (Nagai *et al.*, 2001; Nagai *et al.*, 2003) and inoculated as described in the figure legends.

Apoptosis assays. Caspase-3 and TUNEL assays were performed as described in CHAPTER 1.

RT-PCR of cellular mRNAs. RT-PCR of cellular mRNAs was performed as described in CHAPTER 1. The primers used to amplify bovine OAS-1 mRNA (369-bp product) were 5′-TCTCAGCTTTGTGCTGAGGT-3′ (sense) and 5′-TGAGCTGTGCTGAATTCTGG-3′ (antisense). The PCR amplification of bovine OAS-1 was performed for 40 cycles.

Western blot analysis. At selected time points post-inoculation (p.i.), the cells were treated as previously described (Jordan *et al.*, 2002). Proteins were separated by 10% SDS–PAGE and transferred onto nitrocellulose membranes (Amarsham, Piscataway, NJ, USA). After blocking, the membranes were incubated with primary polyclonal antibody against PKR (D-20; Santa Cruz Biotechnologies, CA, USA) or against phosphorylated eIF2α (Biomol International, Plymouth Meeting, PA, USA) or against OAS-1 (GenWay Biotech Inc., San

Diego, CA, USA), or with mouse monoclonal antibody against β-actin (diluted 1:3000 with PBS containing 1% BSA and 0.1% Tween 20) for 2 h. Subsequently, membranes were incubated with horseradish peroxidase-conjugated secondary antibodies (diluted 1:5000 with PBS containing 2% non-fat milk and 0.1% Tween 20). The immunoreactive protein bands were detected by enhanced chemiluminescence (ECL) detection kit (Amersham).

Extraction and transfection of RNA. Total RNA was extracted using TRIZOL reagent (Invitrogen, Carlsbad, CA, USA) from 6×10^4 mock-infected BFM cells, or BFM cells infected with KS86-1ncp or KS86-1cp at a multiplicity of infection (MOI) of 1 at 48 h p.i. Each RNA sample was treated with 1 U of RNase I (Promega, Madison, WI, USA), which digests ssRNA specifically, or RNase III (New England Biolabs, Beverly, MA, USA), which digests only dsRNA, for 30 min at 37°C. The enzymes were inactivated by heating at 70°C for 20 min. Then the resulted RNA samples were transfected using Lipofectamine 2000 reagent (Invitrogen) into 6×10^4 of confluent BFM cells according to the manufacturer's protocol. Twenty-four hours after the transfection, photographs were taken and apoptosis assays were performed as described above.

RNAi procedure. The author designed Stealth RNAi (Invitrogen) against bovine PKR and OAS-1. The Stealth RNAi against bovine PKR was 5′-GCCGUCUUAAUACGAUCUCCCAGAA-3′ (sense) and 5′-UUCUGGGAGAUCGUAUUAAGACGGC-3′ (antisense) and against the bovine OAS-1 was 5′-GGAGTTCCGCACCCAAGTCAAACAA-3′ (sense) and 5′-UUGUUUGACUUGGGUGCGGAACUCC-3′ (antisense); a control Stealth RNAi

contained the same base composition in a random order, respectively. At 24 h before the virus infection, BFM cells were seeded in 48-well plates in 200 μl of antibiotic-free DMEM supplemented with 10% FCS and incubated at 37°C in a humidified 5% CO_2 atmosphere. The BFM cells were infected with cp BVDV at an MOI of 2 for 1 h at 37°C. After the inoculum was removed by washing the cells in FCS-free DMEM, transfection with 25 pmol of Stealth RNAi against PKR, OAS-1, or each control was performed using Lipofectamine 2000 reagent (Invitrogen) according to the manufacturer's protocol. The medium was then replaced at 4 h post-transfection with DMEM supplemented with 5% FCS. At 24 h p.i., the cells were assayed for the inhibition of PKR and OAS-1 mRNA expression by quantitative real-time PCR as described below.

Quantitative real-time PCR. The RT reaction to initiate cDNA synthesis was performed with SuperScript III RNaseH$^-$ Reverse Transcriptase (Invitrogen) according to the manufacturer's protocol. To determine whether the RNA was single- or double-stranded, the RNA samples were treated with RNase I or RNase III as described in the section of Extraction and transfection of RNA. The viral negative-stranded RNA was primed with 0.8 μM of 324 sense primer (5'-ATGCCC(T/A)TAGTAGGACTAGCA-3'; 5'NCR), and the viral positive-stranded RNA was primed with 326 antisense primer (5'-TCAACTCCATGTGCCATGTAC-3'; 5'NCR) (Vilcek *et al.*, 1994). A quantitative real-time PCR assay was performed by means of a Smart Cycler II (Cepheid, Sunnyvale, CA, USA). Viral RNA was quantitated using Cycleave RT-PCR Pestivirus Detection Kit (TaKaRa, Shiga, Japan) according to the manufacturer's protocol. The quantitation of OAS-1 and PKR mRNAs was performed with SYBR Premix Ex Taq (TaKaRa) using 1 μl of

reverse-transcribed cDNAs. The primers used to amplify bovine PKR mRNA were 5'-CTGGTCGTTCACCATGTTTC-3' (sense) and 5'-CTCAATGGGTGGTCCTTCT-3' (antisense) and the primers of bovine OAS-1 mRNA were the same as described above in the section of RT-PCR of cellular mRNAs. All the samples were analyzed in triplicate. The measured amounts of RNA were normalized to the amount of GAPDH mRNA in each sample as described in CHAPTER 1.

Results

The overexpression of apoptosis-related cellular mRNAs and proteins induced by cp BVDV was correspondingly caused by synthetic dsRNA.

Results in CHAPTER 1 showed that the overexpression of Mx1, iNOS and TNFα mRNAs was caused by cp BVDV infection in primary BFM and primary bovine testicle cells through the comprehensive investigation of apoptosis-related cellular mRNAs. In this study, the author additionally found the overexpression of OAS-1 mRNA (Fig. 1A). In addition, overexpression of PKR mRNA by cp BVDV infection was detected by quantitative real-time PCR (data not shown), and protein overexpression of PKR and phosphorylated eIF2α in the cp BVDV-infected cells (Fig. 1B) was also confirmed as recently reported (Gil *et al.*, 2006). Although the factor(s) leading to the overexpression has remained unclear, the author found that poly(IC), a synthetic dsRNA analog, could induce four apoptosis-related cellular mRNAs (Mx1, iNOS, TNFα and OAS-1) similar to the cp BVDV infection (Fig. 1A and B). On the other hand, with the transfection of poly(I), a ssRNA analog, the overexpression of only two mRNAs, Mx1 and iNOS, was induced even at a concentration of 10 μg/ml (Fig. 1A). When the author tested various concentrations of poly(IC), the overexpression of four apoptosis-related mRNAs was observed at doses greater than 50 ng/ml (data not shown). Furthermore, cp BVDV-like cell death and activation of caspase-3, the apoptosis-executer enzyme, occurred when poly(IC) was transfected into the cells using Lipofectamine 2000 (Fig. 1C) but not when poly(IC) was simply added in the supernatant, even at a high concentration (200 μg/ml, data not shown).

ncp BVDV can reduce apoptosis induced by transfected poly(IC) but cannot completely

inhibit the apoptosis in BFM cells.

It has been shown that ncp BVDV inhibits signal transduction induced by poly(IC) added in the culture supernatant (Iqbal *et al.*, 2004; Schweizer & Peterhans, 2001) and that induced by transfected poly(IC) (Gil *et al.*, 2006; Schweizer & Peterhans, 2001). In contrast to primary bovine turbinate cells used in the previous study of Schweizer and Peterhans (2001), BFM cells induced apoptosis only when poly(IC) was transfected (Fig. 1C). All of the cells transfected with poly(IC) at concentrations greater than 50 ng/ml underwent apoptosis despite of the prior infection with ncp BVDV as shown in Fig. 1D. A slight reduction of caspase-3 activity was observed in the ncp BVDV-infected cells at a poly(IC) concentration of 5 μg/ml, which seemed to be an effect of E^{rns} secreted from BVDV-infected cells (Iqbal *et al.*, 2004). Furthermore, the overexpression of four apoptosis-related cellular mRNAs stimulated by poly(IC), as shown in Fig. 1A, was not inhibited by the prior infection with ncp BVDV, even at the low poly(IC) concentration (50 ng/ml) (data not shown). These results indicate that ncp BVDV does not inhibit signal transduction stimulated by intracellular poly(IC) in BFM cells.

Quantitation of viral ss- and dsRNA using real-time PCR.

To examine whether there are differences in the yields of viral RNA between cp and ncp BVDVs, the author quantitated the amounts of positive-ssRNA and dsRNA of ncp and cp BVDVs using real-time PCR. Viruses were inoculated at an MOI of 5 to analyze the viral RNA replication kinetics of synchronous infections. As shown in Fig. 2, viral RNA of cp BVDV started to increase from 8 h p.i., however, that of ncp BVDV was decreased by 8 h p.i. At 24 h p.i., the copy number of positive-ssRNA in the cp BVDV-infected cells exceeded

approximately 100 times that found in the ncp BVDV-infected cells, while the amount of dsRNA in the cp BVDV-infected cells was 100-200 times than that in the ncp BVDV-infected cells (Fig. 2). Also in the case of multicycle infections at an MOI of 0.1, viral ssRNAs of ncp and cp strains, respectively, were found to increase in the same manner by 48 h p.i. (data not shown), suggesting that each strain replicates with the same efficiency regardless of MOI. The similar results were obtained using two other cp and ncp pair viruses, including BVDV genotype 2 (IS4ncp and IS5cp, KZ91ncp and KZ91cp; Nagai *et al.*, 2001) (data not shown). On the other hand, the copy number of negative-ssRNA, as an indicator of replication, derived from cp BVDV was 100-200 times larger than that from ncp BVDV, corresponding to the difference in the yield of viral dsRNA (Fig. 2).

Viral dsRNA extracted from BFM cells induced apoptosis.

To examine whether viral dsRNA by itself is sufficient to induce CPE via apoptosis, the extracted RNA was transfected into BFM cells. The samples of RNA extracted from mock- and BVDV-infected cells were treated with or without RNase I or RNase III, and each sample was transfected into the same number of normal BFM cells. Only the cells transfected with the extracted RNA from the cp BVDV-infected cells, either without RNase treatments or with RNase I treatment, induced CPE-like cell death (Fig. 3A). The cell deaths were also shown to be triggered via apoptosis as indicated by an ELISA-based TUNEL assay (Fig. 3B). These results showed that cp BVDV yields large amount of dsRNA enough to induce apoptosis, while ncp BVDV replicates at a minimum level yielding unrecognizable amount of dsRNA.

An apoptotic sensitivity to poly(IC) was decreased after the RNAi-mediated knockdown

of PKR and/or OAS-1.

The author first assessed the effects of the RNAi-mediated silencing of PKR and OAS-1 mRNA in cp BVDV-infected BFM cells as described in Materials and methods. By each RNAi treatment, the quantity of PKR mRNA extracted from the cells transfected with PKR siRNA (iPKR) was reduced by approximately 85%, and OAS-1 mRNA was reduced by approximately 90% in the OAS-1 siRNA-transfected cells (iOAS) (Fig. 4A). By the administration of siRNA mixture against PKR and OAS-1 (iMix), the PKR and OAS-1 mRNAs were simultaneously depleted (Fig. 4A). The RNAi-mediated reduction of PKR or OAS-1 protein, and that of both proteins through the double-knockdown in the cp BVDV-infected cells was also confirmed by Western blotting (Fig. 4B). The author next examined the inhibition of the poly(IC)-induced caspase-3 activity to examine the cellular sensitivity against dsRNA after the RNAi-mediated depletions of PKR and OAS-1. The poly(IC)-induced caspase-3 activity was reduced by approximately 30% after the knockdown of PKR, and the activity was reduced by approximately 15% after the knockdown of OAS-1 compared with the activity in control siRNA-transfected case (Fig. 4C). These results showed that the participation of OAS-1 in the induction of poly(IC)-induced apoptosis was less than that of PKR; however, the OAS-1 pathway was also involved in executing apoptosis. Then, after the double-knockdown of PKR and OAS-1, the caspase-3 activity induced by poly(IC) was decreased to the same level as that of mock-treated cells (Fig. 4C). These results suggested that apoptotic sensitivity of BFM cells to transfected dsRNA was functionally depleted through the administration of PKR and OAS-1 RNAi.

Double-knockdown of OAS-1 and PKR with RNAi resulted in the complete inhibition of

cp BVDV-induced cell death.

Subsequently, the effect of PKR and OAS-1 knockdown on the induction of apoptosis in cp BVDV-infected cells was analyzed. Through a time course experiment, cp BVDV-induced caspase-3 activity was reduced by approximately 30% at 48 h p.i. with the administration of PKR RNAi (Fig. 5A), corresponding to the change observed in the case of poly(IC)-induced caspase-3 activity. As observed with the suppression of caspase-3, the RNAi-mediated silencing of PKR in cells infected with cp BVDV resulted in a delay in the appearance of CPE and a reduction of visible cell death (Fig. 5B). In addition, cp BVDV-induced caspase-3 activity was reduced by approximately 15% with the administration of OAS-1 RNAi (Fig. 5C), which corresponds to the reduction in the experiment with transfected poly(IC). However, the reduction of apoptosis in OAS-1 siRNA-transfected cells was not clearly observed when compared with that in control siRNA-transfected cells (data not shown). When the author tested the double-knockdown of PKR and OAS-1, the caspase-3 activity induced by cp BVDV infection was dramatically decreased, in the same manner as that induced by poly(IC), and cp BVDV-induced cell death was completely inhibited as examined by microscopy at 48 h p.i. (Fig. 5D), though the yielded viral titers remained unaffected (Fig. 5E). Although possibilities that cp BVDV may induce apoptosis via additional trigger of PKR or OAS-1 are not still excluded, these results strongly suggest that each of both factors independently activates the pro-apoptotic signaling pathways against dsRNA and that both pathways synergistically participate in the execution of apoptosis. In addition, cp BVDV-induced apoptosis occurred in the same fashion as that stimulated by synthetic dsRNA, suggesting that viral dsRNA is a main trigger of cp BVDV-induced apoptosis.

Discussion

The molecular feature that distinguishes the cp from the ncp biotype of BVDV is the efficient generation of discrete NS3 protein, which is thought to correlate with an up-regulated synthesis of viral RNA, throughout an infection of cp BVDV (Lackner *et al.*, 2004; Meyers & Thiel, 1996; Vassilev & Donis, 2000). The author focused on the effect of viral RNA accumulation in the induction of apoptosis due to the efficient RNA replication of cp BVDV as shown in Fig. 2. In this study, the dsRNA, which is derived from an increased level of viral RNA replication, is shown to be highly involved in the execution of apoptosis by interactions with dsRNA-reactive cellular factors, PKR and OAS-1.

The author found that the up-regulation of four apoptosis-related cellular mRNAs observed in the cp BVDV-infected cells was induced similarly by the transfection of synthetic dsRNA. Among the set of four factors, iNOS was shown to serve as anti-apoptotic factor, and TNFα has been revealed to participate in enhancing the cp BVDV-induced apoptosis as an extrinsic factor in CHAPTER 1. In this study, the author revealed that dsRNA could trigger intrinsic apoptotic factors, PKR and OAS-1, and initiate apoptosis through the interactions with both factors, which are thought to be key events in the cytopathogenicity. The RNAi-mediated knockdown of either PKR or OAS-1 in cp BVDV-infected cells resulted in the reduction of caspase-3 activity and the delay of cell death. By the double-knockdown of both PKR and OAS-1, the apoptotic activity of cp BVDV-infected cells was inhibited almost to the same level as the level observed in mock-infected cells. These results indicate that a pro-apoptotic synergistic effect of OAS-1 and PKR is induced by accumulated viral dsRNA in the cp BVDV-infected cells and that both factors independently play critical roles in initiating apoptosis. The viral titers of cp BVDV when faced with the double-knockdown of

both factors were unchanged compared with the titers in the mock- and control siRNA-transfected cases (Fig. 5E); thus, the inhibition of apoptosis appears to be attributable to the insensitivity of host cells to the PKR and OAS-mediated antiviral pathways probably stimulated by cp BVDV-derived dsRNA, which lead a cytopathic infection of cp BVDV to a noncytopathic one. Furthermore, the functions of PKR and OAS-1 have been suggested to be associated with the clearance of hepatitis C virus (HCV) infection (Knapp *et al.*, 2003), supporting the idea that both factors might play crucial roles in preventing a persistent infection.

The overexpression of four apoptosis-related cellular mRNAs was not observed in the ncp BVDV-infected cells. ncp BVDV seems to yield only a small amount of ssRNA because the overexpression of Mx1 and iNOS mRNAs was caused by synthetic ssRNA as shown in Fig. 1A. The quantitation of viral RNA, as shown in Fig. 2, supported the suggestion that minimal RNA replication occurred in the ncp BVDV-infected cells. In the case of HCV, the limitation of viral RNA replication via the degradation of NS5B, which functions as an RNA-dependent RNA polymerase, is thought to be important to escape the host cell defenses (Gao *et al.*, 2003). Thus, the maintenance of low-level RNA replication as observed in the ncp BVDV infection would be a most crucial strategy for establishing persistent infection, given that the difference in the RNA replication level between ncp and cp BVDV was the common feature among all three pairs of the BVDV strains tested. Conversely, since ncp and cp BVDV both share the ability to inhibit an interferon-related antiviral response (Baigent *et al.*, 2004; Chen *et al.*, 2007) or a signal transduction against dsRNA (Iqbal *et al.*, 2004), it is speculated that excessive amount of dsRNA yielded by cp BVDV surpasses the BVDV capacity to inhibit the antiviral responses.

In this study, the participation of the PKR pathway and the subsequent phosphorylation of eIF2α, which leads to the restriction of mRNA translation, were shown to be involved in cp BVDV infection (Fig. 1B). As the inhibition of eIF2α kinase by 2-aminopurine (2-AP) increased the viral titer of cp BVDV up to 10-fold and as a slight increase of the viral titer was observed by the knockdown of PKR (Fig. 5E), protein synthesis of cp BVDV might be limited following the activation of PKR and subsequent eIF2α phosphorylation. However, despite the excessive induction of antiviral factors such as Mx1 or OAS-1, which restrict viral RNA replication (Castelli *et al.*, 1998; Haller *et al.*, 1998), the mechanism through which cp BVDV replicates more efficiently than ncp BVDV still needs to be elucidated (Lackner *et al*., 2004).

The difference between the biotypes, which can be distinguished *in vitro*, should be clarified because the transmission of BVDV to a fetus and persistent infection are apparently correlated with the biotype of BVDV. In this study, all of the ncp BVDV strains tested were shown to evade apoptosis and to produce a sufficiently small amount of dsRNA to escape recognition by cellular dsRNA-reactive factors. In contrast, the BVDV biotype with cytopathogenic properties commonly correlates with the productivity of dsRNA, and the extracted dsRNA from the cp BVDV-infected cells induced apoptosis in the absence of viral proteins as shown in Fig. 3A, suggesting that dsRNA is a key factor of cytopathogenicity.

Although the observation *in vitro* might be different from that *in vivo*, as apoptosis and the IFN response are manifested from the earliest stages of pregnancy (Splichal *et al.*, 1994), the transplacental and persistent infection could be affected by the dsRNA-induced innate immune responses. Although the dsRNA-induced apoptosis is known to correlate with negative-strand RNA viruses (Takizawa *et al.*, 1996) and DNA viruses (Kibler *et al.*, 1997),

these results show that also in the case of the positive-strand RNA virus, dsRNA can be a main trigger of apoptosis.

Figure legends

Figure 1. Transfection of poly(IC) induced the overexpression of four apoptosis-related cellular mRNAs (Mx1, iNOS, TNFα and OAS-1) as induced by cp BVDV and induced cell death via apoptosis in BFM cells. (A) The overexpression of the four mRNAs induced by cp BVDV infection or transfection with poly(IC). At 4 h after the transfection of poly(I) (lane I) or poly(IC) (lane IC) or 24 h after the cp (KS86-1cp; lane cp) or ncp (KS86-1ncp; lane ncp) BVDV infection at an MOI of 1, total RNA was isolated and RT-PCR was performed as described in Materials and methods. (B) Expression of PKR and phosphorylated eIF2α (P-eIF2α) induced by poly(IC) or cp BVDV. After BFM cells were treated with poly(IC) (lane IC) or infected with cp (lane cp) or ncp (lane ncp) BVDV as described in (A), each protein was detected by immunoblotting as described in Materials and methods. (C) Caspase-3 was activated only in the presence of poly(IC) transfected using Lipofectamine 2000 (LF). BFM cells were mock-treated (lane Mock) or treated with 10 μg/ml of poly(I) (lane I) or poly(IC) (lane IC) with LF (+LF) or without LF (Sup). The activities of caspase-3 were measured at 24 h after the transfection as described in Materials and methods. Each activity was standardized to the value of mock-treated cells without LF, which was set at 100%. (D) Activities of poly(IC)-induced caspase-3 were slightly reduced by prior infection with ncp BVDV. BFM cells were mock-infected or infected with KS86-1ncp at an MOI of 1 at 18 h before the transfection of poly(IC) at the indicated concentrations. The activities of caspase-3 were measured at 24 h after the poly(IC) transfection. Each activity was standardized to the value of mock-infected cells without poly(IC), which was set at 100%. (**$P < 0.01$; determined by Student's t-test)

Figure 2. Viral positive-, negative-ssRNA and dsRNA yielded by cp BVDV significantly exceed those of ncp BVDV. The amount of viral positive- or negative-ssRNA or dsRNA was determined by quantitative real-time PCR as described in Materials and methods. BFM cells were infected with cp (KS86-1cp) or ncp (KS86-1ncp) BVDV at an MOI of 5. Each genome copy number was normalized to the amount of cellular GAPDH mRNA, and standardized to the positive-ssRNA copy number of ncp BVDV at 0 h p.i., which was set at 1.

Figure 3. The extracted viral dsRNA from cp BVDV-infected cells induced the cytopathic effect (CPE) via apoptosis. (A) Transfection of extracted dsRNA from the cp BVDV-infected cells resulted in the appearance of cell death. RNA samples extracted from mock-infected BFM cells (Ct) or BFM cells infected with KS86-1ncp (ncp) or KS86-1cp (cp) were mock-treated (left panels) or treated with RNase I (center panels) or RNase III (right panels), and then transfected into confluent BFM cells as described in Materials and methods. Cell death was observed 24 h later. (B) The apoptotic index was determined using ELISA-based TUNEL assay. The RNA sample extracted from mock-infected BFM cells as a control (lane Ct), and that from cells infected with ncp BVDV (KS86-1ncp; lane ncp) were used for transfection, respectively. The RNA samples of cp BVDV-infected cells that were mock-treated (lane cp) and treated with RNase I (lane cp I) or RNase III (lane cp III) were transfected into BFM cells and incubated for 24 h. The assay was performed as described in Materials and methods. (**$P < 0.01$; determined by Student's t-test)

Figure 4. PKR and OAS-1 was functionally depleted by the administration of RNAi. (A) The reduction of cp BVDV-induced PKR and OAS-1 mRNA by each RNAi. After BFM cells

were infected with KS86-1cp at an MOI of 2 for 1h, the cells were washed with DMEM and each siRNA was transfected as described in Materials and methods. At 24 h after the transfections of siRNA against PKR (iPKR) or control (iCt-PKR), against OAS-1 (iOAS) or control (iCt-OAS), and against both PKR and OAS (iMix) or control (iCt-Mix) in the cp BVDV-infected cells, total RNA was extracted and quantitative real-time PCR was performed as described in Materials and methods. (B) RNAi-mediated reduction of PKR and OAS-1 protein induced by cp BVDV in BFM cells. At 24 h after the transfection of each siRNA as described above in the cp BVDV-infected cells, lysates were collected and Western blotting was performed to detect PKR, OAS-1 and β-actin. (C) Knockdown of PKR or/and OAS-1 reduced the apoptotic sensitivity of BFM cells to poly(IC). Transfections of each siRNA as described above were performed at 36 h before the transfection of 500 ng/ml poly(IC). After 12 h, each caspase-3 activity was measured and standardized to the value of poly(IC)-transfected normal BFM cells, which was set at 100%.

Figure 5. Apoptosis of cp BVDV-infected cells was inhibited after the RNAi-mediated double-knockdown of PKR and OAS-1. (A) Caspase-3 activity induced by cp BVDV was reduced after the knockdown of PKR. BFM cells were mock-infected (Mock) or infected with KS86-1ncp (ncp) or KS86-1cp (cp) at an MOI of 2 at 1 h before the transfections of siRNAs (iPKR and iCt-PKR; see above), and caspase-3 activities were assayed at the indicated time points. Each activity was standardized to the value of mock-infected cells at 24 h p.i., which was set at 100%. (B) The cp BVDV-induced CPE was reduced visibly by PKR siRNA transfection. Each photograph was taken 48 h after the infection. (C) cp BVDV-induced caspase-3 was inhibited by the double-knockdown of PKR and OAS-1. BFM cells were

mock-infected (Mock) or infected with KS86-1cp (cp) or KS86-1ncp (ncp) at an MOI of 2 at 1 h before the transfections of siRNA described above. At 48 h p.i., each caspase-3 activity was assayed and standardized to the value of the mock-transfected case of mock-infected cells, which was set at 100%. (D) The cp BVDV-induced CPE was inhibited visibly by the RNAi-mediated double-knockdown of both PKR and OAS-1. Each photograph was taken 48 h after the infection. (E) Viral titers of cp BVDV at 48 h p.i. in the mock-transfected cells, the cells transfected with siRNA described in Fig. 4A and the cells treated with 100 μM 2-aminopurine (2-AP), which is the inhibitor of eIF2α kinases, were calculated as 50% tissue culture infective dose/ml ($TCID_{50}$/ml) using Madin-Darby bovine kidney (MDBK) cells. (*P < 0.05, **P < 0.01; determined by Student's t-test)

CHAPTER 2　Fig. 1

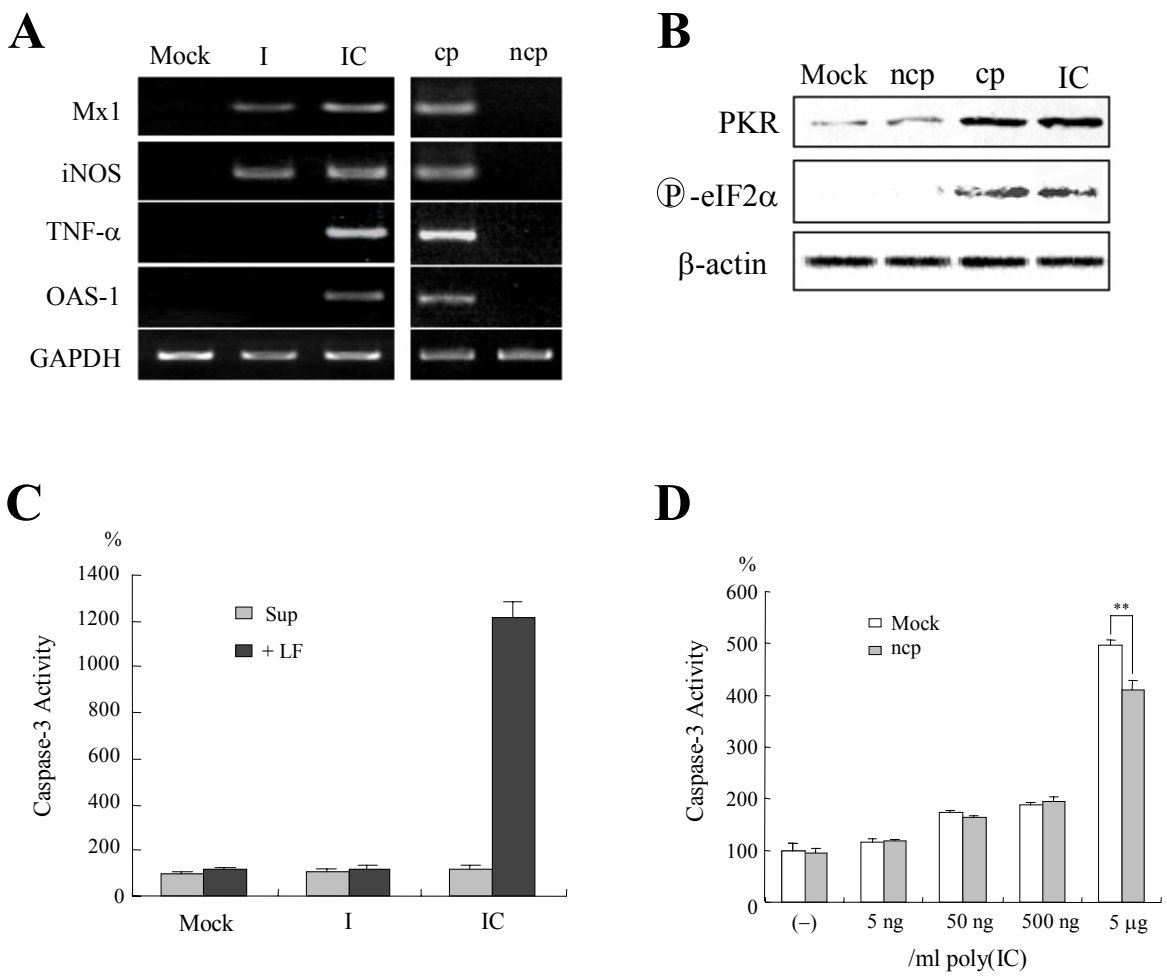

CHAPTER 2 Fig. 2

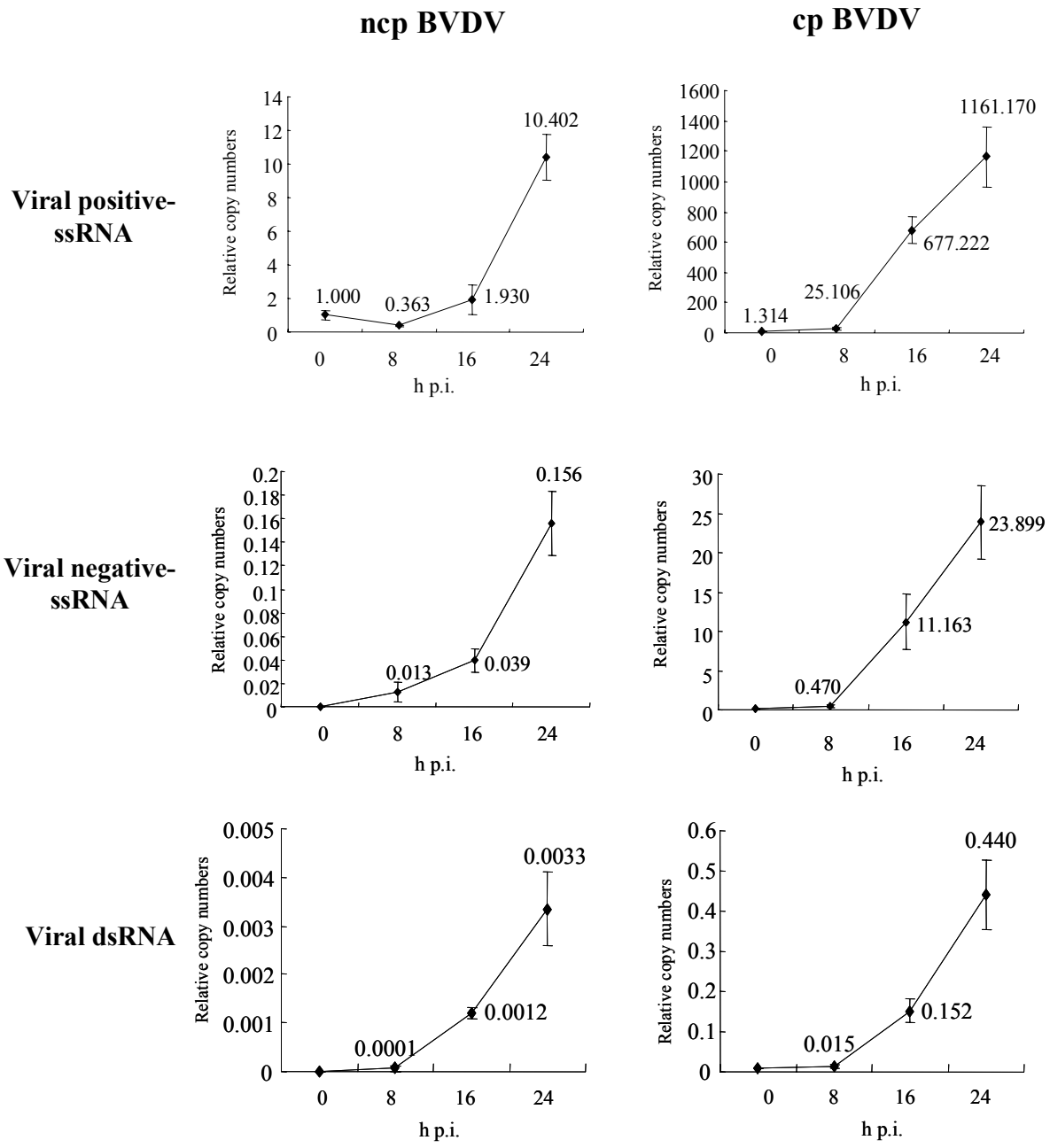

CHAPTER 2 Fig. 3

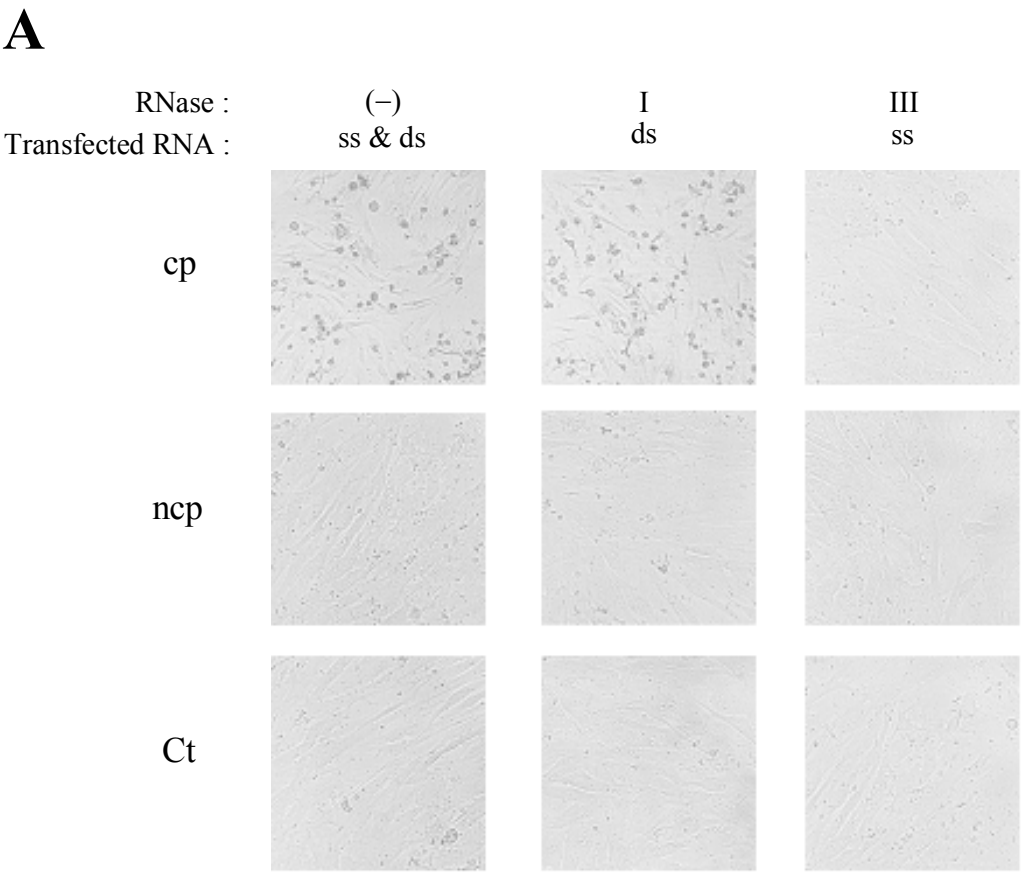

CHAPTER 2　Fig. 4

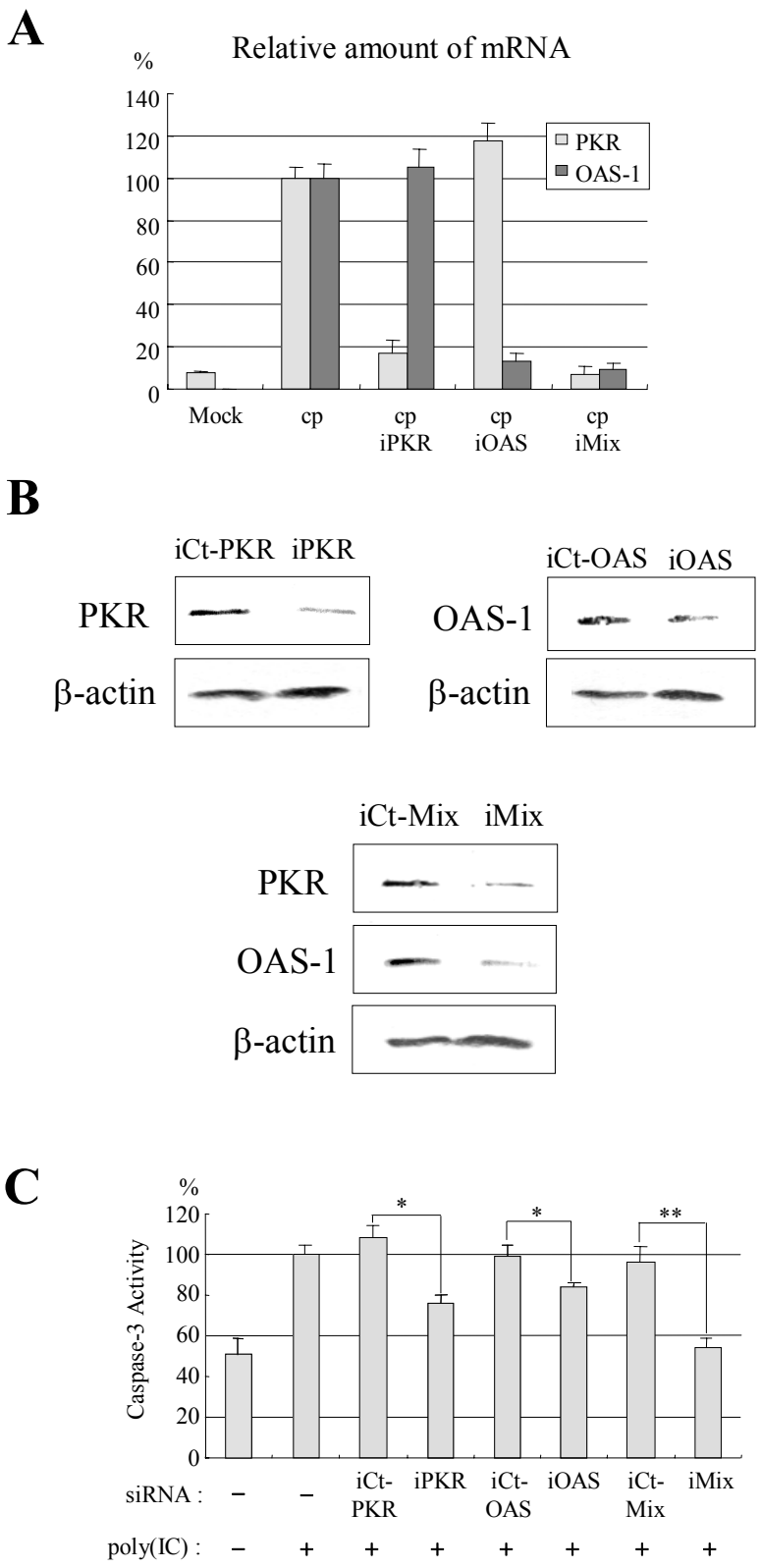

CHAPTER 2 Fig. 5

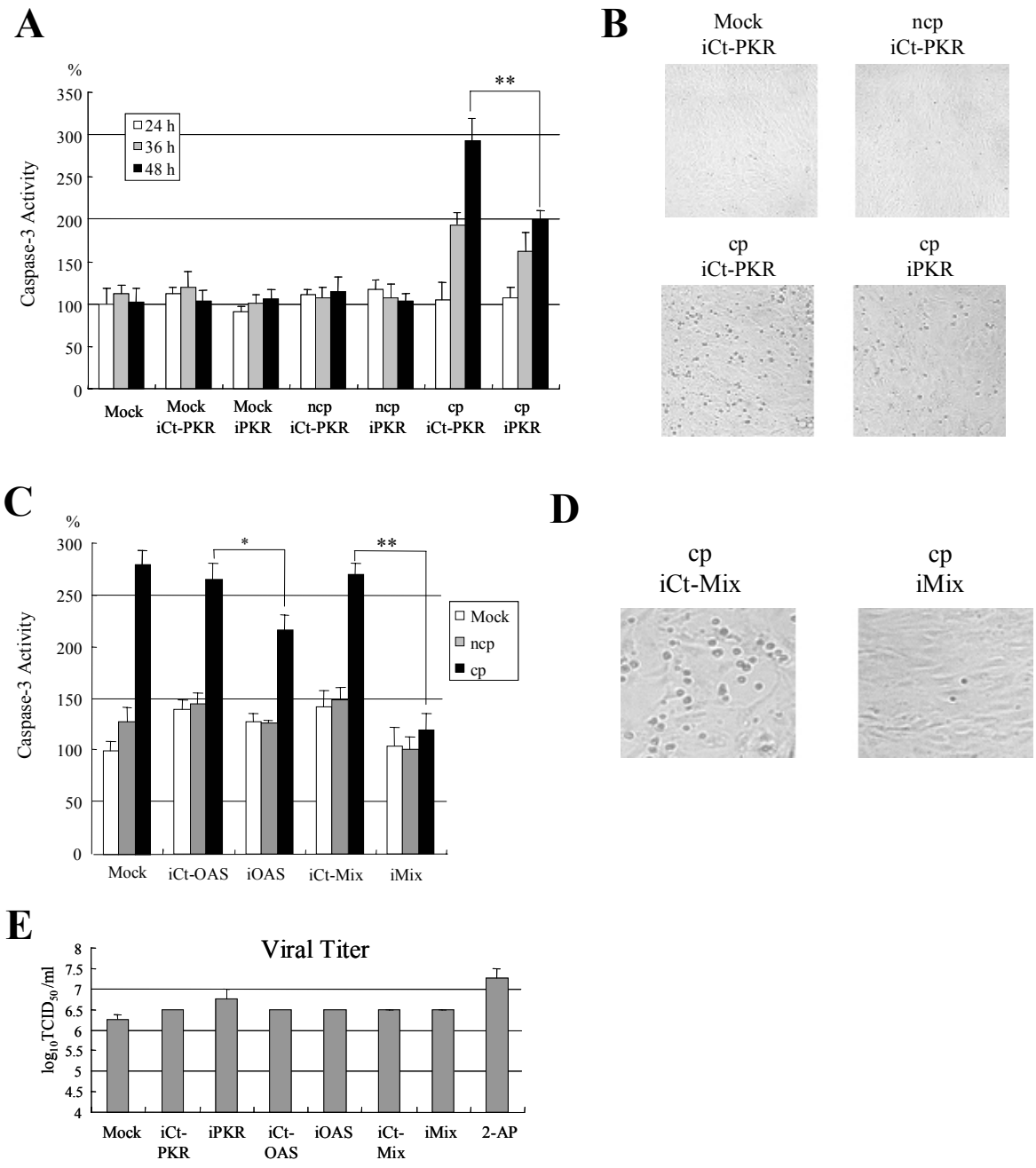

CHAPTER 3

The relationship between the viral RNA level and up-regulation of innate immunity in spleen of cattle persistently infected with bovine viral diarrhea virus

Veterinary Microbiology (2008) 129:69-79

Abstract

Persistent infection in cattle with BVDV may result in growth retardation and immunosuppression. *In vitro* infection with noncytopathogenic (ncp) BVDV has been shown to suppress interferon (IFN) responses, whereas ncpBVDV induces transient strong IFN responses *in vivo* following acute infection of naïve cattle. In this study, the innate immune response of the spleen, a crucial organ for immune system homeostasis, from PI cattle was analyzed. The transcription of five IFN- and apoptosis-related mRNAs (Mx1, iNOS, OAS-1, PKR, and TNFα), which was shown to be up-regulated in response to BVDV replication *in vitro* as shown in CHAPTERs 1 and 2, and the level of viral RNA were quantified using real-time RT-PCR. Up-regulation of Mx1, OAS-1, PKR, and TNFα mRNA expression was detected in the spleens of PI cattle regardless of their age, and induction of apoptosis was also up-regulated in the spleens of PI cattle compared with those of nonPI cattle. Although it cannot be excluded that the innate immune responses may be activated in response to any secondary infections in immunosuppressed cattle, the absence of any pathogenic microorganisms in the PI cattle and the statistically significant correlation between innate immune responses and the viral RNA level indicates that there may be a positive relationship between the increased level of viral RNA replication and up-regulation of innate immunity *in vivo*.

Introduction

PI calves develop lethal mucosal disease following superinfection with antigenically homologous cp BVDV (Brownlie *et al.*, 1984). Even in the absence of cp BVDV, PI cattle may suffer from growth retardation, severe diarrhea, neonatal mortality, and immunosuppression (Johnson & Muscoplat, 1973; Muscoplat *et al.*, 1973; Potgieter, 1995).

Previous *in vitro* studies of cells infected with BVDV have shown that ncp BVDV inhibits endogenous induction of type I IFN (Baigent *et al.*, 2002; Hilton *et al.*, 2006). In spite of the multiple mechanisms adopted by BVDV to evade IFN induction (Iqbal *et al.*, 2004; Nakamura *et al.*, 1995; Schweizer & Peterhans, 2001), acute ncp BVDV infection transiently induces strong IFN responses *in vivo* (Brackenbury *et al.*, 2005; Charleston *et al.*, 2002; Muller-Doblies *et al.*, 2004). However, the study regarding innate immune responses in PI cattle *in vivo* has been hardly carried out. In this study, the author focused on the spleen, a unique lymphoid organ that is important for innate and adaptive immune homeostasis (Mebius & Kraal, 2005), since the viral interaction with immune system seems to play an essential role in immunity to BVDV (Glew *et al.*, 2003; Howard, 1990). Accordingly, the author assessed the possible involvement of innate immunity in the *in vivo* mechanisms of pathogenesis of PI cattle.

Materials and methods

Animals. Twelve nonPI Holstein cattle between 2 and 24 months of age were obtained from National Institute of Animal Health (Tsukuba, Ibaraki, Japan). Twelve PI cattle of different breeds were found in various locations in Japan, and several organs of these cattle were kindly sent from Livestock Hygiene Service Centers (Table 1). The spleens were taken within 1 h after euthanasia, immediately frozen on dry ice, and transported to this laboratory. The nonPI cattle were confirmed to be free of the BVDV genome by reverse transcriptase-polymerase chain reaction **(**RT-PCR).

RNA Isolation. Samples were homogenized using a BioMasher (Nippi, Tokyo, Japan) as described in the manufacturer's protocol. Two milligrams of the homogenate was lysed, and then total RNA was extracted using the SV Total RNA Isolation System (Promega, Madison, WI, USA) according to the manufacturer's protocol.

Quantitative real-time RT-PCR. cDNA synthesis was performed with the ExScript RT Reagent Kit (TaKaRa, Shiga, Japan) according to the manufacturer's protocol. Cellular mRNA and viral RNA were quantified using Power SYBR Green PCR Master Mix (Applied Bio Systems, Warrington, UK) with 2 μl of reverse-transcribed cDNA. Quantitative real-time PCR was performed using the Thermal Cycler Dice System (TaKaRa). The temperature program was consisted of an initial denaturation step at 95°C for 10 min, followed by 45 cycles of 95°C for 15 sec, and 60°C for 30 sec. The primers used to amplify the bovine Mx1, iNOS, TNFα, PKR, and OAS-1 mRNAs and the viral RNA are shown in Table 2. In each run, 10-fold serial dilutions of each RNA sample were tested in duplicate to establish a standard curve for use in calculating the relative amount of each RNA species in the sample.

All samples were analyzed at least three times in duplicate. To confirm the specificity of each PCR product, a melting curve analysis was carried out immediately after the amplification phase of each PCR, and the size of each product was verified by 2% agarose gel electrophoresis. The level of each RNA species was normalized to the amount of GAPDH mRNA in each sample. The relative amount of each mRNA was analyzed using Thermal Cycler Dice Software Ver. 1.02 (TaKaRa).

Western blot analysis. Protein extracts were prepared from the spleens of cattle using a BioMasher (Nippi) according to the manufacturer's protocol. Equal amounts (6 μg) of proteins were separated by 10% SDS–PAGE and transferred onto nitrocellulose membranes (Amersham, Piscataway, NJ, USA). After blocking for 1 h in blocking buffer (0.1% Tween 20 and 5% non-fat milk in PBS), the membrane was incubated with primary chicken polyclonal antibody against OAS-1 (GenWay Biotech Inc., San Diego, CA, USA; diluted 1:3000 with PBS containing 1% BSA and 0.1% Tween 20) for 2 h. Horseradish peroxidase-conjugated rabbit anti-chicken IgG (diluted 1:5000 with PBS containing 2% non-fat milk and 0.1% Tween 20) was used as the secondary antibody. As a loading and transfer control, β-actin was detected using mouse anti-β-actin monoclonal antibody (1:3000 dilution; Chemicon International, Temecula, CA, USA) as the primary antibody and peroxidase-conjugated goat anti-mouse IgG (1:5000 dilution) as the secondary antibody. The protein bands were detected using the Enhanced Chemiluminescence (ECL) Detection Kit (Amersham).

Measurement of capsase-3 activity. Caspase-3 activity was detected using an ApoProbe-3 Kit (BioDynamics Laboratory Tokyo, Japan) as described in CHAPTER 1 with a minor

modification. In brief, after the spleen samples were homogenized using a BioMasher (Nippi), the homogenates were lysed in lysis buffer (50 mM Tris-HCl, pH 7.5, 150 mM NaCl, 1.0 mM EDTA, 1.0 mM Na_3VO_4, 50 mM NaF, and 1 mM DTT) supplemented with Complete Protease Inhibitor Cocktail (Roche Diagnostics, Tokyo, Japan). Three micrograms of each protein lysate were incubated with substrates for 30 min at 37°C, and the fluorescence liberated from the caspase-3-treated substrates was measured using a fluorometer equipped with 360 nm excitation and 460 nm emission filters.

DNA fragmentation assay. To detect characteristic apoptotic DNA ladders, spleen homogenates were resuspended in 100 μl of PBS and gently mixed with 300 μl of buffer containing 10 mM Tris-HCl (pH 7.6), 10 mM EDTA, and 0.6% SDS. The samples were then mixed with 100 μl of 5 M NaCl and incubated overnight at 4°C. After centrifugation at 14,000 rpm for 20 min at 4°C, the supernatants were treated with proteinase K (0.2 mg/ml) for 20 min at 37°C and then mixed with two volumes of ethanol and left overnight at –20°C. The precipitated DNA was treated with 1 μg of RNase A for 20 min at 37°C, then resuspended in TE buffer (10 mM Tris-HCl and 10 mM EDTA, pH 7.6) and visualized by 1.6% agarose gel electrophoresis.

Statistical analysis. Student's *t*-test was used to compare the PI and nonPI cattle, and P values < 0.05 were considered significant. Correlations between the expression levels of various cellular genes or between the levels of viral RNA and cellular gene transcripts were analyzed by Spearman's rank correlation coefficient.

Results

Identification of PI cattle.

PI cattle were identified by detecting BVDV genome from sera using RT-PCR, and the absence of BVDV-specific antibody (< 2) was also confirmed. Other specific pathogens, bacteria, viruses and parasites, were not isolated from these PI cattle. The genotypes of virus isolates from PI cattle were BVDV-1a or -1b, as determined by phylogenetic analysis of the 5'NCR sequences of isolates (Nagai *et al.*, 2004).

mRNA expression of Mx1, PKR, OAS-1, and TNFα is up-regulated in the spleens of PI cattle.

The author first assessed the mRNA expression levels of IFN- and apoptosis-related genes in spleens from 12 nonPI and 12 PI cattle (Table 1). The mRNA species quantified in this study were Mx1, iNOS, TNFα, PKR and OAS-1, which were found to be up-regulated in response to increased viral RNA replication *in vitro* as described in CHAPTERs 1 and 2. The quantity of mRNA in the spleens, expressed as units relative to the amount of GAPDH mRNA, and the median of the nonPI and PI groups are shown in Fig. 1.

The level of mRNA expression of all genes except *iNOS* was found to be significantly up-regulated in the PI cattle regardless of the infecting viral genotype, and the up-regulation of these IFN-stimulated genes (ISGs), *Mx1*, *PKR* and *OAS-1*, indicated an activation of type I IFN responses. Among these up-regulated ISGs, OAS-1 mRNA showed the highest induction with a median value of 34.5-fold, reaching a maximum of 150-fold, whereas the induction of PKR mRNA was up to 10-fold, with a median value of 3-fold (Fig. 1). However, no inductions of ISGs were detected in samples of asymptomatic PI cattle, PI-1 to 3. The level of iNOS mRNA in the PI cattle varied, and it was not significantly different from that in the

nonPI samples, indicating that iNOS was not transcriptionally up-regulated *in vivo*. Western blot analysis of OAS-1, whose promoter activity is primed via an IFN-stimulated response element (ISRE), was performed to assess the level of protein expression following mRNA up-regulation. In spleen samples from all symptomatic PI cattle (PI-4 to 12), OAS-1 was highly induced regardless of age or viral genotype, whereas neither nonPI cattle nor asymptomatic PI cattle (PI-1 to 3) expressed no or low levels of OAS-1 protein (Fig. 2). Interestingly, sample PI-12, in which the level of OAS-1 mRNA expression was found similar to that in the nonPI samples, also contained OAS-1 protein.

mRNA expression of PKR, OAS-1, and TNFα is significantly correlated with type I IFN responses.

Among the five IFN- and apoptosis-related genes quantified in this study, *Mx1*, *PKR*, and *OAS-1* are well-characterized effectors of type I IFN responses (Samuel, 2001). In particular, up-regulated *Mx* gene expression has been used as a sensitive indicator of active type I IFN responses (Fray *et al.*, 2001; Simon *et al.*, 1991). Thus the mRNA levels of four different genes (*iNOS, TNFα*, *PKR*, and *OAS-1*) were compared to that of *Mx1* to determine whether there was coordinated up-regulation by type I IFNs. As expected, a significant positive correlation was detected between Mx1 mRNA expression and that of OAS-1 and PKR (Fig. 3). On the other hand, although a direct connection between type I IFN and TNFα has not yet been defined, a significant correlation was found between them (Fig. 3). No significant correlation was found between the levels of mRNA expression for Mx1 and iNOS.

Correlation between the viral RNA level and type I IFN responses.

The author next quantified the viral RNA levels of each PI cattle. The value of PI-1,

whose viral RNA load was the minimum of all 12 PI cattle, is set at 1 and the fold differences were shown in Fig. 4A. Interestingly, viral RNA loads of asymptomatic PI cattle (PI-1 to 3) were relatively low among the PI cattle, and the highest amount of viral RNA in PI cattle reached to almost 10^4-fold (PI-5 and 6). Then the coordination between the viral RNA level (Fig. 4A) and mRNA expression of Mx1, OAS-1, PKR, and TNFα was examined. Significant correlations were found between the viral RNA level and mRNA expression of Mx1 and OAS-1, while there was no correlation between the viral RNA level and mRNA expression of PKR and TNFα (Fig. 4B).

Apoptosis in the spleens of PI cattle is correlated with the level of type I IFN responses and the accumulation of viral RNA.

The author examined whether apoptosis is induced in response to persistent BVDV infection *in vivo* by measuring the level of caspase-3 activity, and by the detection of characteristic apoptotic DNA ladders. Caspase-3 activity in the PI spleens was significantly elevated up to 6-fold, with a median score of 2.53-fold, compared to that in the nonPI spleens (Fig. 5A). Samples from asymptomatic PI cattle, PI-1 to 3 did not exhibit caspase-3 activities as well as apoptotic DNA ladders. Although spleen samples from PI cattle in which the cp strain was isolated (PI-9 to 11) did not show significantly elevated levels of caspase-3 activity, apoptotic DNA ladders were detected (Fig. 5B). The level of caspase-3 activity showed a significant positive correlation with the viral RNA level and with the mRNA expression of Mx1 and OAS-1 (Fig. 5C), implicating a positive relationship between viral RNA replication and the induction of apoptosis.

Discussion

The present data showed that in the spleen samples from all PI cattle except PI-1, in which extremely poor viral replication was found, IFN responses were induced regardless of age and the presence of cp BVDV. In contrast to previous *in vitro* studies demonstrating inhibitory effects of ncp BVDV infection against IFN responses, PI cattle exhibited strong IFN responses, which correlated with the level of viral RNA.

Since the *Mx* gene is tightly and specifically regulated by type I IFNs, up-regulation of *Mx* gene indicates the activation of the type I IFN pathway (Fray *et al.*, 2001; Simon *et al.*, 1991). The present data also showed a significant positive correlation between the transcriptional up-regulation of OAS-1 and PKR and that of Mx1, indicating that up-regulation of OAS-1 and PKR is in part attributable to the activation of a type I IFN response. Transcription of OAS-1 and PKR mRNA is driven by activation of ISRE promoter elements, which is activated upon binding with IFN-stimulated gene factor 3 (ISGF-3), a type I IFN-inducible transcription factor (Samuel, 2001; Ward & Samuel, 2003). However, different levels of transcription were found for the two factors (Fig. 1), and mRNA expression of OAS-1, but not PKR, was significantly correlated with the level of viral RNA. Unlike OAS-1, which is induced only via IFN-mediated ISRE, PKR is constitutively expressed (Barber *et al.*, 1993; Thomis *et al.*, 1992) via another promoter, the kinase-conserved sequence (KCS) element, which is activated independent of IFNs (Das *et al.*, 2006), although the elements of the bovine PKR promoter have not yet been determined. The inconsistent transcriptional regulation of OAS-1 and PKR may be due to IFN-independent regulation of PKR. It was rather surprising that persistent infection with ncp BVDV induced type I IFN responses, in contrast to previous results obtained *in vitro* (Baigent *et al.*, 2002; Hilton *et al.*, 2006; Schweizer & Peterhans, 2001). Brackenbury et al. (2005) reported that the cells that

produce type I IFN following an acute infection with ncp BVDV were negative for virus infection. Thus, it is speculated that the cells producing IFN in PI cattle might be uninfected cells that were stimulated via extracellular pathway.

Significant correlations between caspase-3 activity and the levels of viral RNA and Mx1 and OAS-1 mRNA were also found in this study, suggesting that the activation of type I IFN and subsequent ISRE-mediated transcriptional regulation are positively correlated with proapoptotic activity. Since the factors driven by ISRE promoter elements contain a variety of apoptosis facilitators (Chawla-Sarkar *et al.*, 2003), it seemed possible that expression of ISGs encoding proapoptotic factors contributed to the induction of apoptosis. The detection of significantly elevated caspase-3 activity in the splenic tissue of PI cattle, but not in that of nonPI cattle, suggests that apoptosis in PI cattle could influence the immune system and might be related in part to immunosuppression. The cell populations in the spleen, which are primed to exhibit antiviral responses and induce apoptotic cell death, must be identified in order to understand the immunological aspects of PI cattle. It is likely that up-regulation of ISGs was induced by the increased level of viral RNA replication detected in most of the symptomatic PI cattle, and that double-stranded RNA (dsRNA), a viral replication intermediate, stimulated apoptosis pathway through binding to dsRNA-reactive proapoptotic ISG products, PKR and OAS-1, as indicated in CHAPTER 2. However, PI cattle may suffer from secondary infections with respiratory or enteric pathogens. The author cannot completely exclude the possibility that the positive correlation between the viral RNA level and innate immune response is attributed to an increased susceptibility to secondary infections due to the immunosuppressive effect of BVDV, although it is unlikely since infection with other pathogenic microorganisms has not been found in the PI cattle. In either case, the present data suggested that the apoptosis and IFN-related pathways were activated in PI cattle

and might influence clinical outcome. Although the author focused on spleens in this study, increased IFN responses and viral replication were similarly detected in other organs, lung, liver and kidney of two PI cattle, although the number of sample was insufficient due to the limitation of the sort of organs obtained from PI cattle (data not shown). More detailed analyses of the immune responses and viral distribution among various organs and tissues are needed to understand the pathogenesis of persistent BVDV infections in further studies.

Figure legends

Figure 1. Relative Mx1, OAS-1, PKR, TNFα, and iNOS mRNA expression in spleens from nonPI (shaded bars) and PI cattle (striped bars). The values are presented as means ± S.D., and each value for nonPI-1, which exhibited representative value of nonPI samples, is set at 1. Summarized values for the nonPI and PI groups are shown in the graph on the right, and significant differences between the values for two groups were calculated. Median values are presented as bars. *, $P < 0.05$; **, $P < 0.01$; ***, $P < 0.001$.

Figure 2. OAS-1 protein expression in PI cattle. Spleen lysates from nonPI and PI cattle were examined by Western blot analysis for the presence of OAS-1 and β-actin, a loading control, as described in the Materials and methods. NonSp, nonspecific.

Figure 3. Correlation of relative Mx1 mRNA expression with relative OAS-1, PKR, and TNFα mRNA expression but not with relative iNOS mRNA expression. Units used for the relative expression levels for cellular mRNAs are the same as that used in Fig. 1. R, Spearman's rank correlation coefficient; NS, not significant.

Figure 4. (A) Relative viral RNA expression in PI cattle. The values are presented as means ± S.D., and the value for the viral RNA expression of PI-1 is set at 1. (B) Correlation of the relative level of viral RNA expression with the relative mRNA expression of Mx1 and OAS-1, but not with that of PKR and TNFα. Units used for the relative expression levels for cellular mRNAs and viral RNA are the same as that used in Fig. 1 and 4A, respectively. R, Spearman's rank correlation coefficient; NS, not significant.

Figure 5. (A) Relative caspase-3 activity in spleen lysates from nonPI (shaded bars) and PI (striped bars) cattle. As a negative control [(−)Ct; black bar], sample PI-8 was treated with AC-DEVD-CHO, a caspase-3-specific inhibitor, at room temperature for 5 min, followed by the procedure described in the Materials and methods. The values are presented as means ± S.D., and each value of nonPI-1 is set at 100%. Summarized values for the nonPI and PI groups are shown in the graph on the right, and significant differences between the values for two groups were calculated. Median values are presented as bars. The presence (+) or absence (–) of clinical symptoms and the isolation of the cp strain in the PI cattle is indicated below. **, $P < 0.01$. (B) Apoptotic DNA ladders from spleens of PI cattle. Nuclear DNA from the spleens of nonPI and PI cattle was isolated by SDS-high-salt extraction as described in the Materials and methods. Equal amounts of DNA were analyzed by gel electrophoresis followed by ethidium bromide staining. (C) Correlation of relative caspase-3 activity with the relative levels of viral RNA and Mx1 and OAS-1 mRNA expression, but not with the relative level of PKR mRNA expression. Units used for the relative expression levels for cellular mRNAs and viral RNA are the same as that used in Fig. 1 and 4A, respectively. R, Spearman's rank correlation coefficient; NS, not significant.

CHAPTER 3 Fig. 1

Mx1

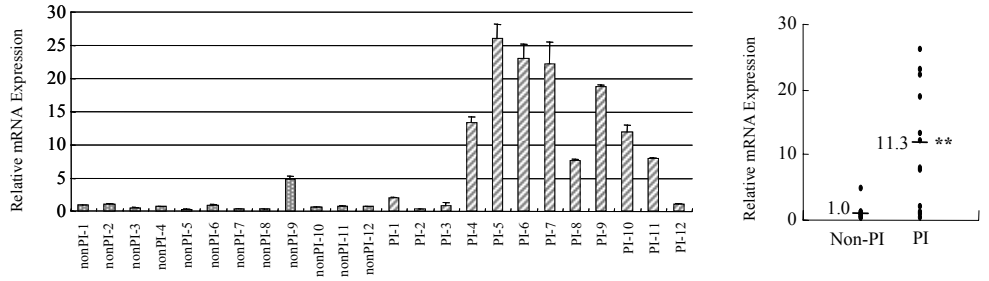

OAS-1

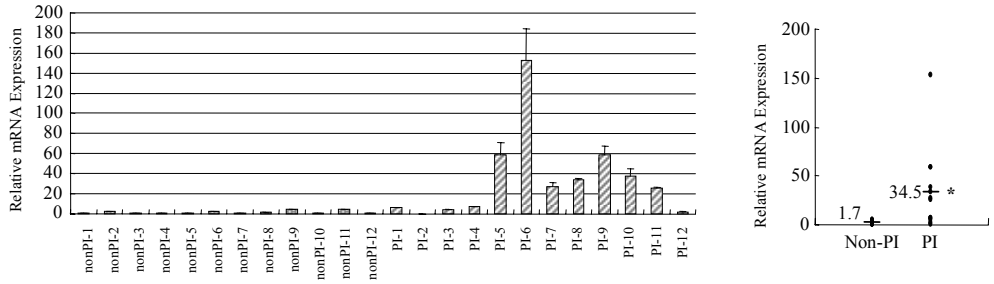

PKR

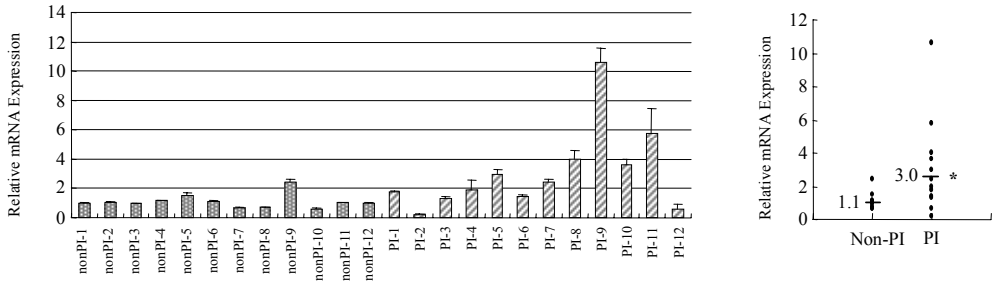

TNF-α

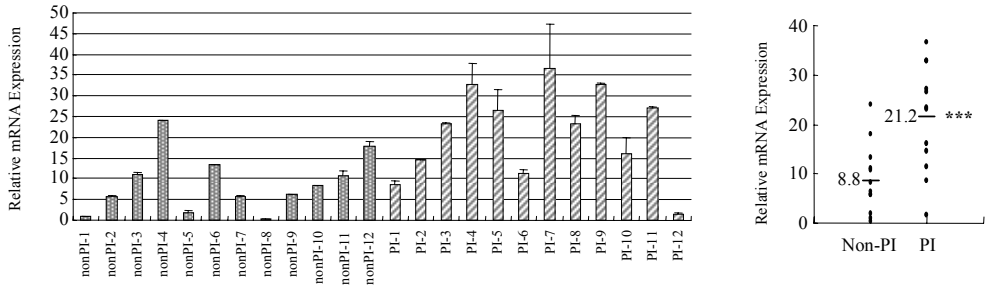

iNOS

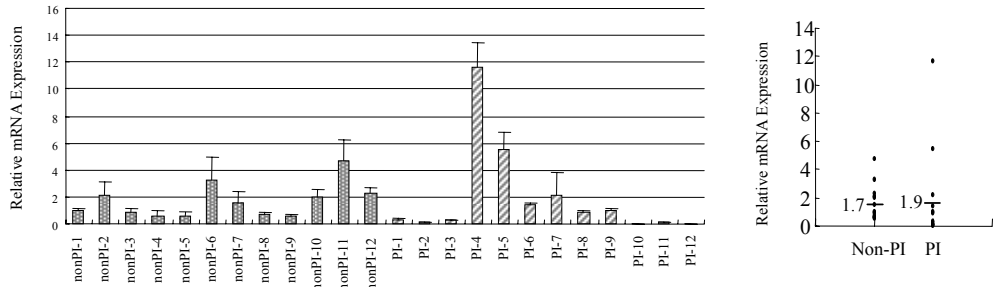

CHAPTER 3　Fig. 2

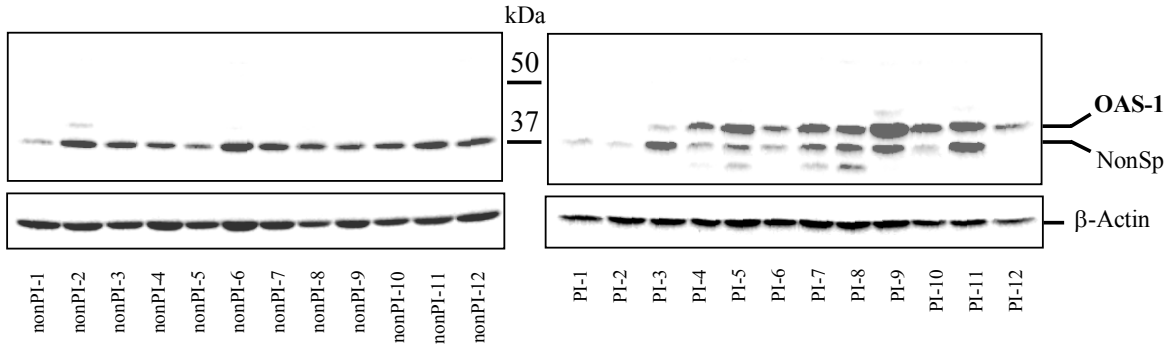

CHAPTER 3　Fig. 3

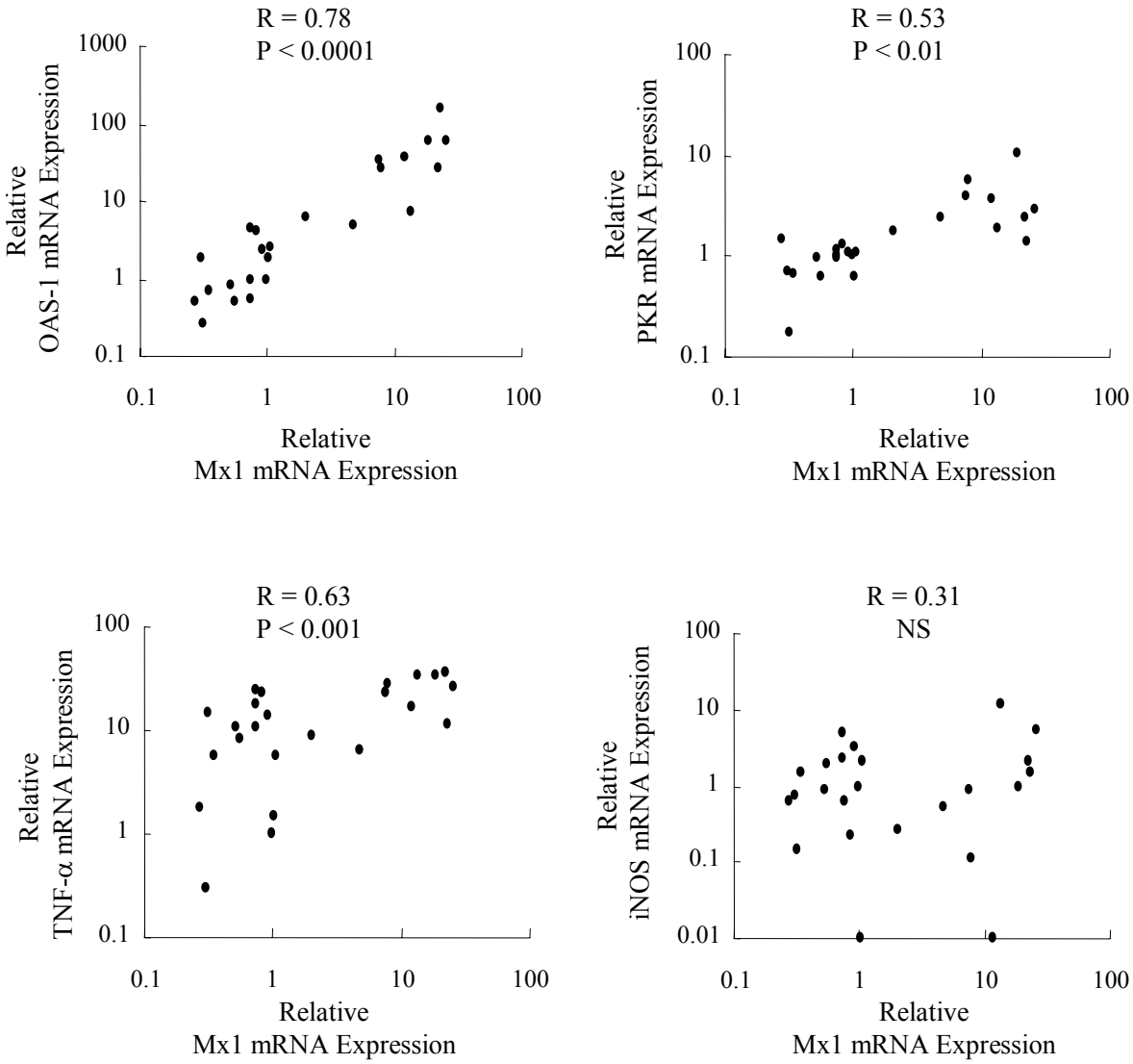

CHAPTER 3 Fig. 4

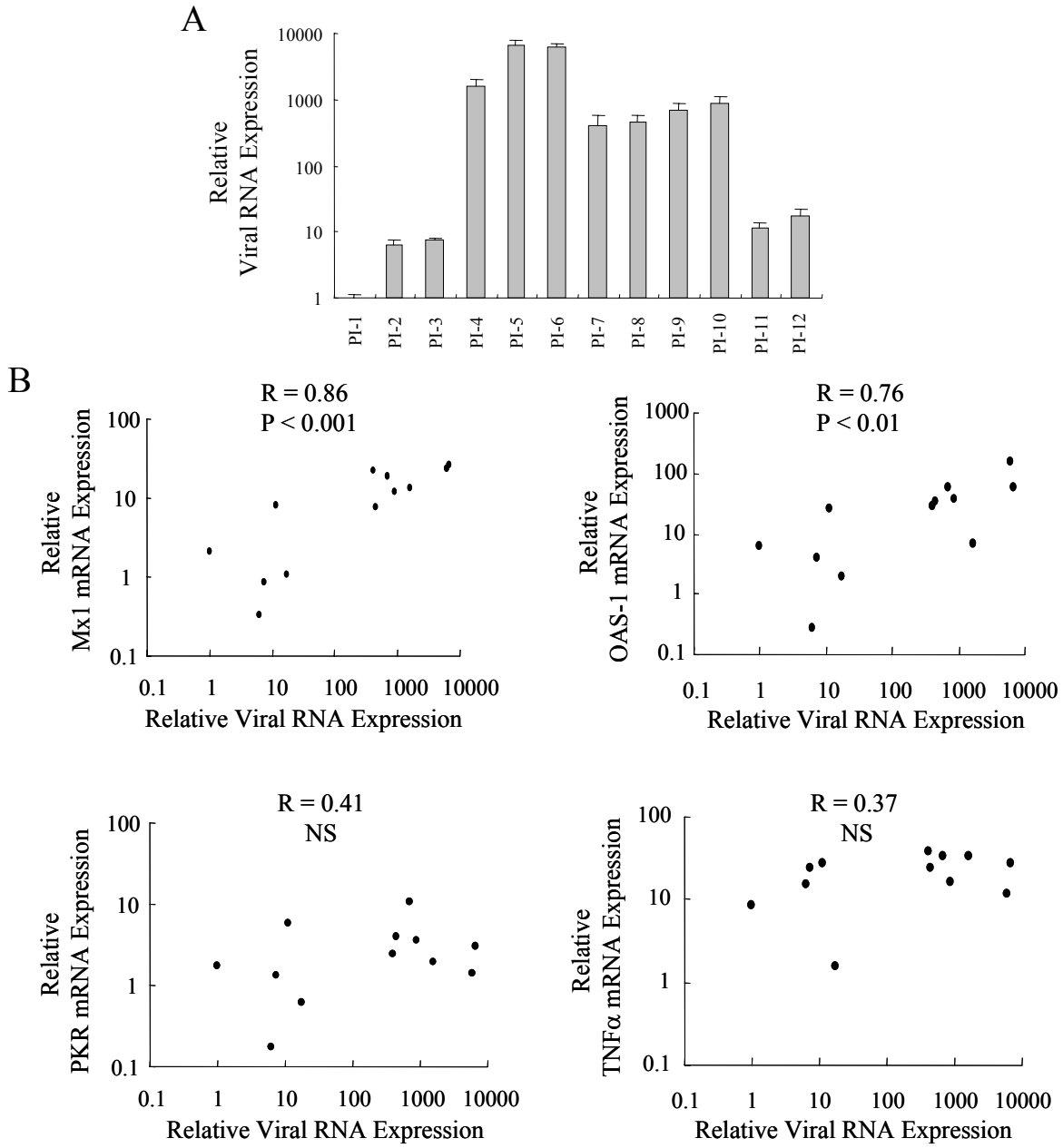

CHAPTER 3 Fig. 5

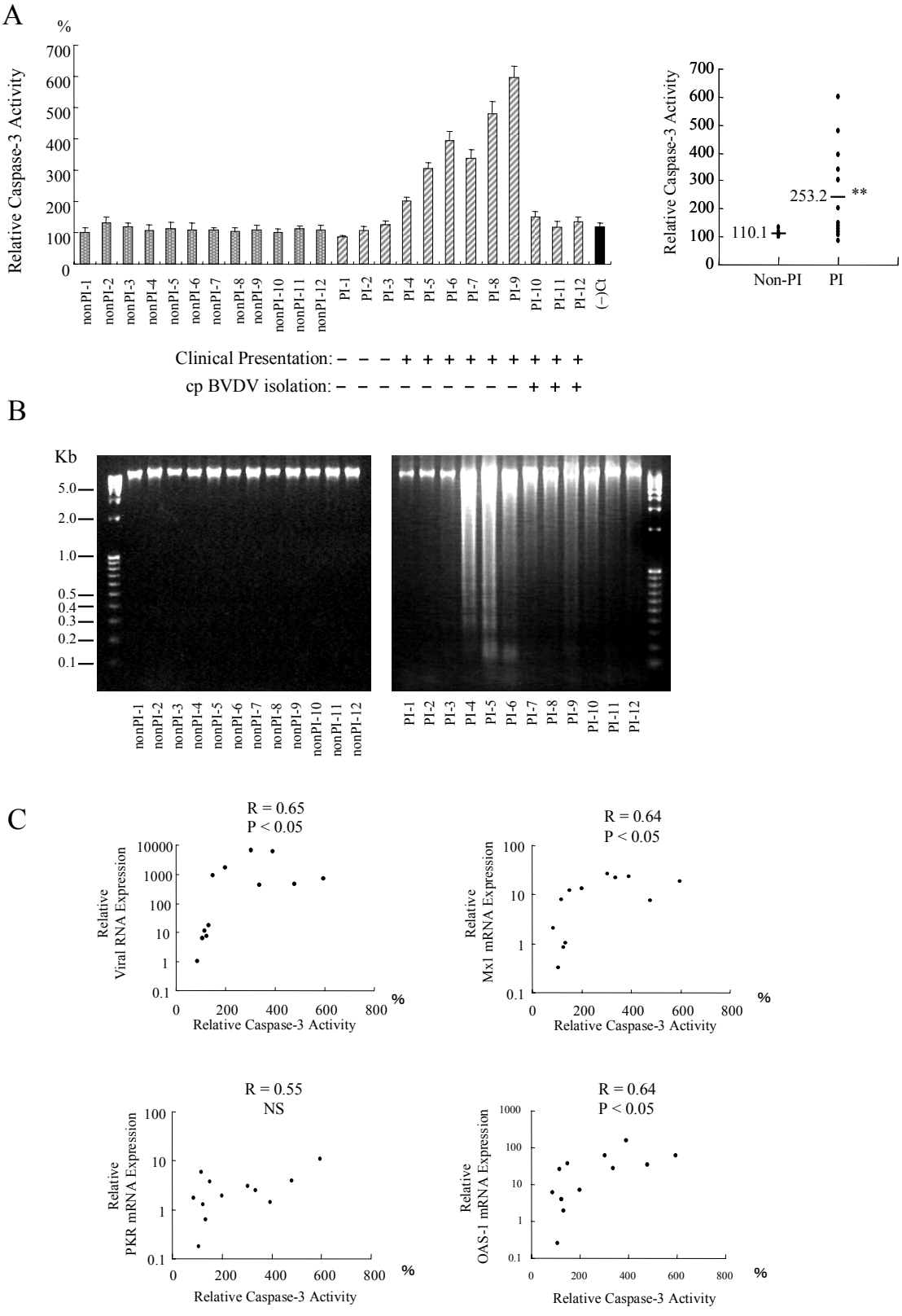

CHAPTER 3 Table 1

Table 1. nonPI- and PI cattle used in this study

Animal No.	Age (month)	Animal No.	Age (month)	Isolated Viral biotype, genotype		Clinical Presentation
nonPI-1	2	PI-1	3	ncp	1a	none
nonPI-2	2	PI-2	14	ncp	1a	none
nonPI-3	4	PI-3	17	ncp	1b	none
nonPI-4	5	PI-4	24	ncp	1a	growth retardation
nonPI-5	5	PI-5	11	ncp	1b	growth retardation, diarrhea
nonPI-6	23	PI-6	12	ncp	1b	growth retardation, mucosal hyperemia
nonPI-7	23	PI-7	4	ncp	1b	growth retardation, diarrhea
nonPI-8	23	PI-8	15	ncp	1b	growth retardation
nonPI-9	23	PI-9	2	ncp	1a	growth retardation
nonPI-10	23	PI-10	11	ncp & cp	1b	growth retardation, diarrhea
nonPI-11	24	PI-11	17	ncp & cp	1b	growth retardation, watery diarrhea
nonPI-12	24	PI-12	8	ncp & cp	1a	acute fever, watery diarrhea, died

CHAPTER 3 Table 2

Table 2. Primers Used for Real-Time PCR

Primer	Sequence 5'-3'	Product size (acc. No., Ref.)
GAPDH F (nt 110-128)	ATGATTCCACCCACGGCAA	122 bp, U85042
GAPDH R (nt 211-231)	ATCACCCCACTTGATGTTGGC	
Mx1 F (nt 1707-1727)	ATCTTTCAACACCTGACCGCG	88 bp, AF047692
Mx1 R (nt 1773-1794)	GGAGCACGAAGAACTGGATGAT	
TNFα F (nt 569-588)	CCTGGTACGAACCCATCTA	125 bp, NM_173966
TNFα R (nt 674-693)	ATCCCAAAGTAGACCTGCC	
iNOS F (nt 857-876)	TCACACAGCTGTGCATCGAC	140 bp, DQ676956
iNOS R (nt 977-996)	TTCCATGGGCACCTCGAGAA	
PKR F (nt 1039-1059)	GTTGGGATGGGCATGATTATG	150 bp, AB104655
PKR R (nt 1168-1188)	AACGTTTGTCTGGCTTCTTGC	
OAS-1 F (nt 135-155)	AGCCATCGACATCATCTGCAC	84 bp, NM_178108
OAS-1 R (nt 198-218)	CCACCCTTCACAACTTTGGAC	
BVDV F (5' NCR; 324)	ATGCCC(T/A)TAGTAGGACTAGCA	288 bp, Vilcek et al., 1994
BVDV R (5' NCR; 326)	TCAACTCCATGTGCCATGTAC	

CHAPTER 4

Oxidative stress induced by bovine viral diarrhea virus infection mediates activation of extracellular signal-regulated kinase in MDBK cells

Abstract

The efforts to identify the cellular signaling cascades triggered upon BVDV infection in MDBK cells revealed marked activation of the mitogen-activated protein kinase (MAPK), extracellular signal-regulated kinase (ERK) 1/2. Phosphorylation of ERK was detected following cp BVDV infection, and was shown to promote pro-survival and proliferative effects. The author also found that serum deprivation (SD) similarly triggered strong ERK phosphorylation. Because culture supernatants from treated MDBK cells could stimulate ERK phosphorylation in untreated cells, it appears that both SD and cp BVDV infection stimulate MDBK cells to release a factor that enhances ERK phosphorylation. The results in this study strongly suggest that this factor is a reactive oxygen species (ROS), because induction of oxidative stress by hydrogen peroxide treatment markedly enhanced ERK phosphorylation, and treatment with antioxidants inhibited ERK phosphorylation enhanced by supernatants from SD, cp BVDV infection and hydrogen peroxide treatment. Taken together, it is likely that ERK signaling is triggered by oxidative stress induced following cp BVDV infection and might be involved in the BVDV pathogenesis.

Introduction

Cellular protein kinases, such as extracellular signal-regulated kinase (ERK) or protein kinase B (Akt), play pivotal roles in cell signal transduction by facilitating the phosphorylation of many cellular substrates that regulate cell growth, differentiation, cell death and stress responses (Manning & Cantley, 2007; Shaul & Seger, 2007). However, the role of these signaling pathways in BVDV infection has not yet been extensively studied. The author therefore analyzed the activation status of these kinases in BVDV infected cells, and found that ERK signaling is activated exclusively in MDBK cells infected with cp BVDV. The author discusses the role of ERK phosphorylatoin in MDBK cells and the possible implications in the BVDV pathogenesis.

Materials and methods

Reagents. LY294002 and PD98059 were purchased from Cayman Chemical (Ann Arbor, MI, USA). N-acetylcysteine and tunicamycin were obtained from Sigma (St. Louis, MO, USA). Hydrogen peroxide (H_2O_2) and glutathione were from Wako (Osaka, Japan).

Cells and viruses. MDBK cell line was maintained in DMEM supplemented with 5% FCS at 37°C in a humidified 5% CO_2 atmosphere. Cells were confirmed to be free of BVDV by reverse transcriptase polymerase chain reaction (RT-PCR). BVDV strains KS86-1cp and KS86-1ncp have been described previously (Nagai *et al.*, 2003). Cells were infected with BVDV at a multiplicity of infection (MOI) of 5 for 1 h, washed twice with serum-free DMEM, and incubated in DMEM containing 5% FCS.

Western blot analysis. The cells were washed twice with PBS and harvested in lysis buffer (50 mM Tris-HCl pH 7.5, 150 mM NaCl, 1 mM EDTA, 1% Triton X-100, 20 mM NaF, 1 mM sodium orthovanadate) that was supplemented with Complete protease inhibitor cocktail (Roche Diagnostics, Tokyo, Japan). Equal amounts of protein (20 μg) from the lysates were separated by 10% SDS–PAGE and transferred onto nitrocellulose membranes (Bio-Rad). After blocking in blocking buffer (0.1% Tween 20 and 5% non-fat milk in PBS), the membranes were incubated with primary phospho-ERK or phospho-Akt-specific rabbit polyclonal antibody (Cell Signaling Technology, Berverly, MA, USA; diluted 1:1000 with PBS containing 1% BSA and 0.1% Tween 20), or monoclonal anti-KDEL (Stressgen, Victoria, Canada; 1:1000 dilution) or β-actin-specific antibody (Chemicon International, Temecula, CA, USA; 1:3000 dilution) as a loading control, followed by the incubation with

horseradish peroxidase-conjugated secondary antibodies (1:5000 dilution). The immunoreactive protein bands were detected by enhanced chemiluminescence (ECL) detection kit (GE Healthcare, Milwaukee, WI, USA).

MTS assay. Cell growth and viability was measured based on MTS assay using CellTiter 96 AQ_{ueous} One Solution Cell Proliferation Assay (Promega, Madison, WI, USA) according to the manufacturer's protocol.

Apoptosis assay

DEVDase activity assay was performed as described in CHAPTER 1.

Results and Discussion

MDBK cells were mock-infected or infected with the BVDV strains KS86-1cp or KS86-1ncp at a multiplicity of infection (MOI) of 5. After 18 h, cells were harvested and activation statuses of protein kinases, ERK and Akt, were analyzed by Western blotting, using phospho-ERK and phospho-Akt-specific antibodies. The phosphorylation level of Akt was unaffected following infection with either biotype of BVDV compared with that of mock-treated sample, but in contrast, phosphorylation of ERK was noticeably enhanced following cp BVDV infection (Fig. 1A). Subsequently, the kinetics of phospho-ERK expression was analyzed using cell lysates from cells at 6, 12, 18 and 24 h after infection with cp BVDV or ncp BVDV. The level of phospho-ERK was increased following cp BVDV infection between 18 and 24 h post-infection (p.i.). In mock- or ncp BVDV-infected cells, phosphorylation levels of ERK were attenuated in a time-dependent manner (Fig. 1B).

Because previous studies have shown that ERK is phosphorylated in response to numerous extracellular factors, such as epidermal growth factor (EGF), hepatocyte growth factor (HGF), nerve growth factor (NGF) or reactive oxygen species (ROS) such as H_2O_2 (Bhat & Zhang, 1999; Huang *et al.*, 2006; Jaramillo & Olivier, 2002; Nakagami *et al.*, 2000; Park *et al.*, 2005; Ramachandiran *et al.*, 2002; Xia *et al.*, 1995), the author tested whether culture supernatant from cp BVDV-infected cells was capable of inducing phosphorylation of ERK in uninfected cells. Cell culture supernatants from mock-, cp BVDV- or ncp BVDV-infected cells at 18 h p.i. were added to normally-maintained confluent MDBK cells. MDBK cells were harvested in lysis buffer at 5, 15, 30 and 60 min after addition, and then analyzed for phosphorylation of ERK by Western blotting. As shown in Fig. 1C, while supernatants from mock- and ncp BVDV-infected cells slightly stimulated phosphorylation of

ERK at 5 and 15 min after addition, supernatant from cp BVDV-infected cells stimulated robust and prolonged phosphorylation of ERK from 5 up to 30 min after addition. This result suggests that phosphorylation of ERK is enhanced by a factor that is released into the supernatant following cp BVDV infection.

Activation of ERK is well known to mediate survival and proliferation, however, several lines of evidence indicate that in several cell types, ERK signaling contributes to cell death *in vitro* as well as *in vivo* (Zhuang & Schnellmann, 2006). In addition, because apoptotic cell death is a hallmark of cp BVDV infection, the author sought to determine the effect of ERK phosphorylation on the induction of apoptosis in cp BVDV-infected MDBK cells. To do this, the author used PD98059, to inhibit MAPK kinase 1 (MEK1), the kinase that phosphorylates ERK. As a negative control, phosphorylation of Akt was inhibited with the phosphatidylinositol 3-kinase inhibitor, LY294002. After infection with BVDV at an MOI of 5 for 1 h, cells were incubated in the presence or absence of 5 μM PD98059 or 1 μM LY294002 for 24 h. In the presence of PD98059 or LY294002, phosphorylation of ERK or Akt, respectively, was confirmed to be specifically attenuated (Fig. 2C). Relative proliferation levels of the cells grown on a 96-well plate were measured by MTS assay. MDBK cells infected with cp BVDV exhibited the highest degree of proliferation, at more than 130% compared with mock-infected cells, and this effect was inhibited by treatment with PD98059, but not by LY294002. In contrast, ncp BVDV infection did not significantly affect the level of cell proliferation. Furthermore, because the data in CHAPTERs 1 and 2 showed that cp BVDV-induced apoptosis is mediated by activation of DEVDase, apoptotic induction levels were analyzed by measuring DEVDase activity as described in Materials and methods. In agreement with the result of the MTS assay (Fig. 2A), cp BVDV-infected cells treated with

PD98059 significantly increased DEVDase activity by up to 300% of control, whereas LY294002 treatment exhibited an increase of only 180%. In mock- or ncp BVDV-infected cells, treatment with these inhibitors resulted in a slight increase in DEVDase activity, up to a maximum of 150% (Fig. 2B). Collectively, it appears that up-regulated phosphorylation of ERK promotes cell survival and proliferation in cp BVDV-infected cells, and that the anti-proliferative effect of PD98059 in cp BVDV-infected cells appears to be the result of increased apoptosis.

To identify the factor that enhances phosphorylation of ERK following cp BVDV infection, the author tested whether various cellular stresses could result in increased phosphorylation of ERK. Infection with cp BVDV is known to induce a variety of cellular stresses, including oxidative and endoplasmic reticulum (ER) stresses (Baigent *et al.*, 2002; Jordan *et al.*, 2002; Schweizer & Peterhans, 1999). The author hypothesized that MDBK cells may activate survival signaling in an effort to counteract the cellular stress caused by cp BVDV. Therefore, MDBK cells were exposed to ER stress by treatment with 2 μg/ml tunicamycin, or oxidative stress by serum deprivation (SD) for 18 h. Specific induction of ER stress by tunicamycin treatment was confirmed by the detection of the commonly accepted ER stress marker, BiP/GRP78, by Western blotting (Fig. 3A). Marked induction of phospho-ERK was detected upon SD (Fig. 3A), but not upon ER stress. Time course analysis revealed that phospho-ERK levels peaked at 12 h after the onset of SD, and then decreased in a time-dependent manner (Fig. 3B, upper panels). In addition, the supernatant from serum-deprived MDBK cells possessed the capacity to induce phosphorylation of ERK in normally cultured cells (Fig. 3B, lower panels). To further examine whether cp BVDV infection and SD induce ERK phosphorylation in an oxidative stress-dependent mechanism,

the author used H_2O_2 to induce oxidative stress, and the antioxidants N-acetylcysteine (NAC) and glutathione (GSH) as a preventive measure against the induction of oxidative stress. As expected, incubation with H_2O_2 at various concentrations stimulated phosphorylation of ERK in a dose-dependent manner (Fig. 3C), and this effect was attenuated by the presence of NAC or GSH (Fig. 3D). In addition, ERK phosphorylation stimulated by addition of supernatant from cp BVDV-infected cells or the serum-deprived MDBK cells was reversed by supplementation with NAC or GSH (Fig. 3D). These findings support the hypothesis that oxidative stress is involved in ERK phosphorylation in cp BVDV-infected MDBK cells.

Activation of ERK has controversial roles in various cell types. Although phosphorylation of ERK is generally accepted to mediate pro-survival effects by inactivating the pro-apoptotic protein, Bad, and facilitating the expression of anti-apoptotic proteins (McCubrey *et al.*, 2007), several lines of evidences describe a role for ERK as a pivotal mediator of cell death in certain cell types such as oligodendrocytes (Bhat & Zhang, 1999), renal epithelial cells (Dong *et al.*, 2004; Ramachandiran *et al.*, 2002; Tikoo *et al.*, 2001), osteoblastic cells (Park *et al.*, 2005) and HeLa cells (Wang *et al.*, 2000). In addition, activation of ERK has been demonstrated to be involved in ROS-induced chemokine gene inductions in macrophages, via ERK-dependent formation of an essential transcriptional complex composed of NFκB, AP-1 and CREB (Jaramillo & Olivier, 2002). Collectively, oxidative stress-induced ERK activation appears to culminate in a variety of effects, including survival, inflammation, and death, depending on the cell type. Oxidative stress has been shown to mediate the disruption of cell metabolism, a process that is implicated in the liver pathogenesis associated with chronic Hepatitis C virus infection (Miura *et al.*, 2008). Therefore, the unusual stimulation of ERK signaling in response to oxidative stress revealed

in this study may account for the pathogenic effects caused by cp BVDV infection. Accordingly, it is important to identify the trigger for oxidative stress and the downstream effectors of ERK activation in cp BVDV-infected cells, in order to better understand the detailed mechanisms that underlie the proinflammatory responses and tissue injury associated with BVDV infection.

Figure legends

Figure 1. Activation of ERK in cp BVDV-infected cells. (A) MDBK cells were mock-infected or infected with either cp or ncp BVDV at an MOI of 5, collected at 18 h p.i., and expression levels of phospho-Akt or phospho-ERK analyzed by Western blot analysis. (B) The kinetics of phospho-ERK expression at the indicated time points p.i. (C) Culture supernatants obtained from mock-infected or either cp or ncp BVDV-infected cells at 18 h p.i. were added to normally maintained MDBK cells for the indicated periods and analyzed by Western blot analysis for ERK phosphorylation.

Figure 2. Effect of ERK phosphorylation on cell proliferation and apoptosis. (A) MDBK cells were infected with cp or ncp BVDV at an MOI of 5 for 1 h, and incubated in the presence of either 10 μM PD98059 (PD) or 1 μM LY294002 (LY). The cells were analyzed for proliferation by MTS assay at 24 h p.i. (B) MDBK cells treated as described in panel A were harvested and lysed at 18 h p.i. and analyzed for DEVDase activity. (C) Phosphorylation levels of ERK or Akt, respectively, in the presence of PD or LY, were detected by antibodies specific for phospho-ERK or phospho-Akt by Western blot analysis. *P*-values were determined using Student's *t*-test. *, $P < 0.01$.

Figure 3. ERK activation is mediated by oxidative stress. (A) ERK phosphorylation is triggered by serum deprivation (SD), but not by ER stress. MDBK cells were serum-deprived or treated with 3 μg/ml of tunicamycin for 24 h, and subjected to Western blotting using anti-phospho-ERK, anti-KDEL or anti-β-actin antibodies. (B) The kinetics of ERK phosphorylation during SD. Cells were harvested and analyzed for phospho-ERK expression

at the indicated time points after onset of SD (upper panels). Normal MDBK cells were incubated with the supernatant from serum-deprived MDBK cells obtained after 18 h of SD for 5, 15, 30 and 60 min (lower panels). The cells were harvested and analyzed by Western bloting for phospho-ERK expression. (C) Activation of ERK by hydrogen peroxide (H_2O_2). MDBK cells were incubated with various concentrations of H_2O_2 for 15 min and analyzed for phospho-ERK expression. (D) ERK phosphorylation induced by the factor released into the supernatant following infection with cp BVDV or SD is prevented in the presence of antioxidants. MDBK cells were pre-treated with or without 15 mM GSH or 15 mM NAC for 1 h, and incubated with culture supernatant from mock-infected cells, cp BVDV infected cells at 18 h p.i., serum-starved cells (SD), or cells treated with 500 μM H_2O_2. After incubation for 10 min, cells were washed, lysed and analyzed for phospho-ERK expression by Western blot analysis.

CHAPTER 4 Fig. 1

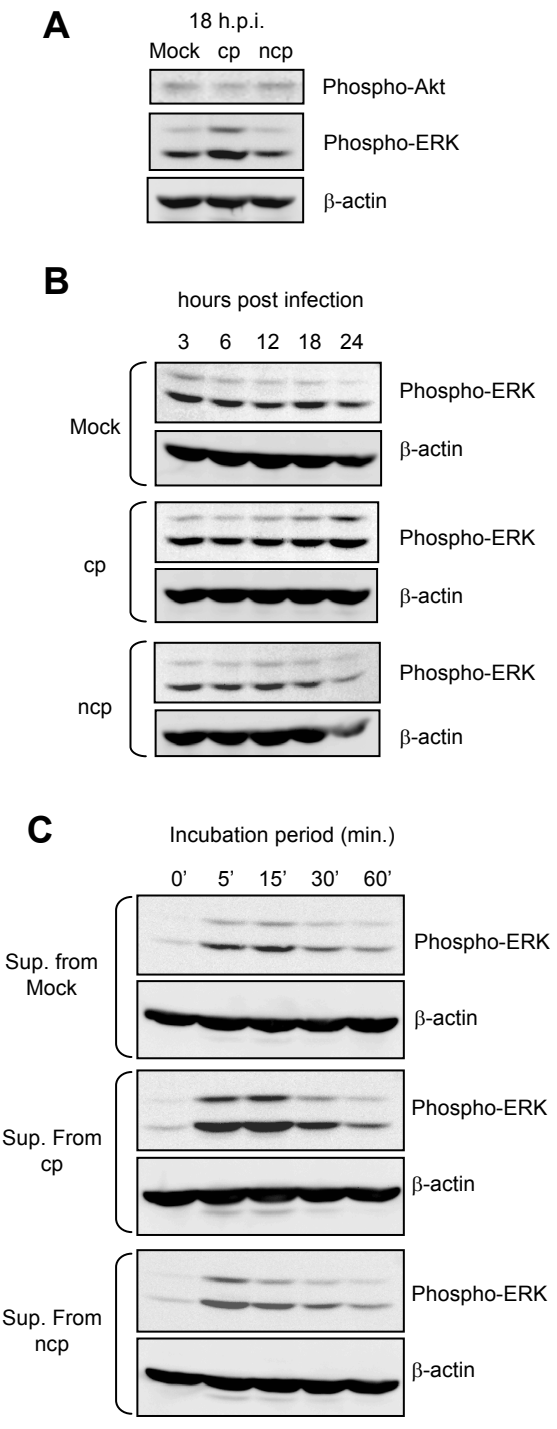

CHAPTER 4 Fig. 2

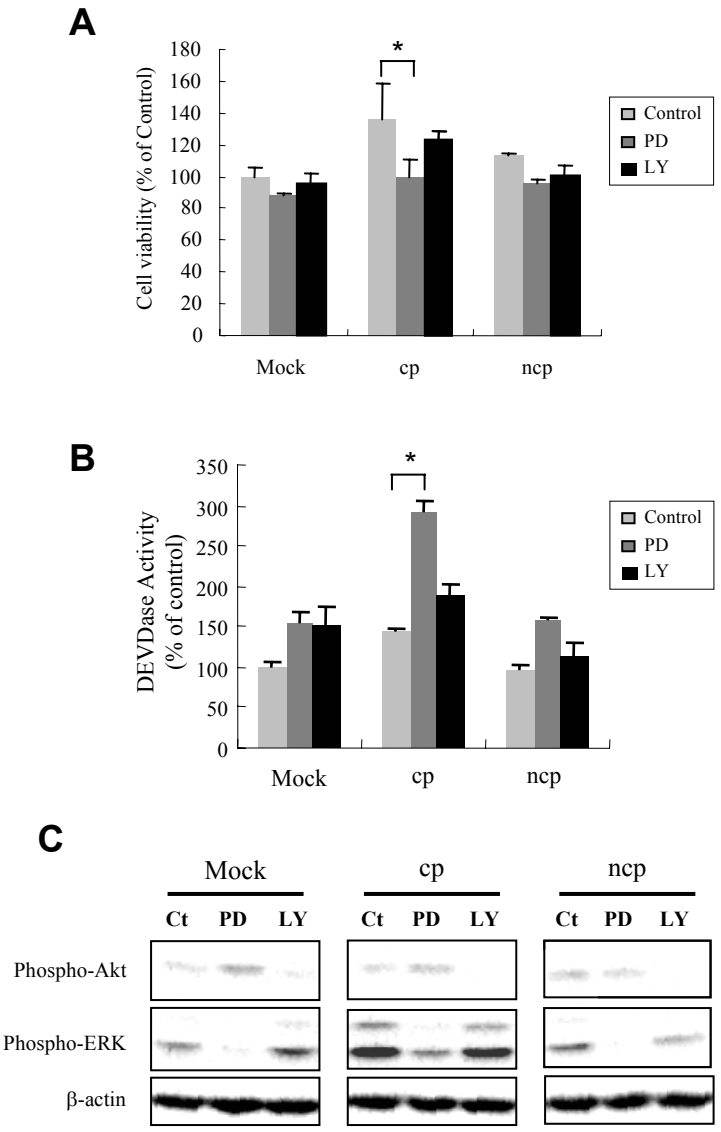

CHAPTER 4 Fig. 3

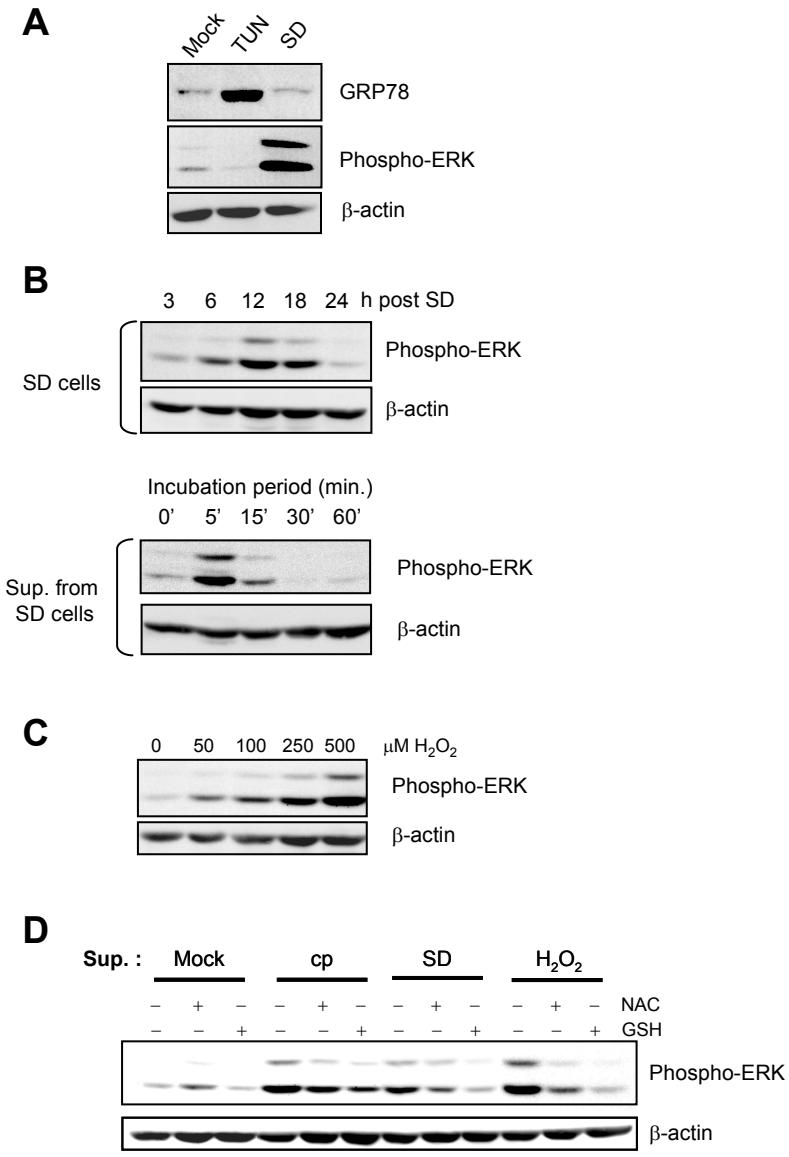

CHAPTER 5

Microarray analysis reveals distinct signaling pathways transcriptionally activated by infection with bovine viral diarrhea virus in different cell types

Abstract

The author performed microarray analysis of BVDV-infected Madin-Darby bovine kidney (MDBK) epithelial cells and bovine fetal muscle (BFM) fibroblast cells. Infection of both cell types with cp BVDV, but not ncp BVDV, stimulated marked up-regulation of numerous genes belonging to diverse functional classes. However, the pattern of gene expression detected in both cell types was highly distinct from each other. Notably, upon cp BVDV infection, BFM cells exhibited marked induction of IFN-stimulated genes (ISGs), whereas MDBK cells characteristically up-regulated endoplasmic reticulum stress-inducible genes, such as tribbles homolog 3, CHOP and asparagine synthase, and showed much weaker induction of ISGs than BFM cells. This study highlights unexpected diversity in the response of different cell types to BVDV infection.

Introduction

Thus far, cell signaling pathways affected by BVDV infection have not been studied in detail, due to the lack of sufficient tools for analyzing expression of bovine genes. However, in recent years, microarray technology has been developed for assessing expression profiles of bovine genes. Using bovine microarrays, the author screened for genes whose expression was significantly changed in Madin-Darby bovine kidney (MDBK) epithelial cells and primary bovine fetal muscle (BFM) fibroblast cells upon BVDV infection. MDBK and BFM cells were used as both cells yield high BVDV titers and induce severe CPEs upon cp BVDV infection. The author identified expression changes in numerous genes involved in cellular responses such as apoptosis, chemokine/cytokine production, immunomodulation, antiviral response, and metabolism. Unexpectedly, highly distinct patterns of genes were found to be affected by BVDV infection between MDBK and BFM cells, indicating considerably different cellular responses to BVDV infection in both cell types.

Materials and methods

Cells and viruses. BFM and MDBK cells were maintained as described in CHAPTER 1 and 4, respectively. BVDV strains KS86-1cp and KS86-1ncp (genotype 1) were used to infect the cells. MDBK and BFM cells were infected with BVDV at a multiplicity of infection (MOI) of 5 for 1 h, washed twice with FCS-free DMEM, then incubated with DMEM containing 5% and 10% FCS, respectively. Endpoint viral titration was performed with four replicates on MDBK cells and the 50% tissue culture infective dose ($TCID_{50}$) determined as described previously (Lackner *et al.*, 2004).

Preparation of total RNA. At 24 h p.i., total RNA for DNA microarray analysis was extracted using SV Total RNA Isolation System (Promega, Madison, WI, USA) as described in CHAPTER 3.

Construction of bovine microarray. A total number of 39,753 probe sets, each consists of nine different 60-mer oligonucleotide probes for each bovine gene, were designed by Roche Diagnostics K.K. based on the data from GenBank. The bovine array was synthesized using the MAS (Roche Diagnostics K.K.) developed as described previously (Singh-Gasson *et al.*, 1999), and contained 356,598 probes.

DNA microarray analysis. Sample labeling, hybridization, and microarray analysis were performed by Roche Diagnostics. Total RNA was first converted to double-stranded cDNA, followed by the synthesis of biotin-labeled cRNA using *in vitro* transcription as previously described (Eberwine *et al.*, 1992; Nuwaysir *et al.*, 2002). cRNA was then purified and fragmented to an average size of 50 to 200 bp. Hybridizations were performed with single

cRNA derived from one biosource (one-color hybridization). The expression level of each bovine gene was calculated by averaging the intensity of signals from nine different probes. The signals between each array were normalized using Robust Multichip Analysis normalization (Irizarry *et al.*, 2003a; Irizarry *et al.*, 2003b). NANDEMO Analysis 1.0.1 software (Roche Diagnostics) was used for further expression analysis. Student's t-test for analyzing the mean log ratios of two samples was applied as a rigorous criterion for significantly changed signal intensity. Changes with $P < 0.05$ were considered statistically significant. It is important that although the array contains 39,753 probe sets, most of the genes are represented by more than one probe set. These arrays also contain some annotative redundancies (a single gene often has several names or GenBank accession numbers corresponding to it). These redundancies were removed and a value of the most significant *P* value was selected when the genes affected by infection were classified into functional classes.

Quantitative real-time RT-PCR. RNA samples used for real-time PCR were prepared from independent cell cultures from those for microarray analysis. cDNA synthesis was performed with PrimeScript RT Reagent Kit (TaKaRa) according to the manufacturer's protocol. The primers used to amplify bovine glyceraldehyde-3-phosphate dehydrogenase (GAPDH), myxovirus resistance-1 (Mx1), 2'-5' oligoadenylate synthetase 1 (OAS-1) and double-stranded RNA (dsRNA) -dependent protein kinase (PKR) mRNAs were described in CHAPTER 3, and those used for bovine beta nerve growth factor (βNGF), C/EBP-homologous protein (CHOP), interleukin 8 (IL-8), tumor necrosis factor (TNF) -related apoptosis-inducing ligand (TRAIL), tribbles homolog 3 (TRB3), Viperin and X-linked inhibitor of apoptosis protein-associated factor-1 (XAF-1) mRNAs are listed in Table 1. Cellular mRNA was

quantified using Power SYBR Green PCR Master Mix (Applied Bio Systems, Tokyo, Japan) and normalized to the amount of GAPDH mRNA as described in CHAPTER 3.

Western blot analysis. Cells were washed twice with PBS, and harvested in lysis buffer (50 mM Tris-HCl pH 7.5, 150 mM NaCl, 1 mM EDTA, 1% Triton X-100, 20 mM NaF, 1 mM sodium orthovanadate) supplemented with Complete protease inhibitor cocktail (Roche Diagnostics). Lysates (20 μg) were separated by 8% SDS–PAGE and transferred onto nitrocellulose membranes (Bio-Rad, Hercules, CA, USA). After blocking with PBS containing 0.1% Tween 20 and 5% non-fat milk, the membranes were incubated with primary monoclonal antibody against BiP/GRP78 (Stressgen, Victoria, Canada) or against β-actin (Chemicon International, Temecula, CA, USA), or rabbit polyclonal antibody against NS3 in PBS containing 1% BSA and 0.1% Tween 20 for 2 h, followed by incubation with horseradish peroxidase-conjugated secondary antibodies (diluted 1:5000 with PBS containing 2% non-fat milk and 0.1% Tween 20). The immunoreactive protein bands were detected by enhanced chemiluminescence (ECL) detection kit (GE Healthcare, Milwaukee, WI, USA).

Apoptosis assay. DEVDase activity assay was performed as described in CHAPTER 1. Fluorescent AMC product formation was measured by reading samples in a fluorometer equipped with 360 nm excitation and 460 nm emission filters.

Results and Discussion

Differential cellular gene expression in cp or ncp BVDV-infected cells.

Infection of confluent MDBK and BFM cells with cp BVDV resulted in obvious CPEs at 48 h p.i. as shown in CHAPTER 2. As CPE is observed at a late time point p.i., it is conceivable that various cytokine productions triggered by BVDV infection would be involved in induction of cell death. The data in CHAPTER 2 demonstrated that viral RNA levels showed a marked increase by 24 h p.i., therefore, this time point was selected to analyze the cellular signaling pathways affected by BVDV replication and probably by proinflammatory cytokines. At 24 h p.i., both BFM and MDBK cells produced similar yields of infectious virion in the supernatants (Fig. 1A). Total RNA was extracted from the cells for use in DNA microarray analysis. Among the values obtained from 39,753 probe sets, filtered data with a maximum t-test *P* value < 0.05 were selected, and comparisons were made between the data from infected samples and a mock-infected control. Scatter plots clearly showed that infection with cp BVDV induced marked up-regulation of numerous genes in both cells, whereas that with ncp BVDV caused relatively subtle changes in gene expression (Fig. 1B). The number of genes up-regulated >8-fold by cp BVDV infection in BFM and MDBK cells were 374 and 58, respectively, whereas the number up-regulated by ncp BVDV infection were only 1 and 3, respectively (Table 2).

Independent confirmation of microarray data by real-time PCR.

The author selected 10 genes whose expression was identified as significantly affected by BVDV infection in the microarray analysis. The genes were selected to represent a wide range of expression patterns and fold changes (FCs) from diverse functional classes (Table 3). Although the microarray data presented in this study are based on a single array for each

virus-cell combination, values from real-time PCR agreed with them, supporting the authenticity of microarray data. But in detail, values of Viperin, TRAIL and OAS-1 in cp BVDV-infected BFM cells obtained from real-time PCR analysis were 20, 10 and 3-fold more than that from microarray analysis. Discrepancy was found only for OAS-1 level in MDBK cells infected with ncp BVDV, which showed 11-fold expression in the microarray analysis whereas no significant change was detected by real-time PCR analysis.

Pathways affected by BVDV infection.

Because infection with cp BVDV, in contrast to infection with ncp BVDV, markedly altered the expression levels of numerous genes (Fig. 1B), the author addresses the possible implications of gene expression changes in each signaling pathway, primarily focusing on the alterations caused by cp BVDV. Genes of known functions whose expression changes were >5-fold following cp or ncp BVDV infection were listed in Table 4. In some cases, genes that perform critical functions belonging to the respective category were added. Additionally, the most highly up-regulated thirty genes by infection with either cp or ncp BVDV in both cells were listed in Tables 5 to 8.

IFN-inducible pathways.

It is well established that infection by cp BVDV, but not by ncp BVDV, results in induction of IFN in cell cultures as shown in CHAPTER 2 and by Baigent et al. (2002). In agreement with these facts, microarray analysis detected the expression of numerous IFN-stimulated genes (ISGs) in BFM fibroblast cells infected with cp BVDV. Among them, expression levels of Viperin, Mx1, IFI44 and IFIT2 were prominent, reaching more than 1000-fold more than that in mock-infected cells. Importantly, real-time PCR analysis detected

an approximately 30,000-fold up-regulation of Viperin in cp BVDV infected cells (Table 3). Among these 4 factors that mediate antiviral responses, it is noteworthy that expression of Viperin has been demonstrated to efficiently inhibit the replication of hepatitis C virus (HCV), a close relative of BVDV, both *in vitro* and *in vivo* (Helbig *et al.*, 2005; Jiang *et al.*, 2008). In agreement with the study in CHAPTER 2, three ISGs, Mx1, PKR and OAS-1, showed high values in cp BVDV-infected BFM cells in this microarray analysis. The microarray data also revealed the previously unobserved induction of antiviral factors, such as GBP4, TRIM5, IRF-10 and BST-2, in cp BVDV-infected cells. It will be important to unravel the roles of these factors in BVDV replication in further studies. Unexpectedly, in contrast to BFM cells, MDBK cells infected with cp BVDV exhibited only a limited number of ISG inductions, such as OAS-1, Mx1, Viperin and RANTES, with approximately 100-fold lower levels than those observed in BFM cells, suggesting the presence of poor IFN responses in MDBK cells. A previous study that screened gene expression in cp BVDV-infected MDBK cells using differential display-PCR technique did not detect expression of IFN-inducible genes (Risatti *et al.*, 2003). This supports the observation that MDBK cells exhibit a weak IFN response. In contrast, ncp BVDV infection resulted in weak ISG inductions in both BFM and MDBK cells. These results indicate that ncp BVDV establishes persistent infection without triggering strong IFN responses, even though it does not completely disrupt them.

IFN mediators and TLRs.

Since strong IFN responses were observed in BFM cells, the author sought to compare the expression levels of genes involved in mediating IFN regulatory pathways. Viral RNA is recognized intracellularly by the RNA helicases RIG-I and MDA-5, and extracellularly by TLR-3, 7 and 8, to initiate innate immune responses. Subsequently, the downstream effectors,

IRF-3, IRF-7, TBK1 and IKKε mediate IFN-α and β production (Thompson & Locarnini, 2007). MDA-5 has been shown to be directly up-regulated by IRF-3, whereas RIG-I up-regulation requires IFN-β signaling through IKKε (Yount *et al.*, 2007). Striking up-regulation of MDA-5 and RIG-I (150-fold and 10-fold, respectively), and moderate increase in IRF-3 and IKKε expression (approximately 2-fold) was observed in BFM cells infected with cp BVDV. In addition, a cytosolic RNA helicase that functions as negative regulator of IFN induction, LGP2 (Yoneyama *et al.*, 2005), was found to be up-regulated by approximately 60-fold. In contrast, ncp BVDV infection in either cell type did not result in marked induction of these mediators, presumably due to an absence of strong IFN responses. Given the significant up-regulation of positive regulators of the IFN response following cp BVDV infection, it appears that IFN responses in BFM cells are amplified in a positive feedback loop, primarily by the expression of MDA-5 and RIG-I. Among the TLRs, TLR-1 to 6 were increased in cp BVDV-infected BFM cells, whereas only TLR-2 and 9 were moderately up-regulated in cp BVDV-infected MDBK cells. Although both TLR-7 and 8 are known as important sensors that trigger innate immune responses against viral infections, their expression levels were not affected by BVDV infection. Interestingly, TLR-5, which recognizes flagellin to initiate innate immune responses (Smith & Ozinsky, 2002), exhibited the strongest up-regulation (30-fold), suggesting that cp BVDV infection may enhance responsiveness to bacterial infection. Further, up-regulated expression of TLR-3, which recognizes dsRNA, a replicative intermediate of viral RNA, may also contribute to the positive feedback loop of IFN response against viral RNA replication in cp BVDV-infected BFM cells.

Ubiquitin-Proteasome System.

ISGs include a number of genes involved in the ubiquitin-proteasome system that play essential roles on the degradative pathway. Indeed, genes related to this pathway, ISG15, UBE1L, LMP-2 and LMP-7, were up-regulated exclusively in cp BVDV-infected BFM cells by 289, 24, 37, and 16-fold, respectively. Notably, induction of ISG15 and its E1-conjugate enzyme, UBE1L, are known to lead to the conjugation of ISG15 to cellular proteins (Loeb & Haas, 1992). Although how this conjugation acts in an antiviral function has not been elucidated, ISG15 conjugation is likely to be an important part of the antiviral response mediated by IFNs. Further functional studies are required to determine the role of the ubiquitin-proteasome system in BVDV infection.

Chemokines/Cytokines.

Upstream activators of IFN responses overlapped with that of NFκB (Hiscott, 2007), and indeed, cp BVDV infection leads to activation of NFκB (Baigent *et al.*, 2002). Expression of various IFN-inducible (RANTES, IL-6, etc) as well as NFκB-inducible (IL-6, 8, 15 and 17, GRO-α, β and γ, CCL20, IP-10 etc.) chemokines and cytokines was observed in cp BVDV-infected BFM cells. Following cp BVDV infection, BFM and MDBK cells up-regulated 25 and 6 genes classified as chemokines/cytokines, respectively. Most of the induction levels of chemokines/cytokines in MDBK cells were lower than those in BFM cells, but interestingly, an up-regulation of approximately 50-fold was found for IL-8 in both cells, which was confirmed by real-time PCR analysis (Table 3). These data suggest that cp BVDV infection triggers expression of diverse proinflammatory chemokines/cytokines in BFM cells, while a number of these genes are limited in MDBK cells. In contrast, ncp BVDV infection affected few genes in either cell type. Because cellular proinflammatory responses such as production of chemokines/cytokines are implicated in the BVDV pathogenesis of MD

(Bielefeldt-Ohmann, 1995), cell types such as fibroblasts may be involved in the disease progression.

Immunomodulation/Cell adhesion.

ISGs induced by cp BVDV infection in BFM cells include genes involved in immunomodulation, such as MHC class I and II, and complement components that are crucial for antigen processing and presentation (Chawla-Sarkar *et al.*, 2003). Most increased was CD83, an NFκB-inducible gene that possesses immune stimulatory capacity and is the maturation marker of dendritic cells (Prechtel & Steinkasserer, 2007). In contrast to BFM cells, expression levels of these immunomodulatory genes were unchanged or down-regulated by cp BVDV infection in MDBK cells, with the exception of CD3γ which was found to be increased by approximately 7-fold.

Cell adhesion molecules also play an important role in the immune response to virus infection, including inflammation or antigen presentation (Kesson *et al.*, 2002). Among the eight cell adhesion-related genes up-regulated by cp BVDV infection in BFM cells, expression of the NFκB-inducible genes VCAM-1 and ICAM-1 were remarkably increased by 450 and 10-fold, respectively. Only expression levels of CD36 were decreased in response to cp BVDV infection, by 3-fold. In the case of ncp BVDV infection, expression levels of genes involved in immunomodulation/cell adhesion functions were almost unaffected or only slightly increased. Together, these findings suggest that cp BVDV infection may stimulate immunomodulatory and cell adhesion functions through activation of IFN and NFκB-dependent pathway in BFM cells.

Apoptotic pathways.

It is well-established that IFNs mediate apoptosis in virus-infected cells by inducing many pro-apoptotic factors (Chawla-Sarkar *et al.*, 2003). Indeed, the author has previously demonstrated that 2 ISGs, PKR, and OAS-1, were up-regulated in BFM cells infected with cp BVDV and play a crucial role in apoptosis as demonstrated in CHAPTER 2. Microarray data showed up-regulation of many known pro-apoptotic ISGs (TRAIL, XAF-1, galectin 9, caspases 4 and 8, PKR and OAS-1) in cp BVDV-infected BFM cells. Among these pro-apoptotic ISGs, TRAIL is a death ligand that shares homology with TNF family members and induces apoptosis via caspase-8 activation (Ashkenazi & Dixit, 1998). XAF-1 is a tumor suppressor gene that directly interacts with and inhibits XIAP, one of the six known inhibitors of apoptosis protein (Liston *et al.*, 2001). Interestingly, it was demonstrated that constitutive expression of XAF-1 alone did not lead to apoptosis, but instead rendered the cells sensitive to TRAIL-induced apoptosis (Leaman *et al.*, 2002). Thus, it is noteworthy that TRAIL was increased in conjunction with XAF-1 by more than 100-fold in cp BVDV-infected BFM cells, and real-time PCR analysis confirmed the increase of TRAIL and XAF-1 by approximately 2000 and 90-fold, respectively (Table 3). Collectively, this data suggests that the coordinate expression of TRAIL and XAF-1 may play a critical role in cp BVDV-induced apoptosis in BFM cells. Furthermore, in agreement with the data in CHAPTER 1, up-regulation of TNFα and its receptors was observed. The author has demonstrated in CHAPTER 1 that TNFα probably induced via NFκB-mediated signaling (Shakhov *et al.*, 1990), participated in enhancing apoptosis in cp BVDV-infected cells by activation of caspase-8 through the extrinsic pathway. Galectin 9 acts as an eosinophil chemoattractant and is known to induce cell aggregation and apoptosis in melanomas (Kageshita *et al.*, 2002). Further, overexpression of galectin 9 sensitized cells to apoptosis through the Fas-mediated pathway. Taken together, cp BVDV infection in BFM cells seemed to stimulate both intrinsic (Grummer *et al.*, 2002b)

and extrinsic apoptotic pathways by affecting the expression of multiple cellular factors. In contrast, infection of MDBK cells by cp BVDV induced only a small number of pro-apoptotic factors (TNFRs and the Bcl-2 family member protein, Bfk, and a few ISGs, OAS-1 and galectin 9), with moderate levels as compared with that in BFM cells. In both cell types, expression changes in anti-apoptotic factors were relatively minor compared to changes in pro-apoptotic factors. In cp BVDV-infected BFM cells, there was a 7-fold down-regulation of PI3K, a crucial component of the Akt-mediated pro-survival pathway. Unexpectedly, cp BVDV infection in MDBK cells stimulated survival factors; expression levels of NAIP and Bcl-2 were increased by 5 and 3-fold, respectively. Collectively, cp BVDV infection seems to direct BFM cells toward apoptosis via activation of IFN- and NFκB-mediated pathways and down-regulation of pro-survival factors, whereas apoptosis in MDBK cells may result from an imbalance between up-regulation of both pro- and anti-apoptotic signals. In contrast, it appears that ncp BVDV avoids apoptosis by evading expression of pro-apoptotic factors, rather than by facilitating expression of anti-apoptotic factors in either cell type.

ER stress-mediated pathways.

A previous study has shown that cp BVDV infection in MDBK cells leads to induction of the ER stress-mediated apoptosis pathway (Jordan *et al.*, 2002). In agreement, the microarray data shows the up-regulation of ER stress-inducible genes CHOP, TRB3 (Ohoka *et al.*, 2005), tryptophanyl-tRNA synthetase and asparagine synthetase (Okada *et al.*, 2002), in cp BVDV-infected MDBK cells. As both BFM and MDBK cells yielded similar viral titers and NS3 protein accumulations (Fig. 1A and 2B), the author assumed that infection with cp BVDV induces comparable ER stress in both cells in response to viral protein synthesis. But unexpectedly, significant up-regulation of ER stress-inducible genes was not detected in cp

BVDV-infected BFM cells, which was confirmed by real-time PCR analysis (Table 3). To further confirm the poor ER stress responses in BFM cells, the author examined the expression of the ER stress-specific protein BiP/GRP78, which was previously shown to be induced in MDBK cells following cp BVDV infection (Jordan *et al.*, 2002). As shown in Fig. 2A, both cp BVDV infection and treatment with tunicamycin, an inducer of ER stress, resulted in marked expression of BiP/GRP78 protein in MDBK cells, but no or only a slight induction was detected in BFM cells. Notably, even following treatment with tunicamycin, BFM cells did not undergo activation of DEVDase, a caspase-3-like enzyme which is the most downstream executioner of apoptosis and mediator of cell death upon cp BVDV infection as shown in CHAPTER 2, in contrast to MDBK cells (Fig.2C). Collectively, it appears that cellular responses including apoptosis and transcriptional regulation to ER stress are distinct between both cells. Furthermore, it is noteworthy that the real-time PCR data indicated that mock-infected BFM cells exhibited constitutively higher expression levels of CHOP and TRB3 mRNAs than mock-infected MDBK cells (Fig. 2D), suggesting the existence of distinct regulatory mechanisms against ER stress at basal levels in BFM and MDBK cells. Involvement of CHOP-mediated oxidative stress and caspase-12 activation in ER stress-mediated apoptosis in cp BVDV-infected MDBK cells has previously been proposed (Jordan *et al.*, 2002). Given the role of TRB3 up-regulation in the induction of apoptosis (Ohoka *et al.*, 2005), up-regulated TRB3 may also play an important role on ER stress-mediated apoptosis in MDBK cells infected with cp BVDV.

Mitogen-activated protein kinase (MAPK) signaling.

MAPK signaling pathways control diverse cellular functions, such as cell differentiation, proliferation, survival and death (Chen *et al.*, 2001). MAPKs require tyrosine and threonine

phosphorylation, both catalyzed by MAP-kinase kinases (MEKs), to become active (Payne *et al.*, 1991; Robbins *et al.*, 1993). Conversely, MAPKs are inactivated through dephosphorylation by the dual-specificity phosphatases known as MAPK phosphatases (MKPs) or human vaccinia H1 gene products (HVHs) (Lewis *et al.*, 1998). In response to infection with cp BVDV, expression changes in both MAPKs and dual-specificity phosphatases were observed in BFM cells, while only the dual-specificity phosphatases were up-regulated in MDBK cells. It is of note that HVH-2 expression increased by 17-fold in MDBK cells, and HVH-3 was up-regulated by 6-fold in both cells. Although the precise functions of these HVHs remain unknown (Keyse, 2008), cp BVDV infection appears to affect MAPK signaling by regulating expression of both MAPKs and its phosphatases. Furthermore, significant down-regulation of JNK3 was observed in cp BVDV- as well as ncp BVDV-infected BFM cells. JNK3 is one of the c-Jun N-terminal protein kinases (JNKs) that are activated in response to a variety of cellular stresses, which leads to transcription of a number of genes through phosphorylation of transcription factors such as c-Jun, ATF-2, Elk-1, NFAT and p53 (Bogoyevitch *et al.*, 2004). In contrast to ubiquitously expressed JNK1 and 2, expression of JNK3 is restricted to the brain, and to a lesser extent the heart and testes. Importantly, JNK3 is known to mediate the apoptotic response and implicated in neurodegenerative diseases such as Parkinson's and Alzheimer's diseases (Bogoyevitch *et al.*, 2004). Although a role of JNK3 in fibroblast cell type is still unclear, decreased expression of JNK3 in BFM cells infected with BVDV may result in altered responsiveness to various cellular stresses.

Cell growth/Differentiation.

Differential expression of genes involved in cell growth and differentiation was found in

both BFM and MDBK cells infected with cp BVDV. BFM cells exhibited strong induction of Rnd1, LMO2 and ETB by 120, 34 and 11-fold, respectively, whereas MDBK induced TC-1, FGF21, IGFBP1, βNGF, lumican and GDF15 by 35, 34, 19, 18, 14 and 13-fold. The most significantly up-regulated gene of this class in BFM cells, Rnd1, has been shown to control rearrangements of the actin cytoskeleton and induce loss of cell-substrate adhesion leading to cell rounding (Nobes *et al.*, 1998). The second most up-regulated gene, LMO2, has been shown to be necessary for angiogenic remodeling of the existing capillary network into mature vasculature and for hematopoiesis (Yamada *et al.*, 2000; Yamada *et al.*, 1998). Conversely, cp BVDV infection of MDBK cells mainly induced expression of growth factors and TC-1, an NFκB-inducible gene that is known to stimulate β-catenin-mediated expression of genes implicated in invasiveness and aggressive behavior of cancers (Jung *et al.*, 2006). Infection by ncp BVDV in either cell type resulted in moderate changes in only 4 or 5 genes. These results indicate that cp BVDV infection may affect the differentiation state by regulating expression of different gene sets in BFM and MDBK cells.

Cell cycle/Oncogene.

Although ncp BVDV infection did not cause dramatic changes in expression of genes in this category, the author found that following cp BVDV infection, pro-growth factors, such as oncogenes, were up-regulated in MDBK cells, whereas growth suppressive genes were predominantly induced in BFM cells. This result from MDBK cells was in good agreement with a previous study demonstrating an up-regulation of proto-oncogenes in lymphoid cells (Neill & Ridpath, 2008). Thus, transcriptional regulation of oncogenes or genes involved in cell cycle following cp BVDV infection appears to be cell type-specific.

Metabolism.

Following cp BVDV infection, the most highly up-regulated gene in BFM cells was an ISG, Viperin (Table 5), while that in MDBK cells was CYP3A5 (Table 7), an oxidoreductase that is involved in drug, cholesterol and lipid metabolism (Lamba *et al.*, 2002). Differential regulation was also observed for other genes of this class; APOL3 and SLC15A3 genes were up-regulated exclusively in BFM cells, while CYP3A5 and ALDH1L2 genes were markedly induced in MDBK cells following cp BVDV infection. These results indicate that cellular metabolic events related to these genes can be significantly affected by cp BVDV infection.

Transcription factors and their modulators.

Because numerous genes were induced following cp BVDV infection in both cells types up-regulation of transcription factors was examined. In agreement with significant up-regulation of ISGs in BFM cells, the transcription factor ISGF3, which binds to IFN-stimulated response elements (ISREs) and transcribes ISGs, was increased by more than 10-fold. In contrast, IκBα which inhibits NFκB, was up-regulated in cp BVDV-infected BFM cells by 13-fold. In spite of this, numerous NFκB-inducible genes were up-regulated following cp BVDV infection. Importantly, since IκBα is itself an NFκB-inducible gene and acts as a negative feedback regulator (Haskill *et al.*, 1991), the abundant IκBα expression seems to be indicative of marked activation of NFκB-mediated transcription, rather than of a down-regulation of NFκB signaling in cp BVDV-infected cells. A small number of transcription factors, EGR-1 and 3, and E1AF, were commonly up-regulated in BFM and MDBK cells, whereas Sox9 and LBP-9 were affected exclusively in MDBK cells infected with cp BVDV. This differential regulation of transcription factors in BFM and MDBK cells may account for the highly distinct expression patterns of genes in both cells.

Conclusions

This study demonstrates the differential regulation of genes in BFM and MDBK cells following BVDV infection. The microarray data discussed above clearly indicate that infection with cp BVDV leads to numerous changes in gene transcription, whereas ncp BVDV can establish infection without significant alteration in gene transcription. This may be attributed to the greater amount of dsRNA produced by cp than ncp BVDV (Lackner *et al.*, 2004; Mendez *et al.*, 1998; Vassilev & Donis, 2000), since dsRNA is a strong inducer of IFN and NFκB signaling (Thompson & Locarnini, 2007). More detailed studies are required to elucidate this point.

Genes belonging to various functional classes, including apoptosis, transcription factors, immunomodulation, and cell cycle, were shown to be differentially altered upon BVDV infection (Table 4). Only a limited number of genes, IL-6, IL-8, HVH3, EGR3 and SPP1, were shown to be similarly regulated in both BFM and MDBK cells. These differences may be attributed to the cell type, as BFM cell is fibroblast, which produces abundant IFNs, and MDBK cell is an epithelial cell. Nevertheless, it was unexpected that MDBK cells would exhibit poor IFN-mediated gene induction, as previous studies have shown the expression of IFN or ISGs in MDBK cells (Barreca & O'Hare, 2004; Muller-Doblies *et al.*, 2002). Given the much smaller number of ISGs induced in MDBK cells compared with those in BFM cells, the author proposes that the fibroblast cell type is more suited for studies regarding interaction between BVDV and IFNs. Equal induction levels in both cells of the NFκB-inducible proinflammatory cytokines, IL-8 or IL-6, indicated that NFκB signaling is similarly activated in MDBK and BFM cells, however, the number of NFκB-inducible cytokines/chemokines is limited in MDBK cells compared with BFM cells. Notably, regardless of the marked increase in antiviral ISGs or proinflammatory responses in BFM cells, both cells produced similar viral

titers (Fig. 1A). Because the ISGs that were found to be up-regulated in this study, including Viperin and PKR, have been identified to efficiently suppress replication of HCV (Jiang *et al.*, 2008), a close relative of BVDV, it will be important to study the interaction between BVDV and these antiviral factors, since BVDV can continue to efficiently replicate in their presence.

It was of particular interest that in spite of the largely different signaling pathways activated by cp BVDV in MDBK and BFM cells, both cells follow the same fate, apoptotic cell death. Data from this study suggests that apoptotic processes in both cells are considerably distinct from each other, since marked transcriptional activation of pro-apoptotic ISGs was found in BFM cells, but not in MDBK cells, whereas ER stress-inducible pro-apoptotic factors were exclusively up-regulated in MDBK cells. Furthermore, it was surprising that BFM cells did not induce activation of DEVDase against ER stress, even by treatment with tunicamycin (Fig. 2C). These results suggest that each cell type may have adopted distinct defense systems against virus infection or the subsequent environmental stresses. Proposed models of cellular signaling pathways activated following cp BVDV infection in BFM and MDBK cells are summarized in Fig. 3.

In this work, the author showed that the microarray technique is very useful to generate comprehensive expression profiles of bovine cells infected with BVDV. Although the author analyzed the data from a single time point after virus infection in this study, it will be necessary to generate transcriptional profiles at multiple time points after infection to elucidate the kinetics of BVDV replication as well as the cell signaling pathways affected by BVDV infection. Further analysis of the functional outcome resulting from the respective gene expression will provide a basis for an understanding of the cellular responses involved in the virus life cycle and its pathogenesis.

Figure legends

Figure 1. Scatter plots of signal intensity comparisons of mock-infected and infected samples. (A) Viral titers of cp and ncp BVDV at 24 h p.i. were calculated as 50% tissue culture infective dose/ml ($TCID_{50}$/ml). (B) Log scale plot of signal intensities of either cp (left panels) or ncp (right panels). BVDV-infected sample compared to the mock-infected sample in BFM (upper panels) or MDBK (lower panels) cells. The diagonal lines indicate changes of 1-, 1.5-, 2-, 4- and 8-fold.

Figure 2. Differential responses to ER stress in MDBK and BFM cells. MDBK or BFM cells were mock-infected or infected with cp or ncp BVDV at an MOI of 5, or treated with 2 μg/ml tunicamycin (TUN) as indicated. After 24 h, cell lysates were harvested and protein expression of (A) BiP/GRP78 or (B) BVDV NS3 and β-actin as a loading control was detected by Western blot analysis as described in Materials and methods. (C) MDBK or BFM cells were mock-treated or treated with 2 μg/ml tunicamycin (TUN) for 24 h. Cell lysates were then subjected to DEVDase assay as described in Materials and methods. Values are expressed relative to the value of mock-treated samples, which were set to 100%, and represent the mean ± S.D. from three independent experiments. (D) Comparison of relative mRNA expression levels of ER stress-inducible genes, CHOP and TRB3, between MDBK and BFM cells. Both cells were mock-infected or infected with cp or ncp BVDV. After 24 h, cells were harvested and analyzed for mRNA expression by real-time PCR analysis as described in Materials and methods. Values determined by the standard $2^{-\Delta\Delta Ct}$ method are expressed relative to the values of GAPDH mRNA in each sample, and represent the mean ± S.D. from three independent experiments. P values were determined for the experimental sample versus the mock-treated sample using Student's t-test. *, $P < 0.01$.

Figure 3. Proposed model of cellular signaling pathways activated upon BVDV replication in MDBK and BFM cells. In MDBK epithelial cells, pro-apoptotic signal is mediated through ER stress-inducible pathway, while IFN responses are weak. NFκB signaling seems to be strongly induced, as indicated by the marked induction of IL-6 or IL-8, but number of NFκB-inducible genes is relatively few. While in BFM fibroblast cells, pro-apoptotic signaling is mediated through IFN-stimulated pathway, but not through ER stress-mediated signaling. It appeared that abundant proinflammatory genes are induced via NFκB-dependent pathway.

CHAPTER 5 Fig. 1

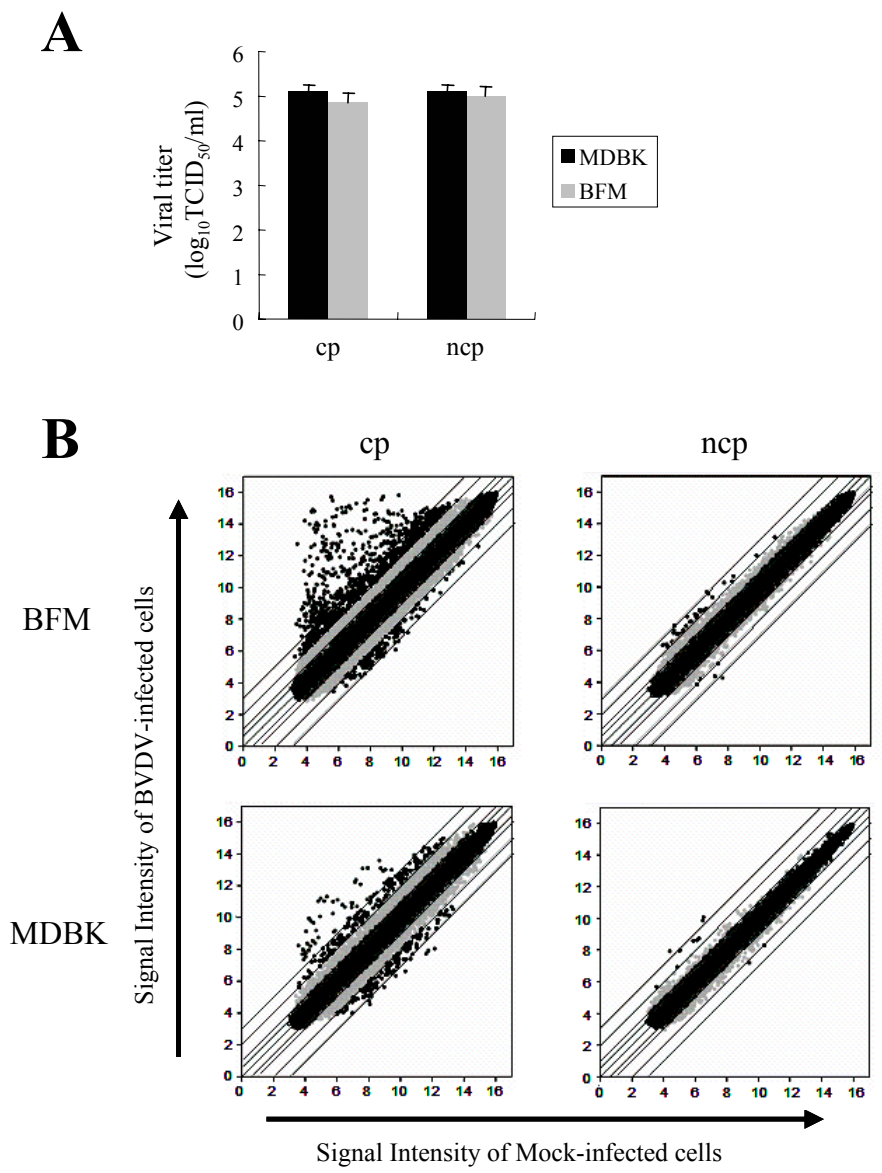

CHAPTER 5 Fig. 2

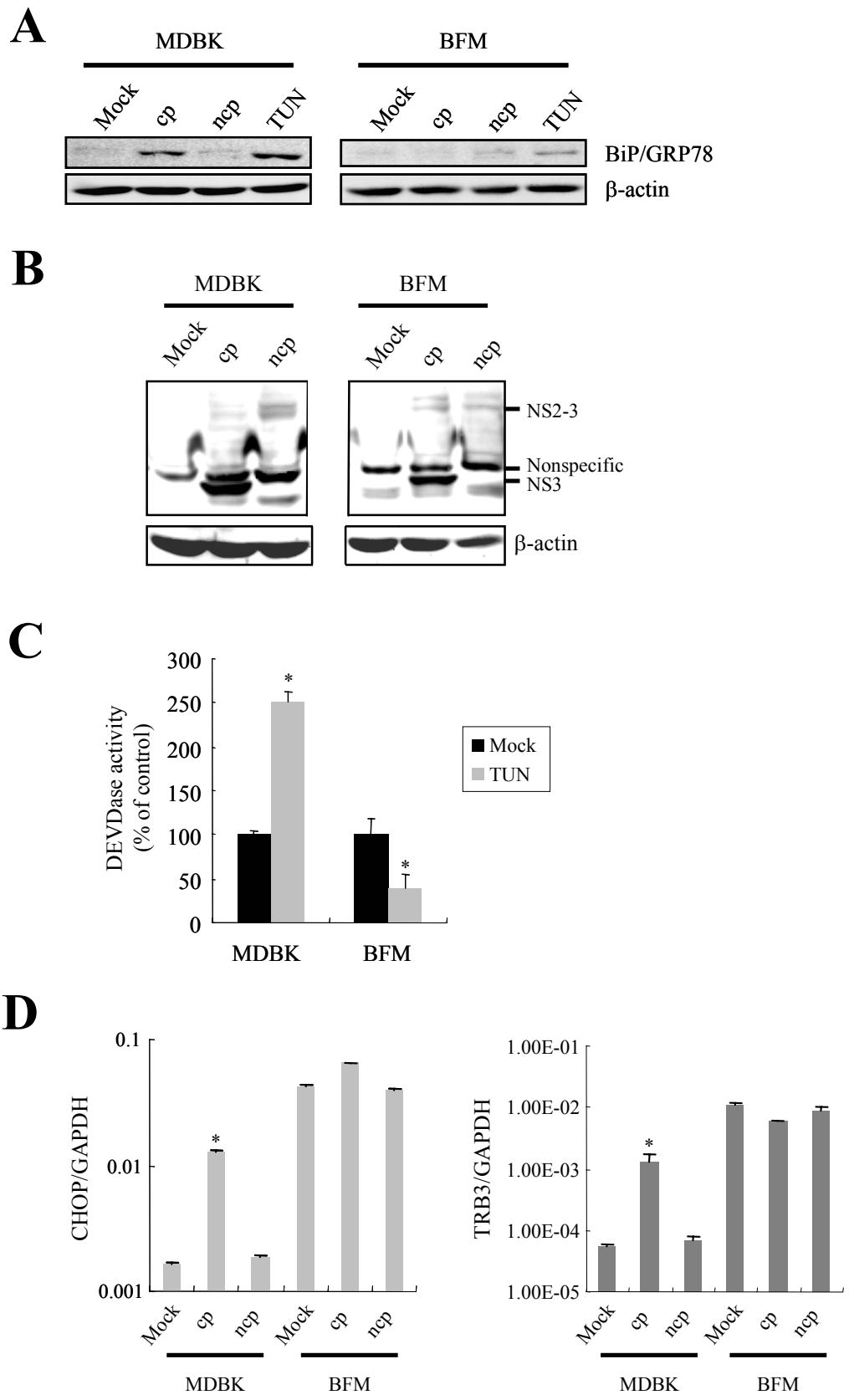

CHAPTER 5 Fig. 3

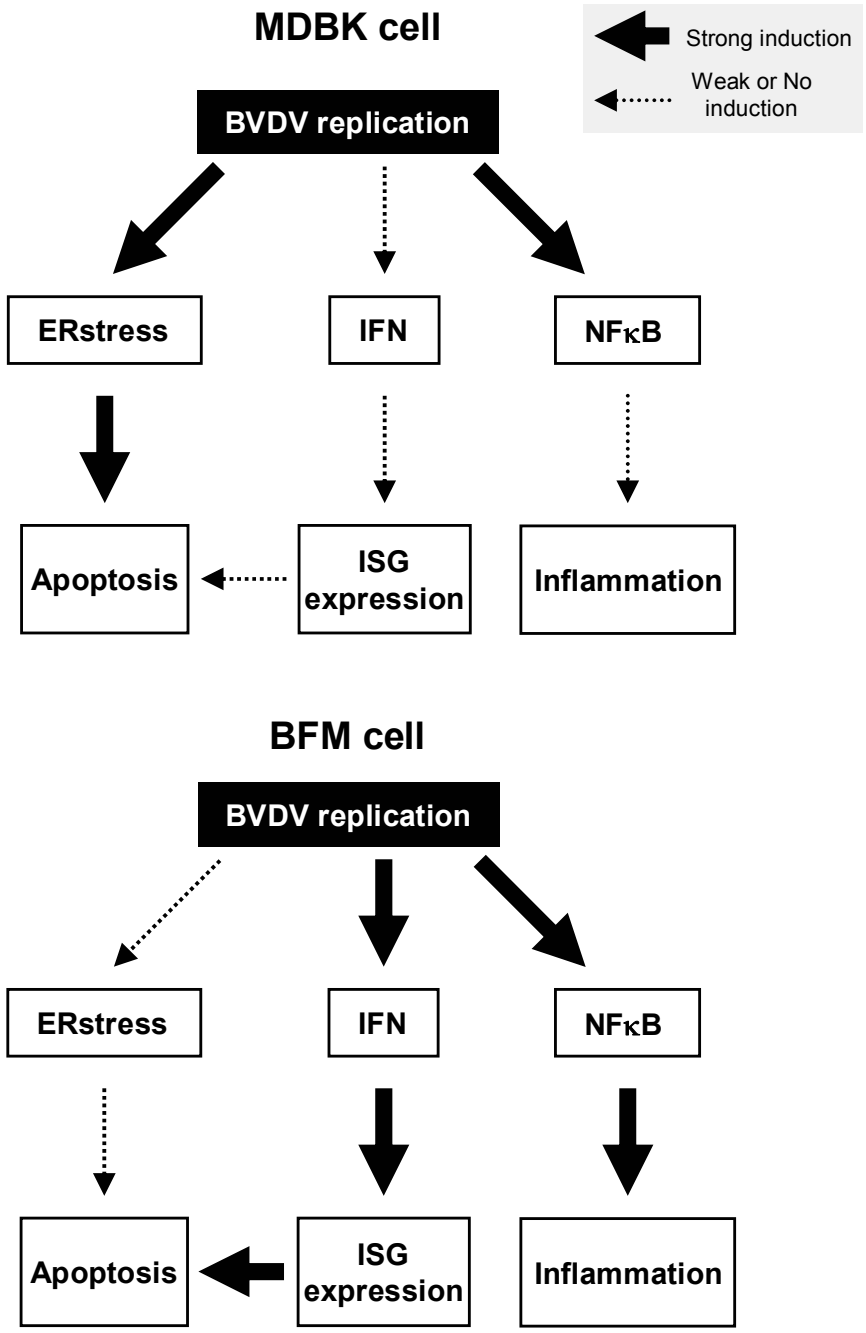

CHAPTER 5 Table 1

Table 1. Primer sets used in this study

Primer	Sequence 5'-3'	Product size, acc. No.
βNGF F (nt 251-270)	TCAGCATTCCCTTGACACAG	108 bp, XM_580907
βNGF R (nt 358-340)	AGTTTGGGGTCCACAGTGA	
CHOP F (nt 454-471)	AGACCAAGGAAGAACCAG	133 bp, BC122721
CHOP R (nt 586-567)	GAGTCGTTCATTCTCTTCAG	
IL-8 F (nt 122-139)	TGAAGCTGCAGTTCTGTC	83 bp, BC103310
IL-8 R (nt 204-187)	ATTTGGGGTGGAAAGGTG	
TRAIL F (nt 76-93)	CGATCCTCATCTTCACAG	129 bp, XM_583785
TRAIL R (nt 204-187)	CTTCCTCCAAGAAGCAAG	
TRB3 F (nt 261-279)	TGTTCATGCTCCGGATGTG	128 bp, BC120209
TRB3 R (nt 388-369)	ACACCTTGCAGATGTACTCC	
Viperin F (nt 890-908)	TTCTTGGATCGCCACAAGG	121 bp, BC105455
Viperin R (nt 1010-991)	CCTTCCGCCCATTTCTACAG	
XAF-1 F (nt 89-108)	CCTACTGCTTGATGTACCTG	80 bp, BC122801
XAF-1 R (nt 168-150)	CTGGCAGTGTTCTTCCATC	

CHAPTER 5 Table 2

TABLE 2. Number of probe sets affected by BVDV infection

Fold Change (FC)	BFM				MDBK			
	cp		ncp		cp		ncp	
	DOWN	UP	DOWN	UP	DOWN	UP	DOWN	UP
1.0 < 1.5	1878	986	2174	1488	5606	4373	2343	4257
1.5 < 2.0	2602	1197	1010	1158	2126	1428	440	585
2.0 < 4.0	1631	1258	202	447	1076	843	167	104
4.0 < 8.0	115	451	2	23	128	170	0	4
8.0 <	7	374	0	1	11	58	0	3

CHAPTER 5 Table 3

TABLE 3. Validation of array data by real-time PCR

Gene	cp				ncp			
	BFM FCs	**Microarray data**	MDBK FCs	**Microarray data**	BFM FCs	**Microarray data**	MDBK FCs	**Microarray data**
β-NGF	1.22	1.01	3.81	18.21	1.01	-1.23	-1.30	1.39
CHOP	1.68	1.45	11.74	7.57	-1.04	-1.56	1.04	1.67
IL-8	52.85	63.18	47.16	52.72	-1.02	3.14	1.03	1.62
Mx1	2529.79	527.69	-1.13	-1.22	22.14	5.20	-1.34	1.79
OAS-1	963.70	363.46	1.14	3.43	23.99	4.26	1.20	11.59
PKR	13.67	9.38	-1.07	-1.18	1.21	2.04	-1.51	-1.02
TRAIL	2069.40	225.99	-1.75	-1.74	6.32	1.87	-1.20	1.07
TRB-3	-1.80	-2.11	27.73	34.38	-1.21	-1.32	2.06	2.05
Viperin	29840.86	1489.18	2.46	2.91	26.63	1.08	1.77	3.08
XAF-1	91.86	152.33	1.12	1.07	2.74	1.48	-1.22	1.34

TABLE 4. Pathways of genes regulated upon infection with BVDV

Gene		cpBVDV FCs in		ncpBVDV FCs in	
Genbank No.	Description	BFM	MDBK	BFM	MDBK
	IFN responses				
XR_027292	guanylate binding protein 4 (GBP4)	296.17	–	–	–
XM_864679	tripartite motif protein TRIM5, transcript variant 2	149.51	–	–	–
XM_870740	interferon regulatory factor 10 (IRF-10)	64.00	–	–	–
BC111668	interferon, alpha-inducible protein 6 (IFI6)	44.20	–	–	–
BC102387	Interferon-induced guanylate-binding protein 1 (GTP-binding protein 1, GBP1)	29.43	–	–	–
NM_001075961	receptor (chemosensory) transporter protein 4 (RTP4)	22.01	–	–	–
NM_001034545	interferon gamma inducible protein 47 (IFI47)	21.78	–	–	–
XM_001255309	interferon regulatory factor 1 (IRF-1)	20.44	–	–	–
XM_592214	hect domain and RLD 5 (HERC5)	17.20	–	–	–
AF214525	interferon-gamma inducible proteasome subunit LMP7	16.14	–	–	–
NM_001015617	Interferon beta precursor (IFN-beta, Fibroblast interferon)	10.84	–	–	–
XM_871059	Bone marrow stromal antigen 2 (BST-2, HM1.24, CD317)	311.36	–	–	2.63
BC118109	myxovirus (influenza virus) resistance 1 (Mx1)	527.69	–	5.20	–
XM_872122	Interferon-induced protein 44 (Antigen p44, IFI44)	1293.51	–	2.67	–
BT025389	interferon-induced protein with tetratricopeptide repeats 2 (IFIT2)	1295.59	–	4.23	–
AB104655	PKR	9.38	–	2.04	–
NM_174366	ISG15 ubiquitin-like modifier	288.66	–	2.91	3.61
NM_178108	2',5'-oligoadenylate synthetase 1 (OAS-1)	363.46	3.43	4.26	11.59
AF355147	GTP-binding protein Mx2	1167.07	3.34	2.76	11.63
NM_001045941	radical S-adenosyl methionine domain containing 2 (Viperin)	1489.18	2.91	–	3.08
AJ007043	RANTES protein	201.15	2.75	–	2.00
BC102471	OAS-like	142.69	2.40	–	–
XM_001251939	Interferon beta-1	5.77	2.16	–	–
BC102161	interferon-related developmental regulator 1 (IFRD1)	–	5.52	–	–
	IFN mediators				
XM_615590	MDA-5	151.19	–	2.10	–
XM_001252348	TRAF-interacting protein with a forkhead-associated domain	105.40	–	–	–
BT020952	LGP2	59.12	–	–	–
XM_580928	RIG-I	11.01	-2.38	–	–
AJ879589	IRF-3	2.57	–	–	–
NM_001030301	TIR domain containing adaptor inducing interferon-beta (TRIF)	2.41	–	–	–
BC114122	IKKepsilon	2.08	–	–	–
	Toll-like receptors				
AY957622	toll-like receptor 1 (TLR-1)	3.07	–	–	-2.19
AY957623	toll-like receptor 2 (TLR-2)	3.44	2.96	–	–
AY957624	toll-like receptor 3 (TLR-3)	3.09	–	–	–
AY957625	toll-like receptor 4 (TLR-4)	7.22	–	–	–
AY957626	toll-like receptor 5 (TLR-5)	31.15	–	–	–
AY957627	toll-like receptor 6 (TLR-6)	3.45	-2.56	–	–
AY957630	toll-like receptor 9 (TLR-9)	–	3.20	-2.28	–
	Ubiquitine-Proteasome system				
NM_174366	ISG15 ubiquitin-like modifier	288.66	–	2.91	3.61
BC102963	proteasome (prosome, macropain) subunit, beta type, 9 (large multifunctional peptidase 2, PSMB9, LMP2)	36.60	–	–	–
NM_001017940	putative ubiquitin-specific protease (bubp43 gene).	36.40	–	–	–
NM_001012284	ubiquitin E1-like enzyme (UBEL1)	23.78	–	–	–
AF214525	interferon-gamma inducible proteasome subunit LMP7	16.14	–	–	–
NM_001040480	proteasome (prosome, macropain) subunit, beta type, 8 (large multifunctional	16.02	–	–	–
XM_586436	ubiquitin-conjugating enzyme RIG-B)	11.06	–	–	–
BC102272	proteasome (prosome, macropain) subunit, beta type, 10	7.51	–	–	–
AF473832	proteasome subunit LMP10	6.35	–	–	–
XM_863936	ubiquitin D, transcript variant 2	4.36	–	–	–
NM_001014889	proteasome (prosome, macropain) activator subunit 2 (PA28 beta, PSME2)	3.90	–	–	–
	Chemokines/Cytokines				
NM_001046551	small inducible cytokine B10 precursor (CXCL10, IP-10)	631.35	–	–	-2.14
BC102064	chemokine (C-C motif) ligand 5 (CCL5)	210.05	–	–	–
U95811	CXCL3/GRO-γ	102.94	–	–	2.04
BT020654	chemokine (C-C motif) receptor-like 1 (CCRL1)	38.65	–	–	–
BC112718	G protein-coupled receptor 84 (GPR84, EX33)	37.40	–	–	–
AY061959	macrophage inflammatory protein 3 alpha (CCL20)	36.21	–	–	–
U95813	CXCL2/GRO-β	33.01	–	–	–
X12497	pre-interleukin-1 α.	30.85	–	–	–
NM_174263	chemokine (C-C motif) ligand 20 (CCL20)	25.97	–	–	–
XM_594243	putative alpha chemokine	10.64	–	–	–
XM_601728	interleukin 1 family, member 6 (epsilon) (IL-1 ε)	9.18	–	–	–
NM_174006	chemokine (C-C motif) ligand 2 (CCL2)	5.94	–	–	–
BC122767	chemokine (C-C motif) receptor-like 2	5.36	–	–	–
U42433	interleukin 15 (IL-15)	5.19	–	–	–
NM_001075253	interleukin 16 (IL-16)	4.81	–	–	–

[a]—, changes less than 2-fold

TABLE 4 —*Continued*

Gene		cpBVDV FCs in		ncpBVDV FCs in	
Genbank No.	Description	BFM	MDBK	BFM	MDBK
BC120352	Interleukin 1 family member 5 (IL-1F5, IL-1 delta)	4.52	–	–	–
BC122679	interleukin 17 receptor C	4.29	–	–	–
XM_871776	interleukin 1 receptor-like 1 isoform 4	3.53	–	–	–
XM_582146	interleukin 32, transcript variant 1 (IL-32)	13.14	–	2.14	–
BC103310	interleukin 8 (IL-8)	63.18	52.72	3.14	–
NM_001048165	chemokine (C-X-C motif) ligand 2 (CXCL2)	35.48	2.65	–	–
U95812	CXCL1/GRO-α	21.71	2.68	–	–
NM_173923	interleukin 6 (interferon beta 2, IL-6)	7.48	4.22	–	–
AF399642	CXC chemokine receptor 4 (CXCR4)	4.61	2.73	-2.53	–
XM_590497	IL-18 receptor alpha (IL-18Rα)	2.43	5.06	–	–
XR_028805	histamine H3 receptor	–	–	–	3.45
	Immunomodulation				
NM_001046590	CD83	133.70	–	–	–
AB008581	MHC class I heavy chain	10.53	–	–	–
DQ140364	haplotype AH20 classical MHC class I antigen (BoLa)	8.57	–	–	–
AB008577	MHC class I heavy chain, clone MP-5.10m.	7.71	–	–	–
BC109586	HLA class I histocompatibility antigen, A-11 alpha chain precursor	7.65	–	–	–
M24090	MHC class I lymphocyte antigen	7.36	–	–	–
U16750	complement component C4	7.13	–	–	–
NM_001040526	complement factor B precursor (C3/C5 convertase)	47.02	-2.10	–	–
BC103357	complement component 2	41.99	-2.27	–	–
D76417	MHC class II DM beta-chain	16.96	-2.49	–	–
NM_001040472	CD3γ molecule (CD3-TCR complex)	–	7.13	–	–
	Cell adhesion				
NM_174484	vascular cell adhesion molecule 1 (VCAM1)	450.71	–	–	–
AY487417	carcinoembryonic antigen-related cell adhesion molecule 1 isoform 3Ls	10.83	–	–	–
U09134	intercellular adhesion molecule-1 (ICAM-1)	9.78	–	–	–
XM_614070	cell adhesion kinase beta	8.79	–	–	–
XM_580533	cell adhesion molecule with homology to L1CAM	5.98	–	2.32	–
S45840	osteopontin (secreted phosphoprotein 1, SPP1)	3.75	3.10	2.02	–
BT029907	adhesion molecule, interacts with CXADR antigen 1 (AMICA1)	3.30	–	–	–
XM_582483	intercellular adhesion molecule-2, transcript variant 1 (ICAM-2)	3.26	–	–	–
BC103112	CD36 molecule (thrombospondin receptor)	-3.43	–	-2.13	–
	Apoptosis				
	Pro-apoptosis				
XM_583785	TNF-related apoptosis-inducing ligand (TRAIL)	225.99	–	–	–
BC122801	XIAP associated factor-1 (XAF-1)	152.33	–	–	–
XM_613366	programmed death ligand 1	30.41	–	–	–
XM_592054	tumor necrosis factor superfamily, member 15, transcript variant 1	12.47	–	–	–
BT021650	BCL2-like 14 (BCL2L14)	9.55	–	–	–
NM_173966	tumor necrosis factor alpha (TNFα)	7.49	–	–	–
BC105222	tumor necrosis factor receptor superfamily, member 1B	7.19	–	–	–
NM_001075310	Bcl-2-like protein 11	5.24	–	–	–
DQ319070	caspase 8	4.32	–	–	–
BC112708	caspase 4	3.86	–	–	–
AF383946	caspase 13A	3.62	–	–	–
BC123503	caspase 3	3.38	–	–	–
AB050006	apoptosis-associated speck-like protein containing a CARD	3.06	–	–	–
AF031589	tumor necrosis factor receptor 2 (TNFR2)	10.38	–	2.26	–
AB104655	PKR	9.38	–	2.04	–
NM_178108	2',5'-oligoadenylate synthetase 1 (OAS-1)	363.46	3.43	4.26	11.59
BC104505	lectin, galactoside-binding, soluble, 9 (galectin 9)	50.59	4.79	–	–
XM_581509	tumor necrosis factor receptor superfamily, member 5 (TNFRSF5)	19.51	2.49	–	–
BC103258	nerve growth factor receptor (TNFRSF16) associated protein 1	–	6.12	–	–
BC122810	pro-apoptotic Bcl-2 protein (Bfk)	–	5.33	–	–
	Anti-apoptosis				
XM_589415	neuronal apoptosis inhibitory protein (NAIP)	–	5.32	–	–
U92434	Bcl-2	–	3.31	–	–
XM_613754	phosphoinositide-3-kinase, catalytic, beta polypeptide (PIK3CB)	-7.01	–	–	–
	ER stress				
NM_001076103	tribbles homolog 3 (TRB3)	-2.11	34.38	–	2.05
NM_001078163	DNA-damage-inducible transcript 3 (CHOP)	–	7.57	–	–
NM_174218	tryptophanyl-tRNA synthetase	–	4.20	–	–
NM_001075653	asparagine synthetase	–	4.04	–	–

TABLE 4 —*Continued*

Gene		cpBVDV FCs in		ncpBVDV FCs in	
Genbank No.	Description	BFM	MDBK	BFM	MDBK
	MAPK				
BC126500	p38Beta2 MAP Kinase	2.92	–	–	–
XM_001257028	dual specificity phosphatase 4 (HVH-2, MKP-2)	2.11	17.01	–	–
XM_583612	dual specificity phosphatase 5 (HVH-3)	5.74	5.97	–	–
NM_001034725	dual specificity phosphatase 10 (MKP-5	3.69	2.96	–	–
XM_001252457	mitogen-activated protein kinase 10 (MAPK10, JNK3)	-8.45	–	-10.49	–
BC113271	extracellular signal-regulated kinase 7 (ERK7)	–	–	–	-3.23
	Cell growth/differenciation				
BC116134	Rhombotin-2 (LIM-only protein 2) (LMO2)	34.60	–	-2.05	–
BC120256	endothelin receptor type B (ETB)	11.55	–	–	–
BC120407	Beta platelet-derived growth factor receptor precursor (PDGF-R-beta)	4.30	–	2.09	–
AF099134	vascular endothelial growth factor-B (VEGF-B)	3.32	–	–	–
U22385	GM-CSF	5.39	5.47	–	–
NM_001046016	Rho-related GTP-binding protein Rho6 (Rho family GTPase 1, Rnd1)	120.99	2.12	–	–
XM_870373	VGF	–	7.36	2.80	–
NM_173934	lumican	–	14.10	–	–
XM_580907	nerve growth factor, beta polypeptide (β-NGF)	–	18.21	–	–
BC111197	insulin-like growth factor binding protein 1 (IGFBP1)	–	19.05	–	–
XM_871003	Growth differentiation factor 15 (GDF15, MIC1)	–	13.28	–	2.57
XM_001253556	Fibroblast growth factor 21(FGF21)	–	34.01	–	2.87
BC103283	TC-1 (c8orf4)	-3.97	35.87	–	3.10
NM_174308	endothelin receptor type A (EDNRA)	-3.39	–	-3.12	–
AB056447	hepatocyte growth factor (HGF)	-2.49	-3.05	–	–
X53553	insulin-like growth factor II (IGF-II)	–	-4.03	–	–
AB004301	growth differentiation factor-5 (GDF-5)	–	–	–	3.52
NM_181010	endothelin 1 (ET-1)	–	–	-3.12	–
	Cell Cycle/Oncogene				
	growth promoter				
XM_878632	Proto-oncogene tyrosine-protein kinase FGR (C-FGR, FGFR1)	4.64	–	–	–
XM_001251257	c-MYC promoter-binding protein IRLB, transcript variant 1	3.01	–	–	–
NM_001046273	G1/S-specific cyclin D1 (PRAD1 oncogene, BCL-1 oncogene)	–	3.34	–	–
NM_174144	pim-1 oncogene (PIM1)	–	9.12	–	2.16
BC118177	RAB39B, member RAS oncogene family	–	8.21	–	–
NM_175050	v-myb myeloblastosis viral oncogene homolog (MYB)	–	3.15	–	–
M82978	c-myb proto-oncogene	-4.53	4.87	–	–
BC126591	FYN oncogene related to SRC, FGR, YES (FYN)	-3.34	2.71	–	–
BC118280	v-fos FBJ murine osteosarcoma viral oncogene homolog	-3.82	–	–	–
XM_001250258	retinoblastoma binding protein 8, transcript variant 1	-3.11	–	–	–
	growth suppressor				
XM_588232	poly [ADP-ribose] polymerase 10 (PARP-10), Myc inhibitor	19.70	–	–	–
NM_174475	3'-5' exonuclease TREX1	15.07	–	–	–
XM_001252683	antagonizer of myc transcriptional activity, transcript variant 1	3.39	–	–	–
XM_591188	p21/WAF1	–	6.22	–	–
	Metabolism				
XM_581308	Apolipoprotein L, 3 (APOL3)	178.94	–	2.40	–
XM_591760	solute carrier family 15, member 3 (SLC15A3)	215.56	–	–	–
XM_001253379	cytochrome P450, family 3, subfamily A, polypeptide 5 (CYP3A5)	1.76	74.40	–	4.34
XR_028169	Aldehyde dehydrogenase 1 family, member L2 (ALDH1L2)	–	33.93	–	2.90
	Transcription factor				
NM_001045868	nuclear factor of kappa light polypeptide gene enhancer in B-cells inhibitor, alpha (NFKBIA, IκBα)	13.48	–	–	–
BT021673	interferon-stimulated transcription factor 3, gamma 48kDa (ISGF3)	10.65	–	–	–
XM_615908	brain-muscle-ARNT-like transcription factor 2a	4.75	–	–	–
AY488117	signal transducer and activator of transcription 1 (STAT1)	3.84	–	–	–
BC114684	upstream transcription factor 1	3.77	–	–	–
BC112570	transcription initiation factor IIB (General transcription factor TFIIB, S300-II)	3.50	–	–	–
XM_588270	signal transducer and activator of transcription 2 (STAT2)	3.27	–	–	–
BC112629	cyclic-AMP-dependent transcription factor ATF-3	3.22	–	–	–
XM_869196	E2F transcription factor 2	3.16	–	2.06	–
NM_001045875	early growth response 1 (EGR1)	3.91	5.06	–	–
XM_604596	early growth response 3 (EGR3)	4.77	4.56	–	–
XM_612436	E1A-F, transcript variant 1 (ETV4)	2.46	9.34	–	2..17
AF278703	Sox9	–	5.73	–	–
XM_001252723	transcription factor LBP-9	–	-6.40	–	–

CHAPTER 5 Table 5

TABLE 5. Genes affected by cp BVDV infection in BFM cells

Genbank No.	FC	P value	Description
UP			
NM_001045941	1489.18	4.24E-05	radical S-adenosyl methionine domain containing 2 (Viperin)
BT025389	1295.59	4.80E-06	interferon-induced protein with tetratricopeptide repeats 2 (IFIT2)
XM_872122	1293.51	0.0007827	Interferon-induced protein 44 (Antigen p44, Non-A non-B hepatitis-associated microtubular aggregates protein)
AF355147	1167.07	3.43E-05	GTP-binding protein Mx2
U96014	715.57	0.000305	ubiquitin cross-reactive protein (UCRP, ISG15)
NM_001029846	664.80	0.0012098	2'-5' oligoadenylate synthetase 1z (OAS1Z)
NM_001046551	631.35	5.50E-05	Small inducible cytokine B10 precursor (CXCL10, Gamma-IP10, IP-10)
BC118109	527.69	0.000145	myxovirus (influenza virus) resistance 1, interferon-inducible protein p78 (mouse)
AB060169	316.37	0.0002373	Mx1B GTP-binding protein
NM_174484	524.90	9.32E-05	vascular cell adhesion molecule 1 (VCAM1)
XM_589840	510.54	3.56E-05	gp50/Trop-2 (LOC539853)
NM_178108	363.46	8.71E-07	2',5'-oligoadenylate synthetase 1, 40/46kDa (OAS-1)
XM_871059	311.36	7.31E-09	BST-2/HM1.24
AY599197	296.38	0.0036544	2'-5' oligoadenylate synthetase 2 (OAS-2)
XR_027292	296.17	5.19E-06	guanylate binding protein 4 (GBP4)
BC102064	290.64	0.0001328	chemokine (C-C motif) ligand 5 (CCL5)
NM_174366	288.66	4.20E-05	ISG15 ubiquitin-like modifier (ISG15)
XM_583785	225.99	0.0018118	TNF-related apoptosis-inducing ligand (TRAIL)
XM_592594	223.36	0.0148752	family with sequence similarity 3, member B (FAM3B)
XM_591760	215.56	0.0006003	solute carrier family 15, member 3
AJ007043	201.15	0.0001419	RANTES protein
BC114020	184.90	0.0001137	guanylate binding protein isoform I or II (GBP-1 or 2)
NM_001075746	109.27	8.53E-06	guanylate-binding protein 5 (GBP-5)
XM_581308	178.94	0.0091452	Apolipoprotein L, 3 (Apol3)
BC122801	152.33	0.0004755	XIAP associated factor-1 (XAF-1)
XM_615590	151.19	8.18E-06	melanoma differentiation associated protein-5 (MDA-5)
NM_001038050	150.55	1.64E-05	putative ISG12(a) protein
XM_864679	149.51	0.0002022	tripartite motif protein TRIM5, transcript variant 2
NM_001046016	146.15	7.68E-06	Rho-related GTP-binding protein Rho6 (Rho family GTPase 1, Rnd1)
NM_001046590	144.14	0.0005009	CD83 molecule
DOWN			
XM_617995	11.32	0.0059456	A kinase (PRKA) anchor protein 6 (AKAP6)
XM_617206	9.18	0.0153462	ADAM metallopeptidase with thrombospondin type 1 motif, 9 preproprotein
XM_586352	8.81	0.0020064	Rho GTPase activating protein 6 (ARHGAP6), transcript variant 4
AF111085	8.79	0.043718	latrophilin 3 splice variant abaf
BC112821	8.56	9.36E-06	FAM107B, C10orf45
XM_001252457	8.45	0.20114	mitogen-activated protein kinase 10 (MAPK10, JNK3)
XM_865202	8.27	0.030116	RBM35A protein, transcript variant 3
XM_868782	8.15	0.023072	Acp1 protein
XM_614107	7.80	0.0063132	OTTHUMP00000017121, retinaldehyde binding protein 1-like 2 (RLBP1L2)
AB033716	7.78	0.0009097	SCF for stem cell factor
XM_615475	7.66	0.0002856	lymphoid enhancer binding factor-1, transcript variant 1
AF111089	7.39	0.0100866	latrophilin 3 splice variant abbg
NM_174233	7.35	2.52E-06	angiotensin II receptor, type 1 (AGTR1)
XM_600139	7.03	0.0010567	putative binding protein 7a5
XM_613754	7.01	0.0005018	phosphoinositide-3-kinase, catalytic, beta polypeptide (PIK3CB)
XR_027969	6.98	0.024936	LIM and calponin homology domains 1 (LIMCH1), transcript variant 1
XM_001253734	6.95	2.81E-05	genethonin 1
XM_584890	6.86	0.00114	Desmoglein 2
NM_174414	6.81	0.019689	phosphodiesterase 1A, calmodulin-dependent (PDE1A)
NM_001076222	6.80	1.54E-05	LIM and cysteine-rich domains 1
XM_582369	6.68	0.0126764	ChaC, cation transport regulator homolog 1 (E. coli)
AY563861	6.52	9.35E-05	clone NG010006A21G10
AF111094	6.50	0.022206	latrophilin 3 splice variant bbbf
XM_580628	6.45	0.021198	zinc finger protein
NM_174375	6.43	0.002374	KIT ligand (KITLG)
XM_867914	6.36	0.0008762	PIG38 protein
NM_001046033	6.36	0.074424	Aspartoacylase (Aminoacylase-2, ACY-2)
BC133516	6.35	0.000844	MAL2 proteolipid
AF111090	6.34	0.025224	latrophilin 3 splice variant abbh
AF111095	6.32	0.02697	latrophilin 3 splice variant bbbg

CHAPTER 5 Table 6

TABLE 6. Genes affected by ncp BVDV infection in BFM cells

Genbank No.	FC	P value	Description
UP			
NM_178108	8.35	1.58E-07	2',5'-oligoadenylate synthetase 1, 40/46kDa (OAS-1)
U96014	7.75	0.00067006	ubiquitin cross-reactive protein (UCRP, ISG15)
NM_173914	6.53	0.000176826	galanin (GAL)
AY650038	5.78	0.00115526	2'-5' oligoadenylate synthetase 1z (OAS-1z)
BC102471	5.73	0.0003769	OAS-like
XM_872122	5.45	0.032382	Interferon-induced protein 44 (Antigen p44, Non-A non-B hepatitis-associated microtubular aggregates protein)
NM_173940	5.21	0.04491	myxovirus (influenza virus) resistance 1, interferon-inducible protein p78 (mouse) (Mx1)
XM_001253432	5.10	0.00027598	ATP-binding cassette sub-family A member 1
XR_028579	4.82	0.00035086	Membrane-associated phosphatidylinositol transfer protein 3 (NIR-1)
BC114759	4.78	0.27296	leucine rich repeat containing 6 (testis)
AY486455	4.78	3.60E-05	alpha-glucocorticoid receptor (GR-A)
BC111664	4.72	0.0049956	extra spindle pole bodies homolog 1
XM_584000	4.66	0.0036156	Bone marrow stromal cell antigen 2
XM_603032	4.66	0.4607	ATP-binding cassette transporter C4
XR_027463	4.65	0.0128522	Eukaryotic translation elongation factor 2
XM_607721	4.59	2.07E-07	homeostatic thymus hormone alpha
AY862879	4.54	0.0068328	large conductance calcium-activated potassium channel alpha subunit isoform A (Kcnma1)
XM_870361	4.43	0.0040848	Tripartite motif-containing 56
NM_174366	4.33	0.006007	ISG15 ubiquitin-like modifier (ISG15)
BT025389	4.24	0.3368	interferon-induced protein with tetratricopeptide repeats 2 (IFIT2)
BC118312	4.22	0.00091436	cDNA clone IMAGE:8284552.
XM_001249644	4.12	9.41E-05	hypothetical protein LOC781234
XM_001253986	4.04	0.031546	mKIAA1477 protein
XM_587985	4.01	0.055762	lethal giant larvae homolog 2
XM_001256258	3.99	0.36554	hypothetical protein LOC789518
XR_027443	3.91	0.11797	LAR-interacting protein 1a (LOC781635)
XM_001255138	3.89	0.00101938	precollagen-D
AB060169	3.88	0.064088	Mx1B GTP-binding protein
NM_001014940	3.77	0.03276	transmembrane protein 35 (TMEM35)
XM_001251051	3.77	0.0065418	KIAA1694 protein
DOWN			
XM_001252457	10.49	0.189132	mitogen-activated protein kinase 10 (MAPK10, JNK3)
XM_001254378	6.92	NA	hypothetical protein LOC786805
BC112590	4.61	0.032914	Bos taurus hypothetical protein MGC137255
XM_617438	4.56	0.02415	Bos taurus similar to solute carrier 19A3 (LOC537280)
BT025464	4.04	0.106282	tumor-associated calcium signal transducer 1 (TACSTD1)
NM_174314	3.80	0.00073862	fatty acid binding protein 4, adipocyte (FABP4)
XM_589483	3.78	0.029084	complement component C5 (LOC512045)
BC118130	3.72	0.14532	hypothetical protein LOC790858
AF012902	3.66	0.076488	plasmalemmal cation channel protein (trp-3)
X91503	3.65	0.0169124	PAS-4 protein
M64756	3.62	NA	beta-casein
XM_001251602	3.57	0.52636	Protein tyrosine phosphatase, receptor type, f polypeptide (PTPRF), interacting protein (liprin), alpha 1
BC102339	3.50	0.053812	interferon-induced transmembrane protein
BC103112	3.43	0.021682	CD36 molecule (thrombospondin receptor)
XR_027448	3.37	0.0190574	beta 1,4-N-acetylgalactosaminyltransferase-transferase-III
XM_615283	3.36	0.077474	RIKEN cDNA 2300009A05 gene (LOC535251)
XM_584034	3.35	0.000081878	Putative lymphocyte G0/G1 switch protein 2, transcript variant 2
XM_864682	3.25	0.0101886	GTPase, IMAP family member 5, transcript variant 2
D45364	3.23	0.05016	PAS-4
XM_614279	3.23	0.00035218	leucine-rich glioma inactivated protein 2
BC123395	3.22	0.088828	Rap1 GTPase-activating protein 1 (Rap1GAP)
S37093	3.15	0.0031714	preproendothelin-1
XM_001252795	3.12	0.022612	hypothetical protein LOC784515
NM_181010	3.12	0.008115	endothelin 1
XM_001256274	3.12	0.75416	myodulin
BC120175	3.10	0.00170158	Pentraxin-related protein PTX3 precursor (Tumor necrosis factor-inducible protein TSG-14)
XM_001256826	3.07	0.120154	Heat shock transcription factor, Y linked 2
XM_001254657	2.94	0.199532	hypothetical protein LOC787186
NM_194465	2.92	0.00029418	IP3 receptor associated cGMP kinase substrate isoform b (MRVI1), transcript variant 2
Z86037	2.91	0.0170298	beta-2-adrenergic receptor

[a]NA, not available

CHAPTER 5 Table 7

TABLE 7. Genes affected by cp BVDV infection in MDBK cells

Genbank No.	FC	P value	Description
UP			
XM_001253379	74.40	1.331E-05	Cytochrome P450, family 3, subfamily A, polypeptide 5 (CYP3A5)
BC103310	52.72	4.06E-09	interleukin 8 (IL-8)
BT021051	35.87	6.639E-05	chromosome 8 open reading frame 4 (c8orf4, TC-1)
XM_602397	38.06	0.017724	cystine/glutamate exchanger
XM_595414	35.44	0.0001275	cytochrome P450 CYP3A24
NM_001076103	34.38	4.895E-05	Tribbles homolog 3 (TRB-3)
XM_001253556	34.01	0.0021376	Fibroblast growth factor 21 (FGF-21)
XR_028169	33.93	0.000514	Aldehyde dehydrogenase 1 family, member L2 (ALDH1L2)
XM_595759	30.30	0.0001249	Inhibin, beta E
S77841	24.21	4.987E-08	follistatin
XM_582369	22.79	0.0065608	ChaC, cation transport regulator homolog 1
XM_869548	22.68	0.0073542	Chromosome 6 open reading frame 146 (c8orf146)
NM_174554	13.56	0.0003647	insulin-like growth factor binding protein 1 (IGFBP1)
XM_580907	18.21	0.0002145	nerve growth factor, beta polypeptide (βNGF)
XM_584419	17.53	0.0026926	polymeric immunoglobulin receptor 3
XM_001257028	17.01	7.468E-06	dual specificity phosphatase 4, MKP-2
NM_001081512	15.39	0.0027842	sprouty homolog 4 (SPRY4)
D89049	13.16	0.0009045	oxidized low density lipoprotein (lectin-like) receptor 1 (OLR1)
NM_173934	14.73	0.0004063	lumican
XM_871003	13.28	0.0002411	Growth differentiation factor 15
XR_027689	11.72	0.0002734	glucose transporter type 3
XM_593270	10.87	0.002299	Coiled-coil domain containing 85B
BT021571	9.93	0.122906	secreted phosphoprotein 1 (osteopontin, bone sialoprotein I, early T-lymphocyte activation 1, SPP1)
XM_582419	9.92	0.0004534	amphiregulin long form
BC123386	9.52	0.000276	sestrin 2
XM_612436	9.34	0.0063788	E1A-F, transcript variant 1
NM_174144	9.12	0.0048044	pim-1 oncogene (PIM1)
XM_001256207	8.97	1.10E-05	hypothetical protein LOC789455
U09198	8.82	5.80E-06	noradrenaline transporter
U52690	8.66	0.0012415	retinal glycine transporter (GlyT-1Ab)
DOWN			
XM_583286	17.27	0.0004182	TXNIP, transcript variant 1
BC119892	14.19	0.0133394	glial fibrillary acidic protein
XM_868524	12.77	0.0040026	renal organic anion transporter 3 (OAT3)
XM_585917	11.41	0.0002095	nwardly rectifying K+ channel
XM_586655	10.33	0.044138	calpain 6
XR_027984	9.46	0.0064924	F-box protein 40
XM_871022	9.46	0.0039462	voltage-dependent calcium channel gamma-4 subunit
XM_001251873	8.74	6.49E-05	fertilin alpha (ADAM 1)
XM_593111	8.29	5.65E-07	I beta-1,6-N-acetylglucosaminyltransferase A form
BC114647	7.93	0.0028178	C1orf110
NM_001045886	7.84	0.0009059	phenazine biosynthesis-like protein domain containing (PBLD)
XM_001250797	7.82	2.19E-05	hypothetical protein LOC782600
XM_595484	7.70	0.002534	kelch-like 14
XM_599177	7.53	0.0006639	multidrug resistance protein 2; MRP2
XM_607511	7.39	0.001163	neo-poly(A) polymerase (PAPOLG)
XM_611708	7.34	0.0001099	dJ85M6.4 (novel 58.3 KDA protein)
XM_001250348	7.28	0.0001348	Bos taurus hypothetical protein LOC782263
XM_588231	7.28	0.0159368	Bos taurus similar to KIAA1881 protein, S3-12
XM_586897	6.92	0.0055416	Bos taurus similar to sprouty homolog 3
XM_584296	6.66	0.000921	coiled-coil domain containing 138
XM_611412	6.64	0.051586	imprinted maternally expressed untranslated mRNA (H19) on chromosome 29
XM_595033	6.62	0.0014528	phosphoinositide-binding proteins
XM_584904	6.55	9.25E-07	peptidyl arginine deiminase, type IV
XM_615409	6.54	0.01329	FYN binding protein (FYB-120/130)
XM_001253683	6.43	0.0012351	Bos taurus hypothetical protein LOC785769
XM_001252723	6.40	0.0013411	transcription factor LBP-9
XM_605364	6.37	0.000479	UDP glucuronosyltransferase 2 family
NM_001034431	6.36	0.00657	erythrocyte membrane protein band 4.9 (dematin, EPB49)
XM_616320	6.33	0.0006094	pleckstrin homology domain containing, family H (with MyTH4 domain) member 2
XM_603302	6.32	0.0128096	DNAH1/KIAA1410 variant protein

CHAPTER 5 Table 8

TABLE 8. Genes affected by ncp BVDV infection in MDBK cells

Genbank No.	FC	P value	Description
UP			
AF355147	11.63	0.0006019	GTP-binding protein Mx2
NM_178108	11.59	3.25E-06	2',5'-oligoadenylate synthetase 1, 40/46kDa (OAS-1)
BC102471	6.54	0.0031304	OAS-like
XM_870511	4.34	0.29318	Cytochrome P450, family 3, subfamily A, polypeptide 5 (CYP3A5)
XM_001255504	4.19	NA	APEG precursor protein
XM_602397	3.77	0.024842	cystine/glutamate exchanger (LOC524078)
BC102318	3.62	0.107438	ISG15 ubiquitin-like modifier
AB004301	3.52	0.0036264	growth differentiation factor-5
M26146	3.51	NA	deoxynucleotidyltransferase (DNTT)
XR_028805	3.45	0.0048678	histamine H3 receptor
XM_595759	3.41	0.0004046	Inhibin, beta E
XM_588125	3.20	0.0061318	ESM-1 protein
NM_001035490	3.10	0.0005807	chromosome 8 open reading frame 4 (C8ORF4)
BC105455	3.08	0.002283	radical S-adenosyl methionine domain containing 2
S77727	3.05	0.010693	endothelium-specific clone A1
AF257506	2.96	0.0149952	stanniocalcin
S77841	2.91	6.40E-05	follistatin
XR_028169	2.90	0.0006532	Aldehyde dehydrogenase 1 family, member L2
XM_001253556	2.87	0.0010989	Fibroblast growth factor 21
U32251	2.87	0.028418	immunoglobulin lambda light chain variable region
AY650038	2.81	0.071738	2'-5' oligoadenylate synthetase 1z (OAS-1z)
NM_181667	2.81	0.53116	ADAM metallopeptidase with thrombospondin type 1 motif, 4 (ADAMTS4)
DQ777771	2.81	0.0033868	breast cancer and salivary gland expression protein (BASE)
XM_868038	2.81	0.059078	solute carrier family 6 (neurotransmitter transporter, GABA)
XM_584000	2.79	0.0028078	Bone marrow stromal cell antigen 2
XM_618422	2.77	0.798	ephrin receptor EphA5
NM_001045936	2.77	0.021744	family with sequence similarity 109, member B (FAM109B)
M64756	2.76	NA	beta-casein
BC126798	2.72	0.062832	galanin
XM_603241	2.70	0.004833	olfactory receptor Olr804
DOWN			
M36808	4.70	0.145156	cellular retinoic acid-binding protein (CRABP)
XM_001254883	4.17	0.06457	chromosome 20 open reading frame 30
AB115780	3.79	0.22298	claudin 3
NM_001001853	3.58	0.0048334	neuroglobin (NGB)
XM_001256109	3.45	0.34242	nucleoside-diphosphate kinase
XM_594791	3.29	0.030082	xPRL-1
XM_870965	3.24	0.10499	Myeloid-associated differentiation marker
BC113271	3.23	0.169226	extracellular signal-regulated kinase 7 (ERK7)
XR_027734	3.22	0.0034396	hypothetical protein LOC782588
XR_027748	3.21	0.0024072	elongation factor 1 alpha
AY741374	3.20	0.0065442	NG010008A20E03
XM_001254447	3.17	0.166508	Acetyl-Coenzyme A acyltransferase 2 (mitochondrial 3-oxoacyl-Coenzyme A thiolase)
XM_586655	3.17	0.0311	calpain 6
AJ488281	3.15	0.0023744	alpha-2C adrenergic receptor (adra2c gene)
AB252572	3.11	0.0024326	urocortin 2
BC112472	3.10	0.072174	major histocompatibility complex, class II, DQ alpha 5
AB099019	3.08	5.38E-07	ubiquinol-cytrochrome-c reductase (subunit II)
XM_001250610	3.05	0.095294	myosin XV
XM_871215	2.97	0.02048	thrombin inhibitor
XM_001255183	2.94	0.042904	hypothetical protein LOC787983
XM_001249557	2.94	0.0192264	ribosomal protein
XM_001251215	2.93	0.0008602	hypothetical protein LOC782582
NM_001013601	2.93	0.52374	histocompatibility complex, class II, DQ alpha, type 1 (BOLA-DQA1)
XM_001252657	2.88	0.22178	hypothetical protein LOC784310
AY834254	2.87	0.0115422	chemokine receptor 3 (CXCR3)
NM_001034432	2.86	0.078196	cAMP responsive element binding protein 3-like 3 (CREB3L3)
XM_608690	2.85	0.2684	hypothetical LOC530225
XR_027256	2.84	0.003694	Elongation factor protein 4
NM_001046121	2.84	0.0173722	solute carrier family 11 (proton-coupled divalent metal ion transporters), member 2
BC116161	2.82	0.025114	hypothetical protein MGC140790

[a]NA, not available

CHAPTER 6

Inhibition of sphingosine kinase by bovine viral diarrhea virus NS3 is crucial for efficient viral replication and cytopathogenesis

Journal of Biological Chemistry (2009) In press

Abstract

Sphingosine-1-phosphate (S1P) is a bioactive sphingolipid implicated in diverse cellular functions including survival, proliferation, tumorigenesis, inflammation, and immunity. Sphingosine kinase (SphK) contributes to these functions by converting sphingosine to S1P. The author reports here that the nonstructural protein NS3 from bovine viral diarrhea virus (BVDV), a close relative of hepatitis C virus (HCV), binds to and inhibits the catalytic activity of SphK1 independently of its serine protease activity, whereas HCV NS3 does not affect SphK1 activity. Uncleaved NS2-3 from BVDV was also found to interact with and inhibit SphK1. The author suspects that inhibition of SphK1 activity by BVDV NS3 and NS2-3 may benefit viral replication, because SphK1 inhibition by siRNA, chemical inhibitor, or overexpression of catalytically inactive SphK1 results in enhanced viral replication, although the mechanisms by which SphK1 inhibition leads to enhanced viral replication remain unknown. A role of SphK1 inhibition in viral cytopathogenesis is also suggested as overexpression of SphK1 significantly attenuates the induction of apoptosis in cells infected with cytopathogenic BVDV. These findings suggest that SphK is targeted by this virus to regulate its catalytic activity.

Introduction

BVDV NS3 exhibits serine protease and helicase/ATPase activities that require its cofactor NS4A (Xu *et al.*, 1997). NS3/4A protease is essential for generating mature NS proteins that are required for viral replication. HCV NS3/4A is well characterized and has been shown to suppress type-I interferons (IFNs) by cleaving the cellular IFN mediators IPS-1 and TRIF (Li *et al.*, 2005; Li *et al.*, 2005). However, neither IFN suppression nor cellular targets have been identified for the BVDV NS3/4A protease (Chen *et al.*, 2007). Moreover, little is known about the regulation of cellular signaling by BVDV NS2-3, NS3, and NS3/4A, which is crucial for the control of both viral replication and biotype.

Recent studies on the mechanisms of viral replication revealed that HCV RNA synthesis occurs on a lipid raft membrane structure where the active viral replicase complex is found (Aizaki *et al.*, 2004; Gao *et al.*, 2004). The significance of the lipid raft as a scaffold for viral replication is further demonstrated by the identification of a novel HCV replication inhibitor, NA255, which prevents the biosynthesis of sphingolipids, the major components of lipid rafts (Sakamoto *et al.*, 2005). Administration of NA255 results in disruption of the HCV replicase complexes from the lipid rafts. This report proposes that the interaction between HCV NS5B and sphingomyelin on lipid rafts plays a crucial role for HCV RNA replication. Cellular sphingolipid metabolism is regulated by a large number of converting enzymes that maintain a homeostasis (Spiegel & Milstien, 2003) but viral mechanisms that affect the sphingolipid metabolism to facilitate viral replication have yet to be identified.

In a search for potential host proteins that interact with BVDV NS3, the author identified sphingosine kinase 1 (SphK1) as a binding partner of NS3 using the yeast two-hybrid system. SphK1 is a lipid kinase that catalyzes the phosphorylation of sphingosine to form

sphingosine-1-phosphate (S1P), a bioactive sphingolipid implicated in diverse cellular functions, including proliferation, survival, tumorigenesis, development, inflammation, and immunity (Shida *et al.*, 2008; Spiegel & Milstien, 2003). Here, the author analyzed the biological significance of the SphK1 interaction with NS3, NS2-3, and NS3/4A. Using purified recombinant SphK1 and NS3, SphK activity was inhibited by the direct association with NS3 via its N-terminal domain, independently of its serine protease activity. The inhibition appears to be specific for BVDV NS3 because HCV NS3 had no effect on SphK activity. Using specific chemical inhibitors, small interfering RNA (siRNA), and a catalytically inactive mutant of SphK1, the author investigated the significance of SphK inhibition in the viral replication.

The present study is the first report demonstrating that SphK1 is targeted by a virus to inhibit its catalytic activity, and this mechanism may contribute to the efficient replication and pathogenesis of BVDV.

Materials and methods

Reagents and antibodies. D-*erythro*-sphingosine and sphingosine kinase inhibitor (SKI) (French *et al.*, 2003) were purchased from Calbiochem (La Jolla, CA, USA). S1P was obtained from Cayman Chemical (Ann Arbor, MI, USA). Anti-Flag M2 monoclonal antibody (mAb; IgG1), anti-Myc mAb (IgG1), and isotype control IgG1 mAb were from Sigma (St. Louis, MO, USA). Anti-BVDV NS3 (IgG2a) and anti-GAPDH mAbs were from TropBio (Townsville, Australia) and Ambion (Austin, TX, USA), respectively. Rabbit polyclonal antibodies (pAbs) against calnexin and SphK1 were from Stressgen (Victoria, Canada) and Exalpha (Maynard, MA, USA), respectively. Mouse pAb against junctional adhesion molecule 1 (JAM-1) was described previously (Makino *et al.*, 2006). Goat anti-mouse IgG, IgG1, IgG2a, or anti-rabbit IgG antibodies conjugated with Alexa-488, Alexa-488, Alexa-594, or Alexa-568, respectively, were from Invitrogen (Carlsbad, CA, USA). Rabbit pAb against HCV NS3 was kindly provided by Dr. Michinori Kohara (the Tokyo Metropolitan Institute of Medical Science, Tokyo, Japan). Protein concentrations in samples were determined with the Protein Quantification Kit-Rapid (Dojindo, Rockville, MD, USA) using bovine serum albumin as a standard. Molybdenum blue spray was from Sigma. Recombinant human SphK1 (hSphK1) was purchased from BPS Bioscience (San Diego, CA, USA).

Cells and viruses. MDBK, LB9.K, and human embryonic kidney HEK293 cell lines were maintained in DMEM supplemented with 5%, 10%, and 10% fetal calf serum (FCS), respectively, at 37°C in a humidified 5% CO_2 atmosphere. MDBK and LB9.K cells were confirmed to be free of BVDV by reverse transcriptase polymerase chain reaction (RT-PCR). BVDV strains KS86-1cp, KS86-1ncp, and Nose have been described previously (Nagai *et al.*,

2003). Unless otherwise indicated, MDBK and LB9.K cells were infected with BVDV using a multiplicity of infection (MOI) of 5 for 1 h, washed twice with FCS-free DMEM, and incubated in DMEM containing 5% or 10% FCS, respectively. Viral titration was performed as described in CHAPTER 5.

RNA extraction. Total RNA was extracted using the SV Total RNA Isolation System (Promega, Madison, WI, USA) according to the manufacturer's protocol.

Plasmids. The bovine SphK1 complementary DNA (cDNA; GenBank database accession number XM_870939.1) was generated from total RNA extracted from MDBK cells by RT-PCR using primers that incorporated *Eco*RI and *Eco*RV sites at the 5' and 3' ends, respectively. Mammalian expression vector of N-terminally Flag-tagged bovine SphK1, designated pFlag-SphK1, was generated by cloning the SphK1 cDNA into pFLAG-CMV2 (Sigma) using *Eco*RI and *Eco*RV sites. The fragments encoding a series of deletion mutants of SphK1 were generated by PCR-mediated site mutagenesis using pFlag-SphK1 as a template. The fragment of catalytically inactive SphK1^{G177D} was generated by PCR-mediated mutagenesis using pFlag-SphK1 as a template with the mutagenic primer 5'-TCGTGGATCAGCCCATCATCGGACATGACCACCAG-3' to substitute Gly^{177} to Asp. The mammalian expression vectors of BVDV NS proteins were generated using SRα promoter vector, pME18S. The Myc-tag sequence together with multiple cloning site from pGBKT7 was amplified by PCR using pGBKT7-NS3 described below as a template and cloned between *Xho*I and *Pst*I sites of pME18S vector. A DNA fragment encoding BVDV NS3, NS2-3, NS3/4A and NS5A was generated from BVDV Nose strain (genotype 1a;

GenBank database accession number AB078951) by SuperScript III One-Step RT-PCR System with Platinum *Taq* High Fidelity (Invitrogen) using primers that incorporated *Nde*I and *Pst*I sites at the 5' and 3' ends, respectively. The fragments were then cloned into pME18S-Myc using *Nde*I and *Pst*I sites to generate pME-NS3, pME-NS2-3, pME-NS3/4A and pME-NS5A. A series of N-terminal deletion mutants of NS3 was generated by PCR-mediated site mutagenesis using pME-NS3 as a template. The fragment of serine protease-negative NS3/4A^{S2051A} was generated by PCR-mediated mutagenesis using pME-NS3/4A as a template with the mutagenic primer 5'-AATATAGGCAGGCCCGCCCATCCCTTCAAGTT-3' to substitute Ser^{2051} to Ala. Hybrid CMV enhancer/ chicken β-actin (CAG) promoter-driven pME18S vectors, termed pCAG, encoding BVDV NS proteins were constructed by a replacement of the SRα promoter with the CAG promoter fragment from pCAGGS vector using *Ssp*I and *Xho*I sites of pME18S vectors. pEF-HCV NS3/4A, which contains HCV NS3/4A cDNA of HCV HCR6 strain (genotype 1b; GenBank database accession number AY045702) cloned into pEF-1 vector (Invitrogen), was kindly provided by Dr. Michinori Kohara (The Tokyo Metropolitan Institute of Medical Science, Tokyo, Japan). All constructs were confirmed by sequencing with an ABI PRISM 3150 genetic analyzer (Applied Biosystems, Tokyo, Japan).

Yeast Two-Hybrid Screening. Potential interacting partners of NS3 were sought using the yeast two-hybrid system according to the manufacturer's manual of MATCHMAKER Library Construction & Screening Kit (Clontech, Palo Alto, CA). The N-terminal domain of NS3 (amino acids 1889 to 2032) derived from BVDV Nose strain was amplified by RT-PCR using primers that incorporated *Nde*I and *Eco*RI sites at the 5' and 3' ends, respectively, and cloned

into the corresponding restriction sites of pGBKT7 in-frame with the Gal4 DNA-binding domain to express N-terminally Myc-tagged partial NS3, designated pGBKT7-NS3. For the construction of MDBK cDNA library, first strand cDNA was synthesized using random primers from 0.6 μg mRNA, which was purified from total RNA using *oligotex-dT30<Super>* mRNA Purification Kit (TaKaRa, Shiga, Japan), and double-stranded cDNA (ds cDNA) amplified by 22 cycles Long Distance (LD) PCR as described in manufacturer's protocol. *Saccharomyces cerevisiae* strain AH109 was transformed with the bait plasmid pGBKT7-NS3, and selected in synthetic medium lacking tryptophan. A positive clone harboring pGBKT7-NS3 was confirmed to express N-terminal 142 amino acids of NS3 protein with anti-Myc mAb by Western blot analysis (data not shown). The MDBK cell ds cDNA library together with *Sma*I-linearized pGADT7-Rec (Clontech) was cotransformed in an AH109 clone harboring pGBKT7-NS3 to clone cDNA into the GAL4 AD expression vector pGADT7-Rec by homologous recombination. The transformed yeast cells were grown on agar plates of synthetic medium lacking histidine, leucine and tryptophan containing 20 μg/ml X-α-Gal (5-bromo-4-chloro-3-indolyl-alpha-O-galactopyranoside). Total 145 clones were identified from 1×10^6 colonies screened in the library. The insert DNA fragments of isolated clones were amplified by PCR using LD-Insert Screening Amplimer Sets (Clontech) according to the manufacturer's protocol, and then determined by sequencing.

Transfection and immunoprecipitation. LB9.K cells were transiently transfected using Lipofectamine 2000 (Invitrogen) as described in the manufacturer's protocol. Transfection efficiency of LB9.K cells was typically 80-90%. LB9.K cells were seeded onto 6-well tissue culture plate 24 h before transfection. Cells were then transfected with 4 μg plasmids per well.

At 24 h post-transfection, cells were washed twice with ice-cold phosphate-buffered saline (PBS) and scraped into 0.2 ml of lysis buffer (50 mM Tris-HCl pH 7.5, 150 mM NaCl, 1 mM EDTA, 1% Triton X-100, 20 mM NaF, 1 mM Na_3VO_4) supplemented with Complete protease inhibitor cocktail (Roche Diagnostics, Tokyo, Japan). The lysates equalized with the same amount of proteins were immunoprecipitated with 3 μg of anti-Flag, anti-Myc, anti-BVDV NS3, or control mouse IgG1 mAbs for 2 h at 4°C, respectively. The immune complexes were precipitated by incubation with protein G Sepharose beads (GE Healthcare, Milwaukee, WI, USA) for another 1 h. The agarose beads were washed four times with 1 ml of wash buffer (50 mM Tris-HCl pH 7.5, 150 mM NaCl, 1 mM EDTA, 0.1% Triton X-100, 20 mM NaF, 1 mM Na_3VO_4). The immunoprecipitates were separated by SDS-PAGE and transferred to nitrocellulose membranes (Bio-Rad, Hercules, CA, USA), probed with antibodies, and immunocomplexes detected by enhanced chemiluminescence (ECL). Antibodies used were: horseradish peroxidase (HRP)-conjugated mAbs against Flag (1:1000 dilution; Sigma), Myc (1:1000; Santa Cruz Biotechnology), and a rabbit pAb against NS3 (1:3000). Images were taken by LAS-4000mini image analyzer system (Fujifilm, Tokyo, Japan).

Subcellular fractionation. Cells were harvested into lysis buffer lacking Triton X-100, sonicated, and centrifuged at 1000×g for 10 min. Subcellular fractionation was performed by sequential centrifugation as described previously (Maceyka *et al.*, 2005). In brief, postnuclear supernatants were centrifuged at 17,000×g for 15 min to obtain the inner membrane fraction. The resulting supernatants were centrifuged at 100,000×g for 1 h to obtain cytosolic and pelleted plasma membrane fractions. The pellet containing inner or plasma membrane was resuspended in lysis buffer (volume comparable to supernatant) and sonicated.

Sphingosine kinase assay. Sphingosine kinase activity was determined as described previously (Olivera *et al.*, 1998). The labeled S1P was separated by TLC on silica gel G60 (Whatman, Clifton, NJ, USA) with 1-butanol/ethanol/acetic acid/water (80:20:10:20, v/v) and visualized by autoradiography. The radioactive spots corresponding to S1P were scraped and counted in a scintillation counter.

Generation of recombinant bovine sphingosine kinase 1. pFlag-SphK1 was transfected into HEK293 cells using Lipofectamine 2000 (Invitrogen) to express the Flag-SphK1, which was subsequently purified by binding to the Flag(M2)-Sepharose (Sigma), followed by elution with the Flag peptide (0.2 mg/ml). The eluted Flag-SphK1 was concentrated using Ultrafree-0.5 Centrifugal Filter Device (50,000 Da cutoff; Millipore, Billerica, MA, USA) and diluted in the sphingosine kinase buffer (20 mM Tris-HCl pH 7.4, 20% glycerol, 1 mM β-mercaptoethanol, 1 mM EDTA, 15 mM NaF, 20 mM Na_3VO_4, and 0.5 mM 4-deoxypyridoxine) supplemented with a Complete protease inhibitor cocktail (Roche Diagnostics). This procedure was repeated five times to reduce the concentration of the Flag peptide.

Generation of GST fusion proteins. NS3 and NS3/4A sequence of BVDV Nose strain was amplified by PCR using the plasmid pME-NS3/4A as a template. The PCR product of NS3 or NS3/4A was cloned into bacterial expression vector pGEX5X-2 using *Sma*I and *Not*I sites. HCV NS3 and NS3/4A sequences were amplified by PCR using the plasmid pEF-HCV NS3/4A as a template. The PCR products were then cloned into pGEX5X-1 using *Eco*RI and

*Xho*I sites. BVDV and HCV NS proteins were expressed in *E.coli* BL21 as GST fusion proteins at the N-terminus. Overnight cultures were grown with shaking at 37°C in Luria-Bertani broth containing 50 μg/ml ampicillin and 20 μg/ml chloramphenicol. The culture was then diluted into fresh Luria-Bertani broth containing 50 μg/ml ampicillin and 20 μg/ml chloramphenicol, and grown with shaking at 37°C to an OD_{600} of 0.6–1.0. Expression of the GST fusion proteins was then induced with 1.2 mM isopropyl β-D-thiogalactopyranoside (IPTG), and the cultures were incubated with shaking at 37°C for a further 3 h. The bacterial cells were then harvested by centrifugation at 6000 × *g* for 10 min at 4°C, resuspended in 10 ml of GST-soluble buffer (40 mM Tris-HCl pH 7.5, 5 mM EDTA, 0.5% Triton X-100), and lysed by sonication. The lysates were mixed well and centrifuged at 20,000 × *g* for 20 min at 4°C. The resultant clarified bacterial lysate was then incubated with GSH-Sepharose 4B for 2 h at 4°C with constant mixing. Subsequently, the GSH-Sepharose beads (with bound protein) were pelleted by centrifugation at 3000 × *g* for 5 min at 4°C and washed five times in GST-soluble buffer. These beads were then either used directly in pull-down assay, or the GST fusion proteins eluted by incubation with cold PBS containing 10 mM GSH for 30 min with constant mixing. This elution procedure was repeated three times. Eluted proteins were concentrated by using Ultrafree-0.5 Centrifugal Filter Device (10,000 Da cutoff; Millipore).

Immunofluorescence microscopy. LB9.K cells were seeded on an eight-well chamber slide (Nunc, Roskilde, Denmark) at 2×10^4 per well 24 h before transfection. Nontransfected cells or the cells transfected with Flag-SphK1 were inoculated with BVDV as described in figure legends. At 18 h p.i., cells were washed twice with PBS, fixed with PBS containing 4%

paraformaldehyde, permeabilized with PBS containing 0.5% Triton X-100, and blocked with PBS containing 10% BSA for 10 min. Nontransfected cells were then incubated with anti-calnexin pAb and mouse anti-BVDV NS3 mAb for 1 h followed by incubation with Alexa-568 conjugated goat anti-rabbit IgG and Alexa-488 conjugated goat anti-mouse IgG antibodies for 1 h at room temperature. Transfected cells were double-stained with mouse anti-Flag mAb (IgG1) and mouse anti-BVDV NS3 mAb (IgG2a) followed by Alexa-488 conjugated goat anti-mouse IgG1 and Alexa-594 conjugated goat anti-mouse IgG2a antibodies, or with mouse anti-Flag mAb and anti-calnexin pAb followed by Alexa-488 conjugated goat anti-mouse IgG and Alexa-568 conjugated goat anti-rabbit IgG antibodies. Cells incubated with secondary antibodies were then washed three times with PBS, mounted in Dako fluorescent mounting medium (Dako Corporation, Carpinteria, CA), then sealed and observed under an LSM 510 microscope (Carl Zeiss, Tokyo, Japan).

Measurement of S1P synthesis. LB9.K cells transiently transfected with pCAG vectors encoding BVDV NS proteins or MDBK cells infected with BVDV were incubated for 4 h in phosphate-free DMEM (Invitrogen), then labeled with fresh phosphate-free DMEM containing [^{32}P]orthophosphate (0.2 mCi/ml) and incubated for 4 h at 37 ℃ in a humidified 5% CO_2 atmosphere. Cells were then scraped on ice into 400 μl of methanol/1 M NaCl/5 M NaOH (100:100:3, v/v), then 200 μl chloroform added. Samples were vortexed thoroughly and centrifuged at 14,000 × *g* for 5 min. The upper aqueous phase containing S1P was transferred to a new tube, and acidified through addition of 20 μl 1 M HCl and 400 μl chloroform/methanol/HCl (100/200/1, v/v). Samples were vortexed thoroughly and phases separated by addition of 120 μl chloroform and 120 μl 2 M KCl. After centrifugation, the

lower organic phase was dried under vacuum and resuspended in chloroform, and resolved by TLC as described above. The radioactive spots corresponding to S1P were scraped from the plates and counted in a scintillation counter.

RNA interference. Duplex siRNAs were purchased from Invitrogen. The siRNA sequence targeting SphK1 was 5'-GCAGUGGCCGCUUCUUUGAACUAUU-3' (sense) and 5'-AAUAGUUCAAAGAAGCGGCCACUGC-3' (antisense), corresponded to 634–658 relative to the first nucleotide of the start codon. The sequence used for scrambled control siRNA was 5'-GCAGGCCCGUUUCUUAGCAUUGAUU-3' (sense) and 5'-AAUCAAUGCUAAGAAACGGGCCUGC-3' (antisense). LB9.K cells were transfected with 20 nM siRNA using siLentfect (Bio-Rad) according to the manufacturer's protocol.

Quantitative real-time RT-PCR. cDNA synthesis was performed with the PrimeScript RT Reagent Kit (TaKaRa) according to the manufacturer's protocol. GAPDH mRNA and viral RNA were quantified using Power SYBR Green PCR Master Mix (Applied Biosystems) as described in CHAPTER 3.

Apoptosis assay. The DEVDase activity assay was performed as described in CHAPTER 1 using Ac-DEVD-AMC as a substrate.

Results

Identification of SphK1 as a binding partner of BVDV NS3 and NS2-3.

To identify potential cellular binding partners of BVDV NS3, the author conducted a yeast two-hybrid screen using the N-terminal 142 amino acids of NS3 as bait, and isolated a cDNA clone encoding partial SphK1 from 1 of 145 total positive colonies. The cDNA sequence encoded 164 C-terminal amino acids of SphK1 (Fig. 1A). Employing the cDNA sequence for bovine SphK1 from the GenBank database, specific primers were designed and used to clone a bovine SphK1 by RT-PCR cloning using total RNA isolated from MDBK cells. Subsequently, a catalytically inactive form of bovine SphK1 was constructed by substituting aspartic acid (D) for glycine (G) at position 177 in the ATP-binding site of the diacylglycerol (DAG) catalytic domain, according to the previous study (Pitson *et al.*, 2000). This SphK1^{G177D} was used for further functional studies as a catalytically inactive SphK1. To investigate whether the cloned bovine SphK1 encodes a *bona fide* SphK, LB9.K cells were transiently transfected with expression vectors containing Flag-tagged SphK1. Similar to the previous study (Olivera *et al.*, 1999), SphK activity in cell lysates from LB9.K cells transiently transfected with SphK1 was increased ~300-fold (Figs. 1B & C). By comparison, expression of catalytically inactive SphK1^{G177D} produced no detectable increase in SphK activity. Western blot analysis using anti-Flag antibody revealed a specific protein band with an apparent molecular weight consistent with the predicted size (~55 kDa) of Flag-tagged SphK1, which was absent in vector-transfected cells (Fig. 1C).

To confirm the interaction between NS3 and SphK1, the author cotransfected Flag-SphK1 and Myc-NS3 in LB9.K cells, immunoprecipitated NS3 using an anti-Myc mAb, and determined whether SphK1 was coprecipitated with NS3 by Western blotting. The author

also cotransfected an empty vector or NS5A as a negative control and uncleaved NS2-3. Both NS3 and NS2-3, but neither NS5A nor vector control, coprecipitated with SphK1 (Fig. 1D). The author attempted to express Myc-tagged NS2 in the same way as above to demonstrate that NS2 does not mediate the binding of NS2-3 to SphK1, but failed to express detectable levels of NS2 protein, most likely due to its instability in LB9.K cells (data not shown).

To confirm the specific interaction of SphK1 with NS3 and/or NS2-3 expressed in the context of BVDV infection, the author transfected an expression vector encoding Flag-SphK following virus infections, immunoprecipitated NS3 and NS2-3 with anti-NS3 mAb, and determined binding to SphK1 by Western blotting. When expressed in the context of BVDV-infection, Flag-SphK1 coprecipitated with NS3 and NS2-3 expressed in cp BVDV-infected cells as well as NS2-3 in ncp BVDV-infected cells (Fig. 1E). To further demonstrate whether NS3 and NS2-3 from BVDV infection interacts with endogenous SphK1, NS3 and NS2-3 were immunoprecipitated with anti-NS3 mAb from the lysates of the BVDV-infected MDBK cells, and their binding to SphK1 was determined by Western blotting using anti-SphK1 pAb. As shown in Fig. 1F, specific interaction of endogenous SphK1 with NS3 and NS2-3 was detected.

NS3 and NS2-3 colocalize with SphK1 in membrane fractions.

Previous studies indicated that BVDV NS3 and NS2-3 are predominantly localized to the endoplasmic reticulum (ER) in cultured cells (Zhang *et al.*, 2003) and SphK1 is diffusely distributed in the cytoplasm (Maceyka *et al.*, 2005). To investigate the localization of these proteins in BVDV-infected LB9.K cells, the author transfected the cells with an expression vector encoding Flag-SphK1 and performed immunostaining using anti-Flag and anti-NS3

mAbs. For positive identification of the ER, cells were stained with a calnexin pAb. The staining patterns of NS3 and NS2-3 (cp BVDV) or NS2-3 (ncp BVDV) overlapped with those of calnexin (Fig. 2B) and partially with those of SphK1 (Fig. 2A). SphK1 also partially colocalized with calnexin (Fig. 2C). The author further examined the localization of endogenous SphK1 and NS3 by subcellular fractionation. The majority of SphK1 and NS3 were found to localize in inner and plasma membrane fractions in MDBK cells (Fig. 2D). Although previous studies have shown that SphK1 in many different cell types is mainly cytosolic (Kihara *et al.*, 2006; Pitson *et al.*, 2003), these data suggest that bovine SphK1 localizes to both cytosolic and membrane fractions.

Mapping the NS3-binding domain on SphK1.

Deletion mutagenesis of SphK1 was performed to identify the NS3-binding domain on SphK1 (Fig. 3A). Flag-tagged SphK1 mutants were coexpressed with Myc-NS3 and immunoprecipitated with anti-Flag mAb. Myc-NS3 coprecipitated with SphK1 mutants containing a region downstream of CaM, which consists of amino acid residues 326–386. This region was also present in the partial SphK1 cDNA sequence isolated from the positive yeast colony in the yeast two-hybrid screen (Fig. 1A). Flag-tagged SphK1 C-terminal deletion mutants of this region were constructed to further determine the NS3-binding domain. The SphK1 mutant consisting of amino acid residues 1–361 coprecipitated with Myc-NS3 but the mutant with residues 1–349 did not (Fig. 3B). Furthermore, the deletion mutant containing amino acids 1–361, but not 1–358, coprecipitated with NS3 (Fig. 3C), suggesting that amino acids 359–361 of SphK1, or the protein folding affected by these residues, are critical for its binding to NS3..

Mapping the SphK1-binding domain on NS3.

Because the N-terminal 142 amino acid residues of NS3 were sufficient to bind to SphK1 in the yeast two-hybrid screen, the author constructed N-terminal deletion mutants of NS3 to determine the regions of NS3 that bind to SphK1 (Fig. 4A). Myc-tagged NS3 mutants were coexpressed with Flag-SphK1 and immunoprecipitated using the anti-Myc mAb. Flag-SphK1 coimmunoprecipitated with the dN1 mutant lacking amino acids 1–32, but not with the dN2 mutant lacking amino acids 1–67 (Figs. 4A & B). As expected from the yeast two-hybrid screen, the N1 mutant containing NS3 amino acids 1–142 coimmunoprecipitated with SphK1, suggesting that amino acids 33–66 of NS3 are critical for its binding to SphK1.

The dose-dependent inhibition of SphK1 activity by NS3.

The author performed *in vitro* SphK assays in the presence and absence of NS3 to assess the functional significance for the binding of NS3 to SphK1. Glutathione S-transferase (GST) fusion proteins GST–NS3, GST–NS5A, or GST alone were expressed and purified from *E. coli* strain BL21 (Fig. 5A). The author failed to express GST–NS2-3, most likely due to toxicity of its highly hydrophobic NS2 domain (Lackner *et al.*, 2004). Recombinant bovine SphK1 (rSphK1) was purified from lysates of HEK293 cells transiently transfected with the Flag-tagged SphK1 expression vector (Fig. 5A). Glutathione (GSH)-Sepharose beads were used to bind and precipitate GST–NS3, GST–NS5A, or GST alone in the presence of rSphK1. The GST pull-down experiments confirmed a specific interaction between rSphK1 and GST–NS3 (Fig. 5B). While GST–NS5A and GST alone showed no specific binding to rSphK1 (Fig. 5B) and had no significant effect on SphK1 activity, GST–NS3 inhibited SphK1

catalytic activity dose-dependently with maximal inhibition (~90%) attained using above a 5-fold molar excess of NS3 to SphK1 (Fig. 5C).

Suppression of SphK1 activity by NS3, NS2-3, and NS3/4A.

Uncleaved NS2-3 and NS3 are expressed in cp BVDV-infected cells, whereas only NS2-3 is detectable in ncp BVDV-infected cells after 9 h p.i. (Lackner *et al.*, 2004). Therefore, the author assessed possible differences in the regulation of SphK1 activity among NS3, NS2-3, and NS3/4A. Plasmids encoding BVDV NS3, NS2-3, and NS3/4A proteins were transiently transfected into LB9.K cells, and the endogenous SphK activity in the cell lysate was measured using the *in vitro* SphK assay. Transfection with various doses of plasmid encoding NS3 exhibited a dose-dependent reduction in SphK activity by up to 30% (Fig. 5D). Cells transfected with plasmids encoding NS2-3 and NS3/4A, showed endogenous SphK activity that was reduced by approximately 15% and 30%, respectively (Fig. 5E). It seemed that the expression of NS4A cofactor does not affect the inhibitory effect of NS3 on SphK1 activity. To further determine whether inhibition of SphK1 activity by NS3 depends on its serine protease activity or not, the author examined the effect of the S2051A NS3/4A mutant, whose serine protease activity is eliminated and the protease-dependent cleavage between NS3 and NS4A is deficient (Xu *et al.*, 1997), on SphK1 inhibition. As shown in Fig. 5E, S2051A mutant efficiently inhibited endogenous SphK1 activity to the same extent as wild type NS3/4A. In addition, SphK1 exhibited no putative NS3/4A recognition sites (Xu *et al.*, 1997) and no detectable degradation when coexpressed with Myc-NS3/4A (data not shown), suggesting that SphK1 inhibition by NS3 is independent of its serine protease activity. In the cells transfected with the NS3 expression plasmid, the endogenous S1P synthesis was reduced

by approximately 15% (Fig. 5F). The weaker inhibition of SphK1 by NS2-3 appeared to be the result of lower expression levels of NS2-3 relative to NS3 and NS3/4A (Fig. 5E, inset). However, the higher level of NS2-3 obtained from lysates of ncp BVDV-infected MDBK cells by immunoprecipitation was shown to significantly inhibit SphK activity by ~50%, similar to the inhibition observed with the NS2-3 and NS3 from cp BVDV-infected MDBK cell lysates (Fig. 5G). These results suggest that SphK1 activity is down-regulated by NS2-3 as well as NS3.

Down-regulation of SphK1 activity and S1P synthesis in BVDV-infected cells.

The kinetics of endogenous SphK1 activity was examined in the context of BVDV infection. At 6 and 12 h p.i., SphK activity in MDBK cells infected with both BVDV biotypes was unaffected or slightly up-regulated. However, at later than 18 h p.i., a time-dependent decrease in SphK activity was observed, which culminated to maximal reductions of 30% and 50% at 48 h p.i. for cells infected with ncp BVDV and cp BVDV, respectively (Fig. 6A). No change in SphK1 mRNA levels was observed in MDBK cells at 24 h p.i. with either BVDV biotype (data not shown). Therefore, it appears unlikely that SphK1 activity is down-regulated at the transcriptional level; it probably occurs concomitantly with the accumulation of newly synthesized viral proteins, NS3 and NS2-3, in the cells. Cellular S1P synthesis levels were reduced by 10% and 20% in cp BVDV- and ncp BVDV-infected cells, respectively, as SphK activity decreased (Fig. 6B).

Overexpression of SphK1 reduced apoptosis induced by cp BVDV infection.

The studies in CHAPTERs 1 and 2 showed that apoptotic cell death induced by

cp BVDV infection is mediated through activation of DEVDase activity. Since several previous studies have demonstrated anti-apoptotic effects of SphK1 (Olivera *et al.*, 1999; Taha *et al.*, 2006; Xia *et al.*, 1999), the author tested whether inhibition of SphK1 by BVDV had any influence in the context of apoptotic induction by overexpression of SphK1 and catalytically inactive SphK1^{G177D}. Overexpression of SphK, but not SphK1^{G177D}, resulted in an approximately 40% reduction in DEVDase activity in cp BVDV-infected cells, whereas mock-infected or ncp BVDV-infected cells were almost unaffected (Fig. 6C). Because overexpression of SphK1 had no significant effect on viral replication (Figs. 7D & E) but counteracted the activation of DEVDase, these data suggest that apoptotic cell death in cp BVDV-infected cells may be exaggerated by the inhibition of SphK.

Inhibition of SphK1 activity significantly enhanced viral replication.

To examine the influence of SphK activity on BVDV replication, the author measured intracellular viral RNA levels in the presence of SKI, which was identified as a highly selective, noncompetitive inhibitor of SphK (French *et al.*, 2003). SKI treatment increased viral RNA levels of both cp BVDV and ncp BVDV infections approximately 2-fold in a dose-dependent manner (Fig. 7A). To further analyze the effect of SphK1 inhibition on BVDV replication more specifically, LB9.K cells were either depleted of SphK1 by siRNA-mediated knockdown or by overexpression of the catalytically inactive SphK1^{G177D}, and then infected with BVDV. Transfection with siRNA significantly inhibited endogenous SphK1 expression levels (Fig. 7B) as well as endogenous SphK1 activity in LB9.K cells by approximately 50% compared to levels in scrambled siRNA-transfected cells (Fig. 7C). Viral RNA levels from both cp BVDV and ncp BVDV infections increased approximately 2-fold

compared to mock-treated or scrambled siRNA-transfected cells (Fig. 7D). Transfection with SphK1^{G177D} also increased viral RNA levels and titers concomitantly by over 160% (Figs. 7E & F). At 48 h p.i., the viral RNA level from cp BVDV infections was 2.5-fold in cells overexpressing SphK1^{G177D} (data not shown). In contrast, transfection with wild-type SphK1, reaching a 300-fold increase in SphK activity, did not affect viral RNA levels and titers (Figs. 7E & F). The author next examined the effect of FCS addition on BVDV replication as FCS is known to mediate SphK activation (Olivera & Spiegel, 1993). FCS addition resulted in a dose-dependent increase in endogenous SphK1 activity (Fig. 7G), and the viral RNA level was reduced by up to 40% in the presence of 10% FCS and the effect was reversible with the addition of SKI (Fig. 7H). The author also examined the effect of S1P, a metabolite of SphK, on the viral RNA replication. However, addition of 1-10 μM S1P did not affect the viral RNA levels (data not shown). These data collectively suggest that SphK inhibition may allow for enhanced BVDV replication, while it appears that S1P does not regulate BVDV replication.

HCV NS3 does not regulate SphK1 activity.

Since BVDV NS3 was shown to inhibit bovine SphK1 activity, thereby promoting efficient viral replication, it was of interest to determine whether NS3 from HCV, a close relative of BVDV, regulate catalytic activity of hSphK1. The author thus examined the effect of purified recombinant HCV NS3 and NS3/4A expressed in *E.coli* (Fig. 8A) on the catalytic hSphK1 activity *in vitro*. Neither GST-HCV NS3 nor NS3/4A had significant effect on hSphK1 activity, even at 10-fold molar excess to hSphK1 (Fig. 8B). Furthermore, transient transfection into HEK293 cells with pEF-HCV NS3 or NS3/4A did not affect the endogenous SphK1 activity, compared with empty vector-transfected cells (data not shown). Taken

together, hSphK1 activity appears to be regulated neither by HCV NS3 nor by HCV NS3/4A. In contrast, BVDV NS3 suppressed hSphK1 activity efficiently by approximately 80% at 5-fold molar excess to hSphK1 (Fig. 8C). Accordingly, the disruption of SphK1 activity appears to be specific to the BVDV NS3.

Discussion

Sphingolipids are predominant components of biological membranes that also play pivotal roles in signal transduction pathways. In particular, the sphingolipid S1P is an intracellular second messenger and an extracellular ligand with diverse cellular functions including survival, proliferation, differentiation, tumorigenesis, inflammation, and immunity (Shida *et al.*, 2008; Spiegel & Milstien, 2003). Despite the profound importance of S1P, no reports have described the direct regulation of SphK activity by a virus, although some studies showed that SphK activity is up-regulated after infection with human cytomegalovirus or respiratory syncytial virus, contributing to efficient viral replication or cell survival, respectively (Machesky *et al.*, 2008; Monick *et al.*, 2004). In the present study, the author demonstrated that BVDV NS3 or NS2-3, but not HCV NS3, directly binds to and inhibits the catalytic activity of SphK1. Inhibition of SphK1 activity was also observed in the context of BVDV infection. This effect seems independent of additional cofactors or auxiliary proteins because the experiments were performed using purified proteins. Studies are currently underway to determine the amino acid residues of NS3 responsible for SphK1 inhibition.

The involvement of sphingolipids in HCV replication has been well described. Replicase complexes of HCV, a close relative of BVDV, associate with lipid rafts enriched in sphingolipids and cholesterol via NS4B, NS5A, and NS5B (Gao *et al.*, 2004). Although the molecular mechanisms characterizing these raft–viral protein interactions are still largely unknown, a direct association of HCV NS5B with lipid rafts via its finger domain is considered essential for HCV replication (Sakamoto *et al.*, 2005). In the presence of a chemical inhibitor of sphingolipid biosynthesis, the association of NS5B with lipid rafts is disrupted and HCV replication is repressed. Because NS5B from HCV shares structural

similarity with that from BVDV (Choi *et al.*, 2004), it is tempting to speculate that BVDV utilizes similar cellular components for replication. Although the molecular mechanisms responsible for enhanced BVDV replication by SphK inhibition are unknown, one may postulate that BVDV NS3 may alter the proportion of intracellular sphingolipid species through inhibition of SphK1 activity so they are more suited for efficient viral replication. Although the author showed that HCV NS3 does not inhibit SphK1 activity in this study, it will be important to determine whether SphK activity is regulated by HCV through other mechanisms or not.

BVDV replication was enhanced by SphK inhibition (Figs. 7A, C, D & E), while conversely, activation of SphK by FCS treatment reduced viral replication (Fig. 7F). This reduction appears specific to the activation of SphK because it was reversed by supplementation with a chemical inhibitor of SphK. Controversially, overexpression of SphK1 did not alter BVDV replication (Figs. 7D & E) despite an approximately 300-fold increase in the intracellular SphK activity (Figs. 1B & C). Previous studies have proposed the posttranscriptional mechanisms for SphK activation by affecting phosphorylation state of SphK, its translocation, or its interactions with other proteins (Taha *et al.*, 2006). Most notably, phosphorylation of Serine 225 in hSphK1 increases catalytic activity and is necessary for the agonist-induced translocation of hSphK1 to the plasma membrane where sphingosine, the substrate of SphK, is concentrated (Johnson *et al.*, 2002; Pitson *et al.*, 2003). Importantly, localization of SphK1 to the plasma membrane, rather than the total SphK level, is the critical factor for enhanced S1P generation and subsequent biological effects (Pitson *et al.*, 2005). Collectively, the posttranscriptional activation state of SphK appears to be crucial for the efficiency of BVDV replication.

BVDV NS3 possesses serine protease and helicase activities that are crucial for efficient viral replication. More importantly, NS3 is abundantly detected in cells infected with cp BVDV. The author thus hypothesized that an inhibitory interaction between NS3 and SphK1 may be a determinant for the induction of cell death. Unexpectedly, uncleaved NS2-3 also interacted with and catalytically inhibited SphK1, and ncp BVDV infection suppressed SphK activity. Because inhibitory regulation of SphK1 is conserved between both the cp and ncp biotypes, SphK1 inhibition itself is not directly linked to the induction of CPE by BVDV. Previously, the author showed that viral cytopathogenicity is mediated via up-regulation of DEVDase activity triggered by intracellular accumulation of double-stranded RNA (dsRNA), a replicative intermediate, resulting from increased viral RNA replication. Therefore, an inhibitory interaction of NS3 with SphK1 seems to have an indirect role in virus-induced cell death because inhibition of SphK1 activity enhances viral RNA replication, which leads to an accumulation of dsRNA. The expression of NS3 by itself has been suspected to be correlated with induction of cell death because abundant levels of NS3 are detected exclusively in cp BVDV-infected cells. Indeed, a previous study suggested that ectopic expression of NS3 using an adenovirus-based vector is sufficient for the induction of apoptosis (St-Louis *et al.*, 2005). However, in this study, the author observed no changes in morphology or DEVDase activity in cells expressing more abundant NS3 relative to cp BVDV-infected cells using the CAG promoter-driven expression vector (data not shown). Thus, it appears that cell death occurs via intracellular events downstream of NS2-3 autoprocessing, presumably as a result of enhanced RNA replication controlled by NS3 expression (Lackner *et al.*, 2004; Mendez *et al.*, 1998; Vassilev & Donis, 2000).

A pro-survival role of S1P has been demonstrated for cells under stress induced by

trophic deprivation or ceramide addition (Olivera *et al.*, 1999). Additionally, overexpression of SphK1 protects many different types of cell from apoptosis mediated by the corresponding stress induction (Maceyka *et al.*, 2005; Olivera *et al.*, 1999; Taha *et al.*, 2006). In the present study, reduced DEVDase activity was observed after overexpression of SphK in cp BVDV-infected cells. Note that oxidative and ER stresses are common characteristics of cp BVDV infections (Jordan *et al.*, 2002; Schweizer & Peterhans, 1999) directly linked to apoptosis. SphK1 overexpression in cp BVDV-infected cells could function to counteract these pro-apoptotic stresses, thereby causing reduced activation of DEVDase. The combined data suggest that inhibitory interaction of NS3 with SphK1 may have a substantial role in enhancing BVDV-induced apoptosis.

Interactions between S1P and its receptors are being increasingly recognized as important in many aspects of immune responses, including lymphocyte chemotaxis. Given the importance of S1P functions in immunity, BVDV-mediated down-regulation of SphK1 that catalyzes the formation of S1P might possibly contribute to BVDV pathogenesis. Further studies are required to analyze the details of SphK inhibition on lymphoid organ or immune cells in cattle persistently infected with BVDV. Moreover, identification of sphingolipid species that are crucial for viral replication or affected through SphK inhibition by NS3 or NS2-3 may provide new insights into the mechanisms of BVDV pathogenesis.

Figure legends

Figure 1. Specific interaction between SphK1 and BVDV NS3 or NS2-3. (A) Schematic representation of bovine SphK1. Functional domains (Sutherland *et al.*, 2006; Taha *et al.*, 2006), diacylglycerol (DAG) catalytic domain, sphingosine-binding domain (SphBD), and calmodulin-binding domain (CaM) are shown. Partial SphK1 cDNA sequence isolated from a positive clone is indicated by a two-headed arrow. (B) LB9.K cells were transiently transfected with empty vector or SphK1 or catalytically inactive SphK1^{G177D} expression vectors. At 24 h post-transfection, cells were harvested and cytosolic SphK activity measured as described in Materials and methods. Data in a graph on the left panel are the means ± S.D. from three independent experiments, each performed in duplicate. (C) Shown on the lower panel is an autoradiogram of a TLC plate used for separation of S1P. The arrowheads indicate the location of S1P visualized with molybdenum blue spray. The upper panel shows the expression of Flag-SphK1 by Western blotting with anti-Flag mAb. (D) Flag-SphK1 expression vector in combination with empty vector, Myc-tagged BVDV NS5A, NS2-3, or NS3 were cotransfected into LB9.K cells. Proteins immunoprecipitated with anti-Myc mAb (even lanes) or isotype control IgG (Isotype Ct; odd lanes) were subjected to Western blotting using anti-Flag mAb. (E) One hour after inoculation with either KS86-1cp or KS86-1ncp at an MOI of 5, Flag-SphK1 expression vector was transfected into LB9.K cells. At 24 h p.i., BVDV NS3 and/or NS2-3 protein was immunoprecipitated with isotype control IgG or anti-NS3 mAb as indicated. Immunoprecipitated proteins were subjected to Western blotting using anti-Flag mAb. (F) Twenty four hours after infection with either KS86-1cp or KS86-1ncp at an MOI of 5 in MDBK cells, NS3 and/or NS2-3 protein was immunoprecipitated with isotype control IgG or anti-NS3 mAb as indicated.

Immunoprecipitated proteins were subjected to Western blotting using anti-SphK1 pAb. These data were representative of at least three independent experiments.

Figure 2. Colocalization of SphK1 with NS3 or NS2-3 in ER membrane of mammalian cells. LB9.K cells were transiently transfected with Flag-SphK1 expression vector. After 6 h, cells were inoculated with cp BVDV or ncp BVDV and further incubated for 18 h. Transfected cells were immunostained with (**A**) anti-Flag mAb (green) and anti-BVDV NS3 mAb (red), (**B**) anti-BVDV NS3 mAb (green) and anti-calnexin pAb (red), and (**C**) anti-Flag mAb (green) and anti-calnexin pAb (red). (D) MDBK cells were mock-infected or infected with either KS86-1cp or KS86-1ncp at an MOI of 5. At 20 h p.i., cells were lysed and subcellularly fractionated into cytosol (S), inner membrane (IM) (mitochondria, ER, and Golgi), and plasma membrane (PM), as described in Materials and methods. Equal amounts (20 μg) of lysates were subjected to Western blotting with anti-SphK1 pAb and antibodies against GAPDH, Calnexin, or JAM-1 as specific organelle markers.

Figure 3. Identification of the NS3-binding site in SphK1. (A) Schematic representation of SphK1 and its deletion mutants. Myc-NS3 expression vector in combination with expression vectors for Flag-SphK1 and its mutants were cotransfected into LB9.K cells. Proteins immunoprecipitated with anti-Flag mAb (even lanes) or isotype control IgG (Isotype Ct; odd lanes) were subjected to Western blotting using anti-Myc mAb. (B) To further determine the critical amino acids of SphK1 for specific binding to NS3, deletion mutants ranging from the N-terminal 325–386 amino acids were immunoprecipitated with Flag-SphK1. (C) According to the result obtained in (**B**), deletion mutants ranging from the N-terminal 349–361 amino

acids were immunoprecipitated with Flag-SphK1. The data are representative of at least three independent experiments.

Figure 4. Mapping of the SphK1-binding site on BVDV NS3. (A) Schematic representation of NS3 and its deletion mutants. (B) SphK1 expression vector in combination with expression vectors of Myc-NS3 and its deleted mutants were cotransfected into LB9.K cells. Proteins immunoprecipitated with anti-Myc mAb (even lanes) or isotype control IgG (Isotype Ct; odd lanes) were subjected to Western blotting using anti-Flag mAb. Data shown in each panel are representative of at least three independent experiments.

Figure 5. NS3 inhibits SphK1 activity *in vitro*. (A) Coomassie brilliant blue-stained SDS-PAGE of the purified proteins as indicated above the lanes (Flag-SphK1 and GST–NS proteins). (B) GST, GST–NS3, and GST–NS5A bound to GSH-Sepharose was incubated with 1 μM purified recombinant Flag-SphK1 for 2 h. Beads were washed four times with wash buffer, then SphK1 associated with GST–NS3 was resolved by SDS-PAGE and detected by Western blotting with anti-Flag mAb (upper panel). GST–NS3 and GST–NS5A bound to GSH beads were visualized by blotting with anti-GST mAb (lower panel). (C) The effect of GST–NS3, GST–NS5A, or GST control on the catalytic activity of purified recombinant bovine SphK1 (10 nM) was determined using the *in vitro* SphK assay over a range of increasing concentrations of GST–NS proteins or GST. Shown on the left panels are autoradiograms of TLC plates used for separation of S1P. The arrowhead indicates the location of S1P. Data in a graph on the right panel represent the means ± S.D. from three independent experiments. (D) Increasing doses (0.25, 0.5, and 1 μg) of pCAG empty vector or

pCAG vector encoding Myc-tagged NS3 were transfected into LB9.K cells. At 24 h post-transfection, cell lysates were subjected to the *in vitro* SphK assay as described in Materials and methods. (E) pCAG vectors encoding Myc-tagged NS3, NS2-3, or NS3/4A, or empty vector were transfected into LB9.K cells. At 24 h post-transfection, cell lysates were harvested and subjected to the *in vitro* SphK assay. Inset shows expression levels of NS proteins by Western blotting with anti-Myc mAb. (F) LB9.K cells transfected with empty vector or pCAG-NS3 were labeled with [^{32}P]orthophosphate at 24 h post-transfection for 4 h, then harvested and analyzed for endogenous S1P synthesis as described in Materials and methods. (G) MDBK cells were mock-infected or infected with cp BVDV or ncp BVDV at an MOI of 5. After 24 h p.i., cells were harvested into lysis buffer and immunoprecipitated by anti-NS3 mAb for 2 h followed by incubation with Protein G Sepharose beads for 1 h. Beads were then extensively washed, mixed with 10 nM purified recombinant bovine SphK1, and subjected to the *in vitro* SphK assay. Inset shows expression levels of NS3 and NS2-3 proteins bound to beads by Western blotting with anti-NS3 mAb. Data (mean ± S.D.) shown in each panel are representative of at least three independent experiments.

Figure 6. Kinetics of sphingosine kinase activity and the effect of SphK1 overexpression in BVDV-infected cells. (A) MDBK cells infected with either KS86-1cp or KS86-1ncp at an MOI of 5 were harvested at the indicated time points p.i., and SphK activity determined by the *in vitro* SphK assay as described in Materials and methods. (B) MDBK cells infected with cp BVDV or ncp BVDV were labeled with [^{32}P]orthophosphate at 18 h p.i. for 4 h, harvested, and analyzed for endogenous S1P synthesis as described in Materials and methods. Data are expressed as percent relative to the mock-infected samples set to 100% and represent the

mean ± S.D. from at least three independent experiments. (C) Overexpression of SphK1 inhibited DEVDase activation in cp BVDV-infected cells. LB9.K cells were transiently transfected with empty vector, or wild type SphK1 (WT) or SphK1^{G177D} (G177D) expression vectors. After 24 h, cells were infected as described above. At 24 h p.i., cells were harvested and the cell lysates assessed for DEVDase activity. Data are expressed as percent relative to the mock-infected samples transfected with empty vector. The data represent the mean ± S.D. from three independent experiments.

Figure 7. Effects of SphK1 activity on BVDV replication. (A) The effect of SphK1 inhibitor (SKI) on BVDV RNA replication. After infection with either KS86-1cp or KS86-1ncp at an MOI of 5 for 1 h, MDBK cells were treated with 0, 1, and 5 μM SKI. After 48 h p.i., cells were harvested and the BVDV RNA level determined by real-time PCR analysis. (B), (C) & (D) SphK1 knockdown with siRNA enhanced BVDV replication. LB9.K cells were mock-transfected (–) or transfected with siRNA targeted to SphK1 (+) or scrambled control siRNA (scr.) at a final concentration of 20 nM. At 24 h post-transfection, cells were mock-infected or infected with BVDV as described above. Cells were further incubated for 24 h, then harvested and assessed for (B) the endogenous SphK1 expression by Western blotting using anti-SphK1 pAb, and (C) the endogenous SphK1 activity and (D) the BVDV RNA level by real-time PCR analysis. (E) LB9.K cells were transiently transfected with empty vector or SphK1 expression vector (WT or G177D). After 24 h, cells were infected as described above. At 24 h p.i., cells were harvested and BVDV RNA level determined by real-time PCR analysis. At the same time, the viral titer (F) in the culture supernatant was assessed. (G) & (H) The effect of SphK1 activation by FCS on BVDV RNA

replication. MDBK cells were infected as described above, and incubated with DMEM containing 0, 2, 5, or 10% FCS, or 10% FCS with 5 μM SKI. After 24 h p.i., cells were harvested and assessed for (G) the endogenous SphK1 activity and (H) the BVDV RNA level determined by real-time PCR analysis. The data are expressed relative to the control-treated data, which were set to 1.0, and represent the mean ± S.D. from at least three independent experiments, each performed in duplicate.

Figure 8. NS3 from BVDV, but not from HCV, inhibits catalytic activity of hSphK1 *in vitro*. (A) Coomassie brilliant blue-stained SDS-PAGE of the purified proteins as indicated above the lanes (left panel), and corresponding Western blotting analysis using anti-HCV NS3 pAb are shown (right panel). (B) The effect of GST-HCV NS3, GST-HCV NS3/4A, or the GST control on the catalytic activity of purified recombinant hSphK1 (10 nM) was determined by an *in vitro* SphK assay over a range of increasing concentrations of GST-NS proteins or GST. Shown on the upper panel is an autoradiogram of a TLC plate used for separation of S1P. Data in a graph on the lower panel represent the means ± S.D. from three independent experiments. (C) The effect of GST-HCV NS3, GST-BVDV NS3, or the GST control on the catalytic activity of purified hSphK1 (10 nM) was determined by an *in vitro* SphK assay. GST-HCV NS3, GST-BVDV NS3, or GST was added to hSphK1 in 5-fold molar excess. Shown on the left panel is an autoradiogram of a TLC plate used for separation of S1P. The arrowhead indicates the location of S1P. Data in a graph on the right panel are the means ± S.D. from three independent experiments.

CHAPTER 6 Fig. 1

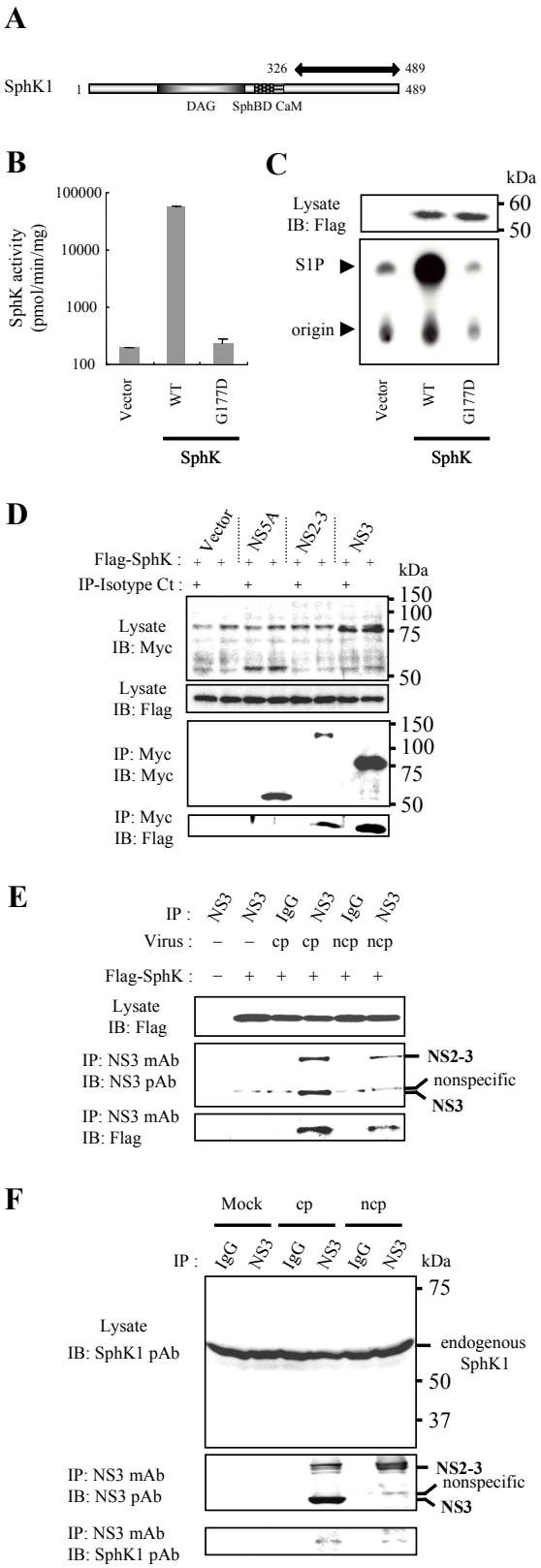

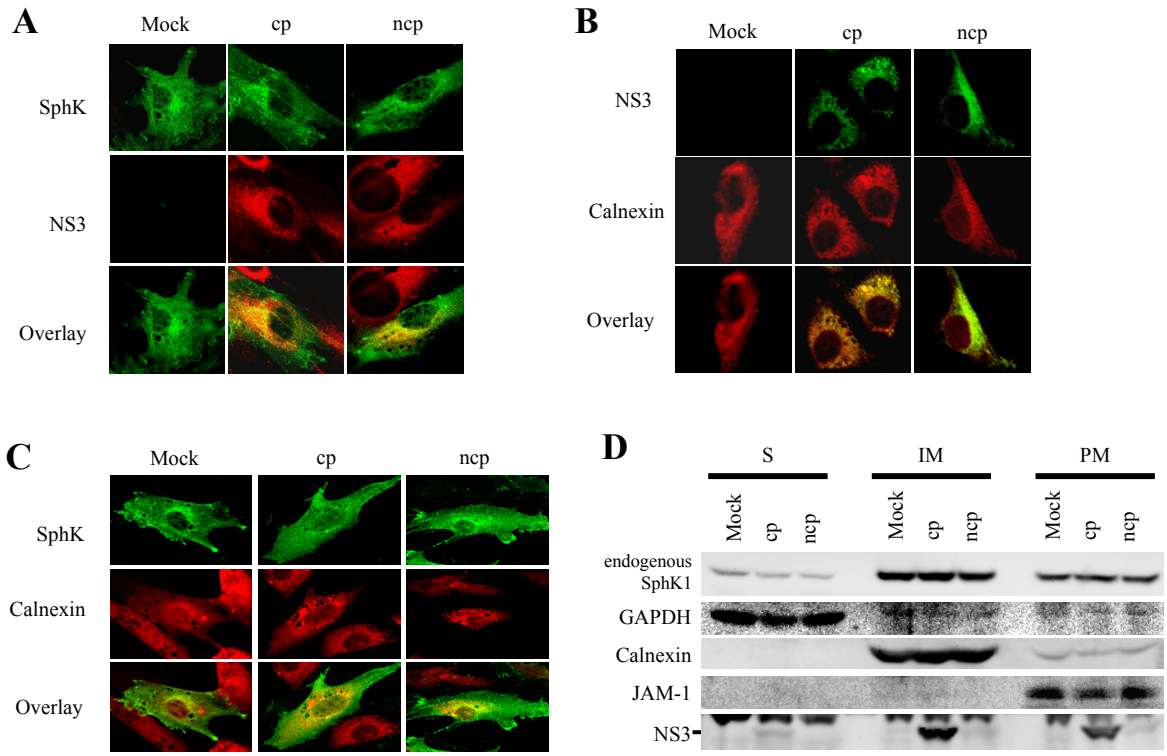
A
Mock
cp
ncp
SphK
NS3
Overlay
B
Mock
cp
ncp
NS3
Calnexin
Overlay
C
Mock
cp
ncp
SphK
Calnexin
Overlay
D
S
IM
PM
Mock
cp
ncp
Mock
cp
ncp
Mock
cp
ncp
endogenous SphK1
GAPDH
Calnexin
JAM-1
NS3

CHAPTER 6 Fig. 3

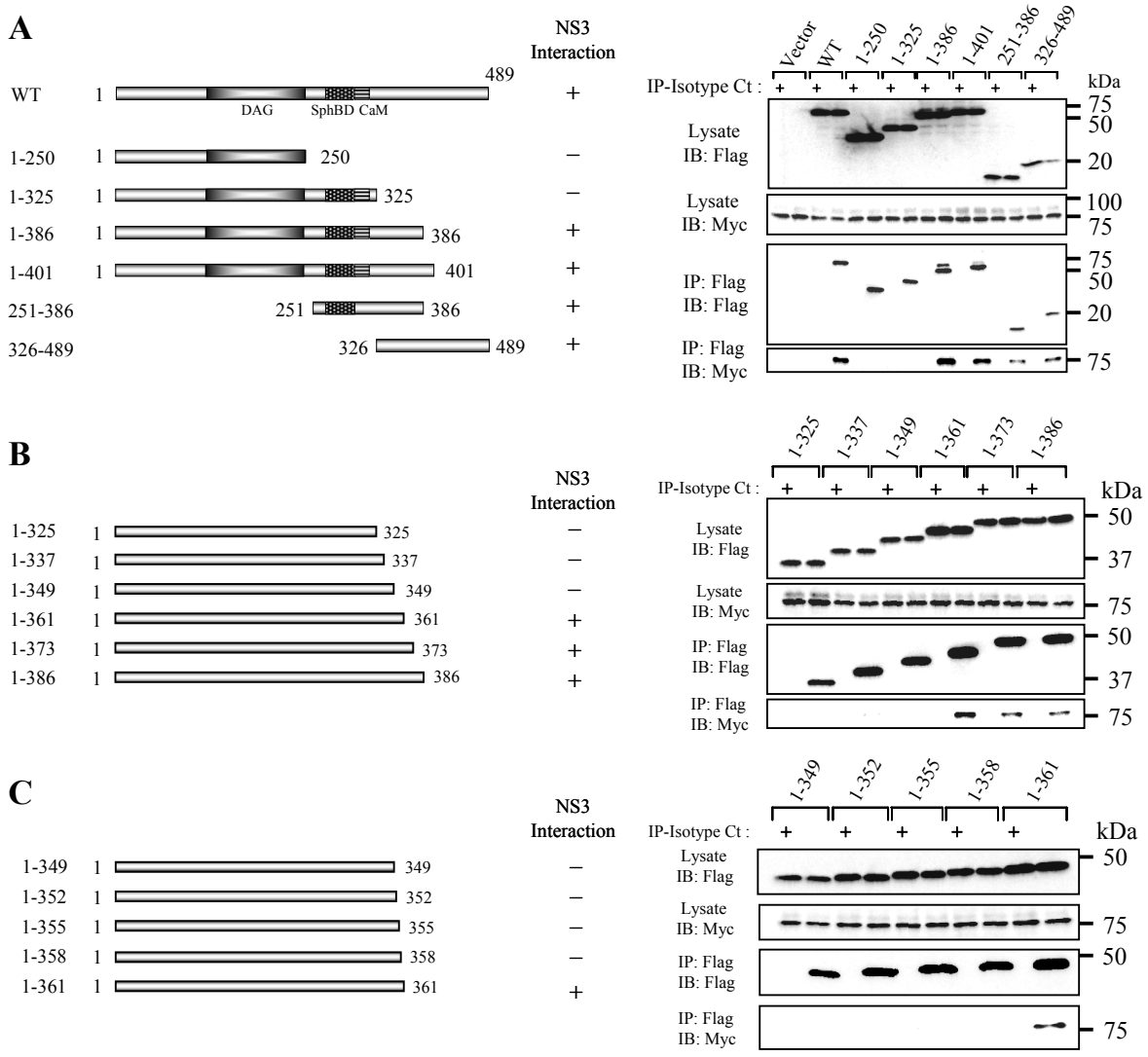

CHAPTER 6 Fig. 4

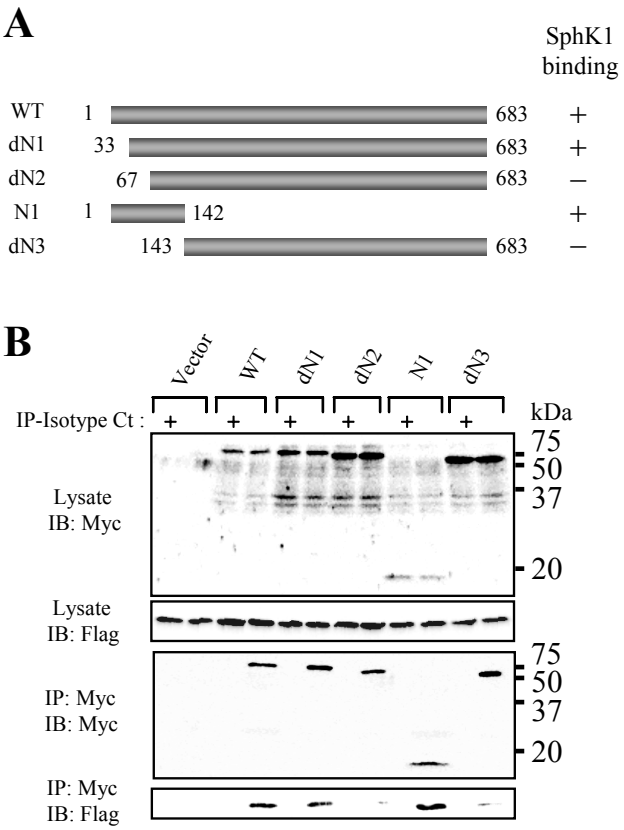

CHAPTER 6 Fig. 5

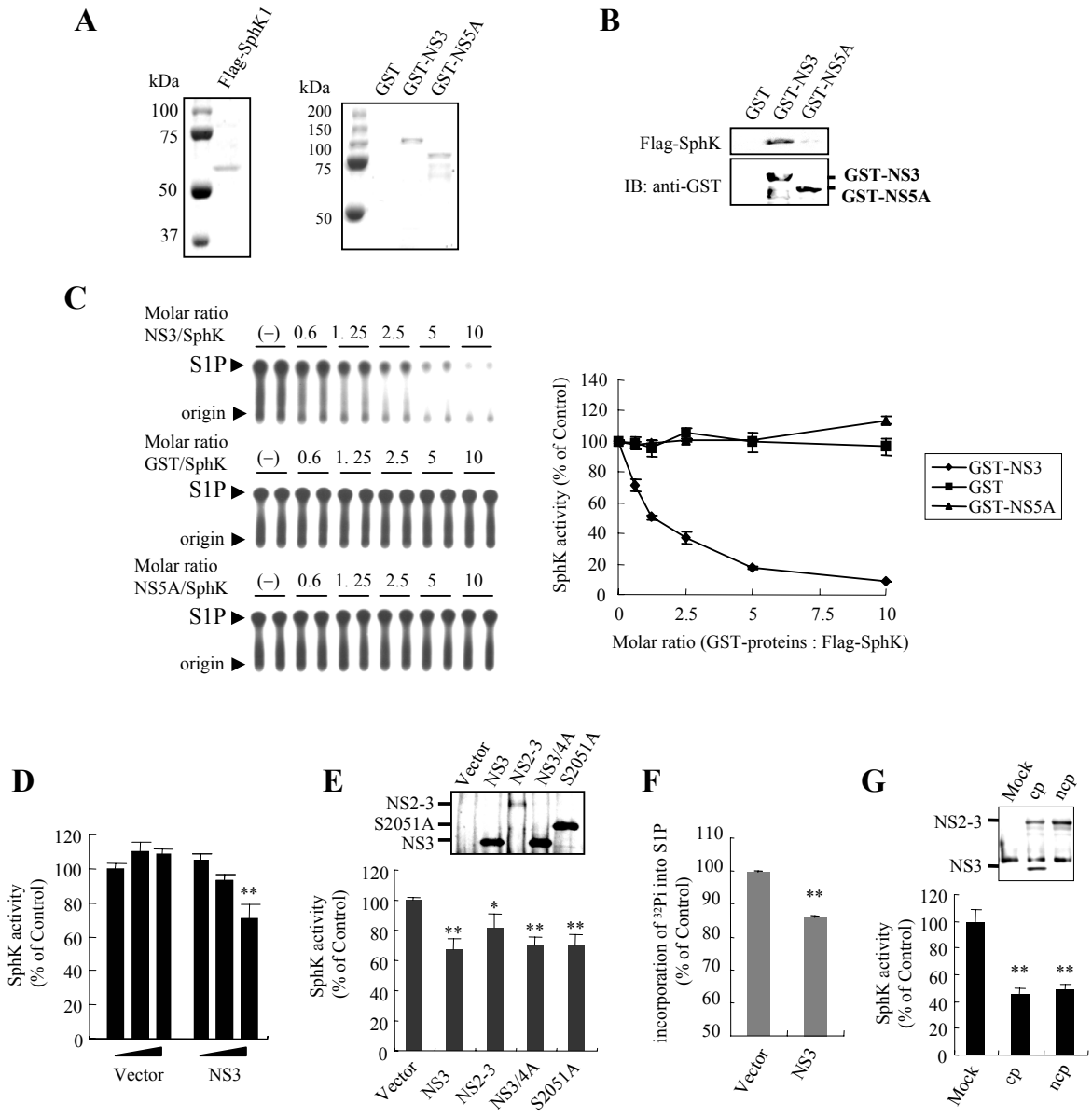

CHAPTER 6　Fig. 6

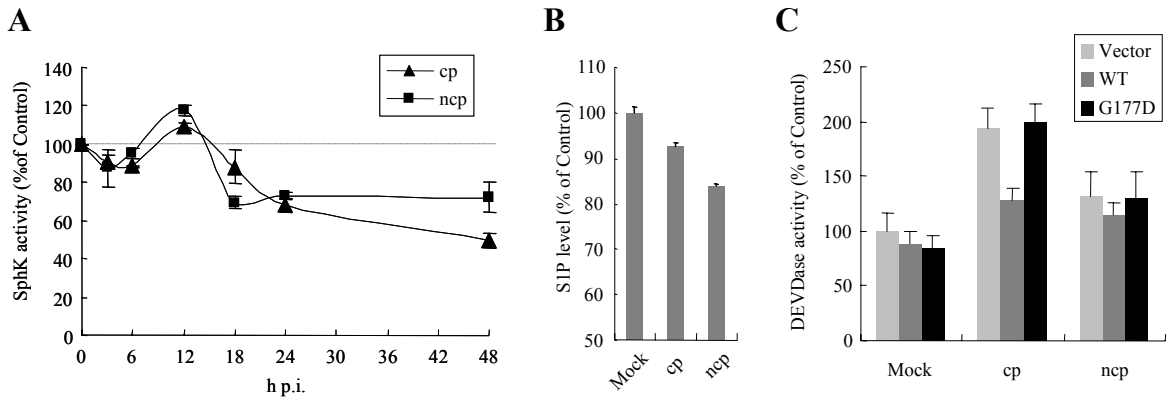

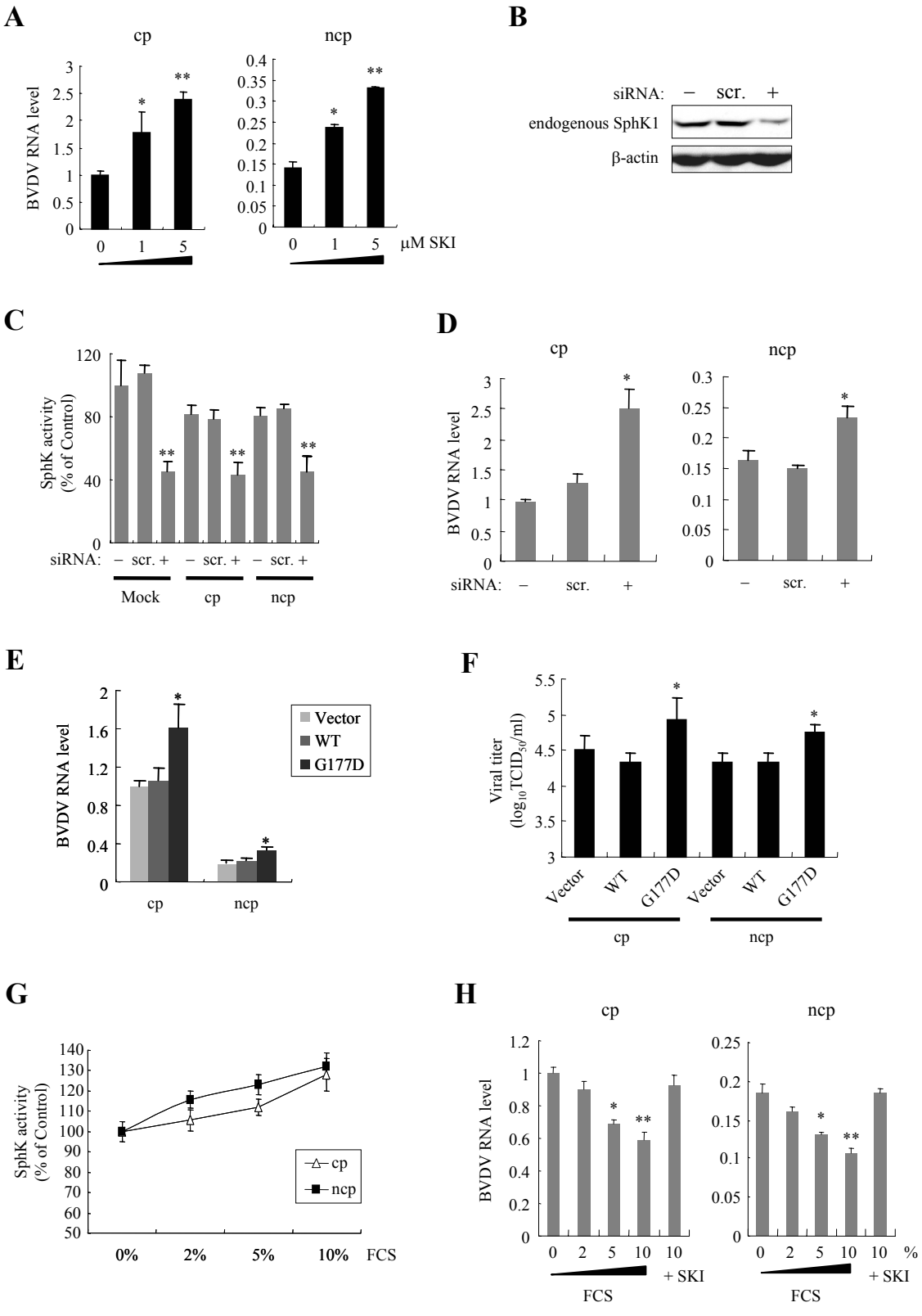
A
cp
ncp
BVDV RNA level
μM SKI
B
siRNA: – scr. +
endogenous SphK1
β-actin
C
SphK activity (% of Control)
siRNA: – scr. + – scr. + – scr. +
Mock
cp
ncp
D
cp
ncp
BVDV RNA level
siRNA: – scr. +
E
BVDV RNA level
Vector
WT
G177D
cp
ncp
F
Viral titer (log10TCID50/ml)
Vector
WT
G177D
cp
ncp
G
SphK activity (% of Control)
cp
ncp
0% 2% 5% 10% FCS
H
cp
ncp
BVDV RNA level
FCS
+ SKI

CHAPTER 6　Fig. 8

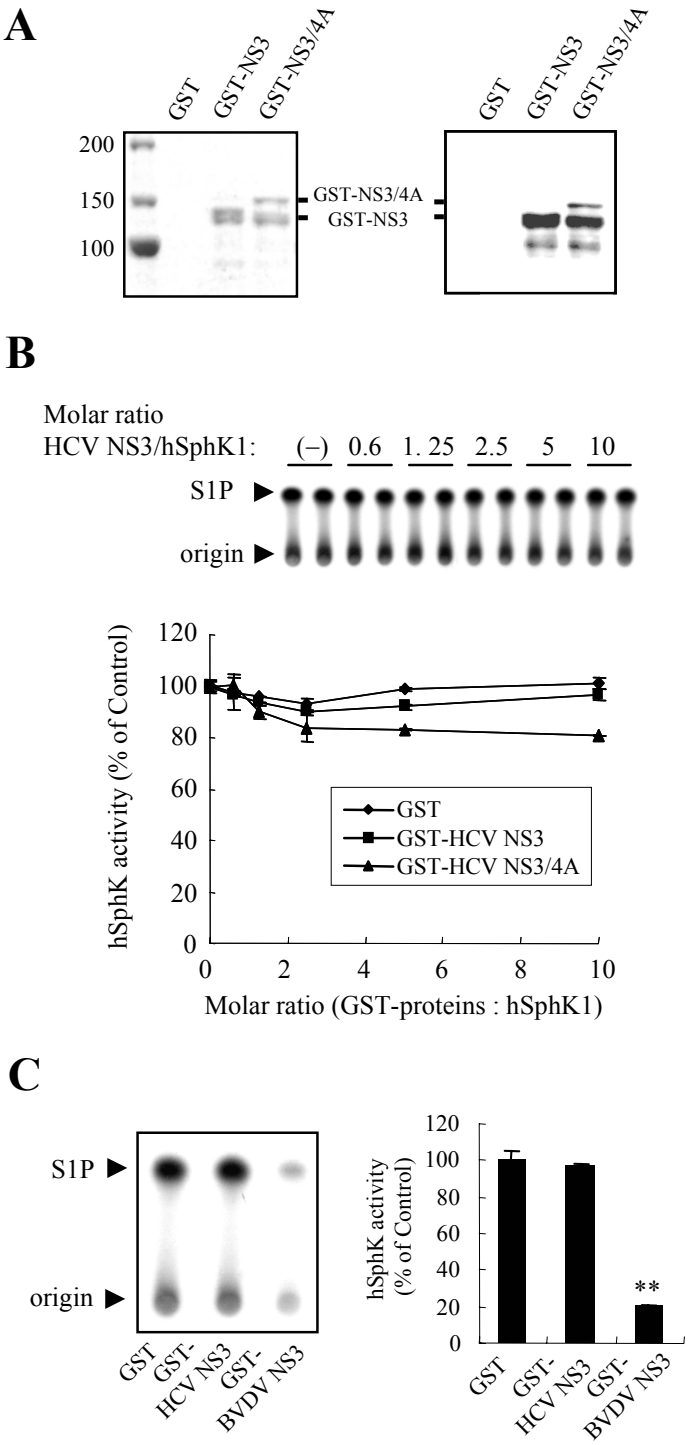

GENERAL CONCLUSION

In the thesis, the author described BVDV interactions with host innate immune responses that are involved in the BVDV pathogenesis. As apoptotic cell death and inflammatory responses are implicated in the tissue injury associated with BVDV infection, the author focused on the mechanism for BVDV-induced cell death *in vitro*, which may be reflected in the BVDV pathogenesis *in vivo*.

In CHAPTER 1, the author sought for an apoptotic signaling activated following cp BVDV infection, and identified a novel pro-apoptotic signaling pathway mediated by TNFα. Pro-apoptotic role of TNFα in cp BVDV-infected cells via extrinsic pathway was confirmed by inhibition of TNFα signaling through antisense transfection or incubation with TNFα mAb.

In CHAPTER 2, the author subsequently showed that TNFα expression is stimulated by the presence of increased level of dsRNA resulted from enhanced viral RNA replication. Additionally, the presence of abundant dsRNA was shown to be the trigger for induction of antiviral or pro-apoptotic genes, ISGs (Mx1, PKR and OAS-1) and iNOS, in cp BVDV-infected BFM cells. The crucial role of dsRNA as a trigger for apoptosis was further demonstrated by the knockdown of PKR and OAS-1, both of which are apoptosis mediators that are activated upon binding to dsRNA. Simultaneous knockdown of both PKR and OAS-1 resulted in marked inhibition of cp BVDV-induced apoptosis, supporting an essential role of dsRNA in the viral induction of apoptosis.

In CHAPTER 3, the author further investigated the involvement of dsRNA in the induction of innate immune responses *in vivo*. The author compared the level of viral RNA load in spleens obtained from PI cattle with the levels of gene transcriptions related to the apoptosis and ISGs, and found significant positive correlations with ISGs, Mx1 and OAS-1, suggesting the role of viral RNA levels as a trigger for IFN responses in PI cattle. Significant

positive relationship between viral RNA load and apoptosis level was also detected. More importantly, PI cattle with higher dose of viral RNA load exhibited severe clinical presentation. These data collectively suggest the positive relationship between the viral RNA levels and the induction of innate immune responses, which may be related to the viral pathogenesis. These results from CHAPTER 1-3 collectively suggest the importance of viral RNA replication as a trigger for innate immune responses and cell death *in vitro* and *in vivo*.

In CHAPTER 4, the author described a role of cellular kinase signaling pathway activated by oxidative stress induced following cp BVDV infection. Although oxidative stress triggered by cp BVDV infection has been implicated in induction of cell death in certain cells, the author demonstrated that it can activate extracellular signal-regulated kinase (ERK) signaling and promote cell proliferation and survival in MDBK cells. As ERK activation is known to mediate numerous cellular signaling cascades through phosphorylation of cellular substrates, disordered ERK signaling initiated by reactive oxygen species may account for unusual activation of cellular signaling following cp BVDV infection.

In CHAPTER 5, the author analyzed comprehensive mRNA expression in different cell types by means of bovine microarray. The microarray data detected up-regulation of numerous ISG inductions, cytokines and the stress-inducible genes in cp BVDV-infected cells, in agreement with the results in CHAPTERs 1-4. Most interesting was the completely different sets of genes up-regulated between BFM and MDBK cells. BFM cells exhibited strong IFN-responses and no ER stress-mediated gene transcriptions, while MDBK cells conversely induced strong ER stress and weak IFN responses. Although a crucial role of interaction between ISGs and dsRNA in the cytopathogenesis has been shown in CHAPTER 2, these results strongly indicate that involvement of the IFN-related apoptosis pathway is restricted to the fibroblast cell type. On the other hand, cp BVDV-infected MDBK cells seem

to induce cell death via ER stress-mediated apoptosis pathway, given the much lower ISGs expression compared with BFM cells. As both cell types similarly undergo apoptotic cell death upon infection with cp BVDV, it was unexpected to observe such distinct signaling pathways between both cell types. These findings may be important to understand the basis for pathogenesis correlated with apoptotic cell death. Gene expression profiles of various cell types are necessary to be examined to reveal the cell type-specific responses to BVDV infection.

In CHAPTER 6, the author identified specific interaction between NS3 and sphingosine kinase 1 (SphK1). NS3 was found to suppress catalytic activity of SphK1. SphK1 is implicated in cell survival signaling by counteract with apoptosis induction mediated by various cellular stress, such as serum deprivation. Indeed, as overexpression of SphK1 significantly reduced apoptosis induction in cp BVDV-infected cells, the inhibitory interaction of NS3 with SphK1 seems to result in enhanced cell death induced by stresses in cp BVDV-infected cells. Inhibition of SphK1 activity by NS3 seemed to have a positive effect on viral replication because SphK1 inhibition by a chemical inhibitor, knockdown with siRNA and overexpression of catalytically inactive SphK1 all resulted in enhanced viral replication up to 2-fold. Sphingolipids are known to serve as a scaffold of viral RNA replication complex in HCV, therefore, regulation of SphK activity by NS3 may affect the sphingolipid metabolism, thereby facilitating efficient viral replication.

As described above, the author described novel signaling pathways activated upon BVDV infection and host-virus interactions in the thesis. Because the cellular responses to BVDV have been poorly studied thus far, these findings in the thesis will contribute to unravel the mechanism for viral pathogenesis. Although the author extensively investigated

the function of NS3 protein in the thesis, only a few viral protein interactions with host factors have been clarified so far, such as N^{pro} and E^{rns}. However, it has been demonstrated that the regulation of IFN signaling is not enough to explain the successful establishment of persistent infection in the fetus, indicating that additional mechanisms, possibly other than IFN system, may exist to exhibit strong antiviral responses in host cells. It will be vital to screen and examine the roles of viral proteins in the interaction with host factors to elucidate yet unknown mechanisms involved in the viral persistence and pathogenesis.

ACKNOWLEDGEMENTS

The author would like to acknowledge the following people for their invaluable assistance:

Dr. Hiroomi Akashi (The University of Tokyo)

Dr. Yukinobu Tohya (The University of Tokyo)

Dr. Kentaro Kato (The University of Tokyo)

Dr. Makoto Nagai (Ishikawa Nanbu Livestock Hygene Service Center)

Dr. Michiko Hayashi (Ishikawa Nanbu Livestock Hygene Service Center)

Dr. Toshiaki Terasaki (Tokyo Metropolitan Livestock Hygene Service Center)

Dr. Hitoki Kondo (Tokyo Metropolitan Livestock Hygene Service Center)

Dr. Kazuki Ishibashi (Fukuoka Chuo Livestock Hygene Service Center)

Dr. Keiichi Goto (Fukuoka Chuo Livestock Hygene Service Center)

Dr. Katsuhiko Fukai (Tochigi Kenoh Livestock Hygene Service Center)

Dr. Koji Matsumoto (Shizuoka Chubu Livestock Hygene Service Center)

Dr. Shinichi Hatama (National Institute of Animal Health)

Dr. Takashi Isobe (National Institute of Animal Health)

Dr. Shokichi Iwamura (National Institute of Animal Health)

Dr. Michinori Kohara (Tokyo Metropolitan Institute of Medical Science)

Dr. Max J. Paape (Beltsville Agricultural Research Center)

The author would like to thank Kyoko Kano for secretarial work and all the members in Department of Veterinary Microbiology, Faculty of Agriculture, the University of Tokyo, for their invaluable help and encouragement.

Finally, the author would like to express special thanks to his family.

REFFERENCES

Adler, B., Adler, H., Pfister, H., Jungi, T. W. & Peterhans, E. (1997). Macrophages infected with cytopathic bovine viral diarrhea virus release a factor(s) capable of priming uninfected macrophages for activation-induced apoptosis. *J Virol* **71**, 3255-3258.

Adler, H., Jungi, T. W., Pfister, H., Strasser, M., Sileghem, M. & Peterhans, E. (1996). Cytokine regulation by virus infection: bovine viral diarrhea virus, a flavivirus, downregulates production of tumor necrosis factor alpha in macrophages in vitro. *J Virol* **70**, 2650-2653.

Aizaki, H., Lee, K. J., Sung, V. M., Ishiko, H. & Lai, M. M. (2004). Characterization of the hepatitis C virus RNA replication complex associated with lipid rafts. *Virology* **324**, 450-461.

Ashkenazi, A. & Dixit, V. M. (1998). Death receptors: signaling and modulation. *Science* **281**, 1305-1308.

Auch, C. J., Saha, R. N., Sheikh, F. G., Liu, X., Jacobs, B. L. & Pahan, K. (2004). Role of protein kinase R in double-stranded RNA-induced expression of nitric oxide synthase in human astroglia. *FEBS Lett* **563**, 223-228.

Baginski, S. G., Pevear, D. C., Seipel, M., Sun, S. C., Benetatos, C. A., Chunduru, S. K., Rice, C. M. & Collett, M. S. (2000). Mechanism of action of a pestivirus antiviral compound. *Proc Natl Acad Sci U S A* **97**, 7981-7986.

Baigent, S. J., Goodbourn, S. & McCauley, J. W. (2004). Differential activation of interferon regulatory factors-3 and -7 by non-cytopathogenic and cytopathogenic bovine viral diarrhoea virus. *Vet Immunol Immunopathol* **100**, 135-144.

Baigent, S. J., Zhang, G., Fray, M. D., Flick-Smith, H., Goodbourn, S. & McCauley, J. W. (2002). Inhibition of beta interferon transcription by noncytopathogenic bovine viral diarrhea virus is through an interferon regulatory factor 3-dependent mechanism. *J Virol* **76**, 8979-8988.

Barber, G. N., Wambach, M., Wong, M. L., Dever, T. E., Hinnebusch, A. G. & Katze, M. G. (1993). Translational regulation by the interferon-induced double-stranded-RNA-activated 68-kDa protein kinase. *Proc Natl Acad Sci U S A* **90**, 4621-4625.

Barreca, C. & O'Hare, P. (2004). Suppression of herpes simplex virus 1 in MDBK cells via the interferon pathway. *J Virol* **78**, 8641-8653.

Becher, P., Orlich, M. & Thiel, H. J. (2001). RNA recombination between persisting pestivirus and a vaccine strain: generation of cytopathogenic virus and induction of lethal disease. *J Virol* **75**, 6256-6264.

Behrens, S. E., Grassmann, C. W., Thiel, H. J., Meyers, G. & Tautz, N. (1998). Characterization of an autonomous subgenomic pestivirus RNA replicon. *J Virol* **72**, 2364-2372.

Bendfeldt, S., Grummer, B. & Greiser-Wilke, I. (2003). No caspase activation but overexpression of Bcl-2 in bovine cells infected with noncytopathic bovine virus diarrhoea virus. *Vet Microbiol* **96**, 313-326.

Bhat, N. R. & Zhang, P. (1999). Hydrogen peroxide activation of multiple mitogen-activated protein kinases in an oligodendrocyte cell line: role of extracellular signal-regulated kinase in hydrogen peroxide-induced cell death. *J Neurochem* **72**, 112-119.

Bielefeldt-Ohmann, H. (1995). The pathologies of bovine viral diarrhea virus infection. A window on the pathogenesis. *Vet Clin North Am Food Anim Pract* **11**, 447-476.

Bielefeldt Ohmann, H. & Babiuk, L. A. (1988). Influence of interferons alpha I1 and gamma and of tumour necrosis factor on persistent infection with bovine viral diarrhoea virus in vitro. *J Gen Virol* **69**, 1399-1403.

Blair, L. A., Maggi, L. B., Jr., Scarim, A. L. & Corbett, J. A. (2002). Role of interferon

regulatory factor-1 in double-stranded RNA-induced iNOS expression by mouse islets. *J Biol Chem* **277**, 359-365.

Bogoyevitch, M. A., Boehm, I., Oakley, A., Ketterman, A. J. & Barr, R. K. (2004). Targeting the JNK MAPK cascade for inhibition: basic science and therapeutic potential. *Biochim Biophys Acta* **1697**, 89-101.

Brackenbury, L. S., Carr, B. V., Stamataki, Z., Prentice, H., Lefevre, E. A., Howard, C. J. & Charleston, B. (2005). Identification of a cell population that produces alpha/beta interferon in vitro and in vivo in response to noncytopathic bovine viral diarrhea virus. *J Virol* **79**, 7738-7744.

Brownlie, J., Clarke, M. C. & Howard, C. J. (1984). Experimental production of fatal mucosal disease in cattle. *Vet Rec* **114**, 535-536.

Brownlie, J., Clarke, M. C. & Howard, C. J. (1989). Experimental infection of cattle in early pregnancy with a cytopathic strain of bovine virus diarrhoea virus. *Res Vet Sci* **46**, 307-311.

Brune, B., von Knethen, A. & Sandau, K. B. (1999). Nitric oxide (NO): an effector of apoptosis. *Cell Death Differ* **6**, 969-975.

Buckwold, V. E., Beer, B. E. & Donis, R. O. (2003). Bovine viral diarrhea virus as a surrogate model of hepatitis C virus for the evaluation of antiviral agents. *Antiviral Res* **60**, 1-15.

Budihardjo, I., Oliver, H., Lutter, M., Luo, X. & Wang, X. (1999). Biochemical pathways of caspase activation during apoptosis. *Annu Rev Cell Dev Biol* **15**, 269-290.

Castelli, J., Wood, K. A. & Youle, R. J. (1998). The 2-5A system in viral infection and apoptosis. *Biomed Pharmacother* **52**, 386-390.

Cebulla, C. M., Miller, D. M. & Sedmak, D. D. (1999). Viral inhibition of interferon signal transduction. *Intervirology* **42**, 325-330.

Chan, F. K. & Lenardo, M. J. (2000). A crucial role for p80 TNF-R2 in amplifying p60 TNF-R1 apoptosis signals in T lymphocytes. *Eur J Immunol* **30**, 652-660.

Charleston, B., Fray, M. D., Baigent, S., Carr, B. V. & Morrison, W. I. (2001). Establishment of persistent infection with non-cytopathic bovine viral diarrhoea virus in cattle is associated with a failure to induce type I interferon. *J Gen Virol* **82**, 1893-1897.

Charleston, B., Brackenbury, L. S., Carr, B. V., Fray, M. D., Hope, J. C., Howard, C. J. & Morrison, W. I. (2002). Alpha/beta and gamma interferons are induced by infection with noncytopathic bovine viral diarrhea virus in vivo. *J Virol* **76**, 923-927.

Chawla-Sarkar, M., Lindner, D. J., Liu, Y. F., Williams, B. R., Sen, G. C., Silverman, R. H. & Borden, E. C. (2003). Apoptosis and interferons: role of interferon-stimulated genes as mediators of apoptosis. *Apoptosis* **8**, 237-249.

Chen, Z., Rijnbrand, R., Jangra, R. K., Devaraj, S. G., Qu, L., Ma, Y., Lemon, S. M. & Li, K. (2007). Ubiquitination and proteasomal degradation of interferon regulatory factor-3 induced by Npro from a cytopathic bovine viral diarrhea virus. *Virology* **366**, 277-292.

Chen, Z., Gibson, T. B., Robinson, F., Silvestro, L., Pearson, G., Xu, B., Wright, A., Vanderbilt, C. & Cobb, M. H. (2001). MAP kinases. *Chem Rev* **101**, 2449-2476.

Chen, Z., Benureau, Y., Rijnbrand, R., Yi, J., Wang, T., Warter, L., Lanford, R. E., Weinman, S. A., Lemon, S. M., Martin, A. & Li, K. (2007). GB virus B disrupts RIG-I signaling by NS3/4A-mediated cleavage of the adaptor protein MAVS. *J Virol* **81**, 964-976.

Choi, K. H., Groarke, J. M., Young, D. C., Kuhn, R. J., Smith, J. L., Pevear, D. C. & Rossmann, M. G. (2004). The structure of the RNA-dependent RNA polymerase from

bovine viral diarrhea virus establishes the role of GTP in de novo initiation. *Proc Natl Acad Sci U S A* **101**, 4425-4430.

Chon, S. K., Perez, D. R. & Donis, R. O. (1998). Genetic analysis of the internal ribosome entry segment of bovine viral diarrhea virus. *Virology* **251**, 370-382.

Clemens, M. J. (1997). PKR--a protein kinase regulated by double-stranded RNA. *Int J Biochem Cell Biol* **29**, 945-949.

Collett, M. S., Anderson, D. K. & Retzel, E. (1988a). Comparisons of the pestivirus bovine viral diarrhoea virus with members of the flaviviridae. *J Gen Virol* **69**, 2637-2643.

Collett, M. S., Larson, R., Belzer, S. K. & Retzel, E. (1988b). Proteins encoded by bovine viral diarrhea virus: the genomic organization of a pestivirus. *Virology* **165**, 200-208.

Collett, M. S., Wiskerchen, M., Welniak, E. & Belzer, S. K. (1991). Bovine viral diarrhea virus genomic organization. *Arch Virol Suppl* **3**, 19-27.

Das, S., Ward, S. V., Tacke, R. S., Suske, G. & Samuel, C. E. (2006). Activation of the RNA-dependent protein kinase PKR promoter in the absence of interferon is dependent upon Sp proteins. *J Biol Chem* **281**, 3244-3253.

Diderholm, H. & Dinter, Z. (1966). Interference between strains of bovine virus diarrhea virus and their capacity to suppress interferon of a heterologous virus. *Proc Soc Exp Biol Med* **121**, 976-980.

Dong, J., Ramachandiran, S., Tikoo, K., Jia, Z., Lau, S. S. & Monks, T. J. (2004). EGFR-independent activation of p38 MAPK and EGFR-dependent activation of ERK1/2 are required for ROS-induced renal cell death. *Am J Physiol Renal Physiol* **287**, F1049-1058.

Eberwine, J., Yeh, H., Miyashiro, K., Cao, Y., Nair, S., Finnell, R., Zettel, M. & Coleman, P. (1992). Analysis of gene expression in single live neurons. *Proc Natl Acad Sci*

U S A **89**, 3010-3014.

Elbers, K., Tautz, N., Becher, P., Stoll, D., Rumenapf, T. & Thiel, H. J. (1996). Processing in the pestivirus E2-NS2 region: identification of proteins p7 and E2p7. *J Virol* **70**, 4131-4135.

Fray, M. D., Mann, G. E. & Charleston, B. (2001). Validation of an Mx/CAT reporter gene assay for the quantification of bovine type-I interferon. *J Immunol Methods* **249**, 235-244.

French, K. J., Schrecengost, R. S., Lee, B. D., Zhuang, Y., Smith, S. N., Eberly, J. L., Yun, J. K. & Smith, C. D. (2003). Discovery and evaluation of inhibitors of human sphingosine kinase. *Cancer Res* **63**, 5962-5969.

Gao, L., Aizaki, H., He, J. W. & Lai, M. M. (2004). Interactions between viral nonstructural proteins and host protein hVAP-33 mediate the formation of hepatitis C virus RNA replication complex on lipid raft. *J Virol* **78**, 3480-3488.

Gao, L., Tu, H., Shi, S. T., Lee, K. J., Asanaka, M., Hwang, S. B. & Lai, M. M. (2003). Interaction with a ubiquitin-like protein enhances the ubiquitination and degradation of hepatitis C virus RNA-dependent RNA polymerase. *J Virol* **77**, 4149-4159.

Gil, J. & Esteban, M. (2000). Induction of apoptosis by the dsRNA-dependent protein kinase (PKR): mechanism of action. *Apoptosis* **5**, 107-114.

Gil, L. H., van Olphen, A. L., Mittal, S. K. & Donis, R. O. (2006). Modulation of PKR activity in cells infected by bovine viral diarrhea virus. *Virus Res* **116**, 69-77.

Glew, E. J., Carr, B. V., Brackenbury, L. S., Hope, J. C., Charleston, B. & Howard, C. J. (2003). Differential effects of bovine viral diarrhoea virus on monocytes and dendritic cells. *J Gen Virol* **84**, 1771-1780.

Goetschy, J. F., Zeller, H., Content, J. & Horisberger, M. A. (1989). Regulation of the

interferon-inducible IFI-78K gene, the human equivalent of the murine Mx gene, by interferons, double-stranded RNA, certain cytokines, and viruses. *J Virol* **63**, 2616-2622.

Grassmann, C. W., Isken, O. & Behrens, S. E. (1999). Assignment of the multifunctional NS3 protein of bovine viral diarrhea virus during RNA replication: an in vivo and in vitro study. *J Virol* **73**, 9196-9205.

Gregory, C. D., Dive, C., Henderson, S., Smith, C. A., Williams, G. T., Gordon, J. & Rickinson, A. B. (1991). Activation of Epstein-Barr virus latent genes protects human B cells from death by apoptosis. *Nature* **349**, 612-614.

Grummer, B., Bendfeldt, S., Wagner, B. & Greiser-Wilke, I. (2002b). Induction of the intrinsic apoptotic pathway in cells infected with cytopathic bovine virus diarrhoea virus. *Virus Res* **90**, 143-153.

Gu, B., Liu, C., Lin-Goerke, J., Maley, D. R., Gutshall, L. L., Feltenberger, C. A. & Del Vecchio, A. M. (2000). The RNA helicase and nucleotide triphosphatase activities of the bovine viral diarrhea virus NS3 protein are essential for viral replication. *J Virol* **74**, 1794-1800.

Haller, O., Frese, M. & Kochs, G. (1998). Mx proteins: mediators of innate resistance to RNA viruses. *Rev Sci Tech* **17**, 220-230.

Haskill, S., Beg, A. A., Tompkins, S. M., Morris, J. S., Yurochko, A. D., Sampson-Johannes, A., Mondal, K., Ralph, P. & Baldwin, A. S., Jr. (1991). Characterization of an immediate-early gene induced in adherent monocytes that encodes I kappa B-like activity. *Cell* **65**, 1281-1289.

Heitmeier, M. R., Scarim, A. L. & Corbett, J. A. (1998). Double-stranded RNA-induced inducible nitric-oxide synthase expression and interleukin-1 release by murine macrophages

requires NF-kappaB activation. *J Biol Chem* **273**, 15301-15307.

Helbig, K. J., Lau, D. T., Semendric, L., Harley, H. A. & Beard, M. R. (2005). Analysis of ISG expression in chronic hepatitis C identifies viperin as a potential antiviral effector. *Hepatology* **42**, 702-710.

Hilton, L., Moganeradj, K., Zhang, G., Chen, Y. H., Randall, R. E., McCauley, J. W. & Goodbourn, S. (2006). The NPro product of bovine viral diarrhea virus inhibits DNA binding by interferon regulatory factor 3 and targets it for proteasomal degradation. *J Virol* **80**, 11723-11732.

Hiscott, J. (2007). Convergence of the NF-kappaB and IRF pathways in the regulation of the innate antiviral response. *Cytokine Growth Factor Rev* **18**, 483-490.

Hoff, H. S. & Donis, R. O. (1997). Induction of apoptosis and cleavage of poly(ADP-ribose) polymerase by cytopathic bovine viral diarrhea virus infection. *Virus Res* **49**, 101-113.

Howard, C. J. (1990). Immunological responses to bovine virus diarrhoea virus infections. *Rev Sci Tech* **9**, 95-103.

Huang, J., Wu, L., Tashiro, S., Onodera, S. & Ikejima, T. (2006). Fibroblast growth factor-2 suppresses oridonin-induced L929 apoptosis through extracellular signal-regulated kinase-dependent and phosphatidylinositol 3-kinase-independent pathway. *J Pharmacol Sci* **102**, 305-313.

Inaba, Y., Tanaka, Y., Kumagai, T., Omori, T. & Ito, H. (1968). Bovine diarrhea virus. II. END phenomenon: exaltation of Newcastle disease virus in bovine cells infected with bovine diarrhea virus. *Jpn J Microbiol* **12**, 35-49.

Iqbal, M., Poole, E., Goodbourn, S. & McCauley, J. W. (2004). Role for bovine viral diarrhea virus Erns glycoprotein in the control of activation of beta interferon by

double-stranded RNA. *J Virol* **78**, 136-145.

Irizarry, R. A., Bolstad, B. M., Collin, F., Cope, L. M., Hobbs, B. & Speed, T. P. (2003a). Summaries of Affymetrix GeneChip probe level data. *Nucleic Acids Res* **31**, e15.

Irizarry, R. A., Hobbs, B., Collin, F., Beazer-Barclay, Y. D., Antonellis, K. J., Scherf, U. & Speed, T. P. (2003b). Exploration, normalization, and summaries of high density oligonucleotide array probe level data. *Biostatistics* **4**, 249-264.

Jaramillo, M. & Olivier, M. (2002). Hydrogen peroxide induces murine macrophage chemokine gene transcription via extracellular signal-regulated kinase- and cyclic adenosine 5'-monophosphate (cAMP)-dependent pathways: involvement of NF-kappa B, activator protein 1, and cAMP response element binding protein. *J Immunol* **169**, 7026-7038.

Jiang, D., Guo, H., Xu, C., Chang, J., Gu, B., Wang, L., Block, T. M. & Guo, J. T. (2008). Identification of three interferon-inducible cellular enzymes that inhibit the replication of hepatitis C virus. *J Virol* **82**, 1665-1678.

Johnson, C. M., Perez, D. R., French, R., Merrick, W. C. & Donis, R. O. (2001). The NS5A protein of bovine viral diarrhoea virus interacts with the alpha subunit of translation elongation factor-1. *J Gen Virol* **82**, 2935-2943.

Johnson, D. W. & Muscoplat, C. C. (1973). Immunologic abnormalities in calves with chronic bovine viral diarrhea. *Am J Vet Res* **34**, 1139-1141.

Johnson, K. R., Becker, K. P., Facchinetti, M. M., Hannun, Y. A. & Obeid, L. M. (2002). PKC-dependent activation of sphingosine kinase 1 and translocation to the plasma membrane. Extracellular release of sphingosine-1-phosphate induced by phorbol 12-myristate 13-acetate (PMA). *J Biol Chem* **277**, 35257-35262.

Jordan, R., Wang, L., Graczyk, T. M., Block, T. M. & Romano, P. R. (2002). Replication

of a cytopathic strain of bovine viral diarrhea virus activates PERK and induces endoplasmic reticulum stress-mediated apoptosis of MDBK cells. *J Virol* **76**, 9588-9599.

Jung, Y., Bang, S., Choi, K., Kim, E., Kim, Y., Kim, J., Park, J., Koo, H., Moon, R. T., Song, K. & Lee, I. (2006). TC1 (C8orf4) enhances the Wnt/beta-catenin pathway by relieving antagonistic activity of Chibby. *Cancer Res* **66**, 723-728.

Kageshita, T., Kashio, Y., Yamauchi, A., Seki, M., Abedin, M. J., Nishi, N., Shoji, H., Nakamura, T., Ono, T. & Hirashima, M. (2002). Possible role of galectin-9 in cell aggregation and apoptosis of human melanoma cell lines and its clinical significance. *Int J Cancer* **99**, 809-816.

Kaufman, R. J. (1999). Double-stranded RNA-activated protein kinase mediates virus-induced apoptosis: a new role for an old actor. *Proc Natl Acad Sci U S A* **96**, 11693-11695.

Kawai, T., Takahashi, K., Sato, S., Coban, C., Kumar, H., Kato, H., Ishii, K. J., Takeuchi, O. & Akira, S. (2005). IPS-1, an adaptor triggering RIG-I- and Mda5-mediated type I interferon induction. *Nat Immunol* **6**, 981-988.

Kelling, C. L., Steffen, D. J., Topliff, C. L., Eskridge, K. M., Donis, R. O. & Higuchi, D. S. (2002). Comparative virulence of isolates of bovine viral diarrhea virus type II in experimentally inoculated six- to nine-month-old calves. *Am J Vet Res* **63**, 1379-1384.

Kesson, A. M., Cheng, Y. & King, N. J. (2002). Regulation of immune recognition molecules by flavivirus, West Nile. *Viral Immunol* **15**, 273-283.

Keyse, S. M. (2008). Dual-specificity MAP kinase phosphatases (MKPs) and cancer. *Cancer Metastasis Rev* **27**, 253-261.

Kibler, K. V., Shors, T., Perkins, K. B., Zeman, C. C., Banaszak, M. P., Biesterfeldt, J.,

Langland, J. O. & Jacobs, B. L. (1997). Double-stranded RNA is a trigger for apoptosis in vaccinia virus-infected cells. *J Virol* **71**, 1992-2003.

Kihara, A., Anada, Y. & Igarashi, Y. (2006). Mouse sphingosine kinase isoforms SPHK1a and SPHK1b differ in enzymatic traits including stability, localization, modification, and oligomerization. *J Biol Chem* **281**, 4532-4539.

Knapp, S., Yee, L. J., Frodsham, A. J., Hennig, B. J., Hellier, S., Zhang, L., Wright, M., Chiaramonte, M., Graves, M., Thomas, H. C., Hill, A. V. & Thursz, M. R. (2003). Polymorphisms in interferon-induced genes and the outcome of hepatitis C virus infection: roles of MxA, OAS-1 and PKR. *Genes Immun* **4**, 411-419.

Kummerer, B. M. & Meyers, G. (2000). Correlation between point mutations in NS2 and the viability and cytopathogenicity of Bovine viral diarrhea virus strain Oregon analyzed with an infectious cDNA clone. *J Virol* **74**, 390-400.

Kummerer, B. M., Stoll, D. & Meyers, G. (1998). Bovine viral diarrhea virus strain Oregon: a novel mechanism for processing of NS2-3 based on point mutations. *J Virol* **72**, 4127-4138.

Lackner, T., Muller, A., Konig, M., Thiel, H. J. & Tautz, N. (2005). Persistence of bovine viral diarrhea virus is determined by a cellular cofactor of a viral autoprotease. *J Virol* **79**, 9746-9755.

Lackner, T., Muller, A., Pankraz, A., Becher, P., Thiel, H. J., Gorbalenya, A. E. & Tautz, N. (2004). Temporal modulation of an autoprotease is crucial for replication and pathogenicity of an RNA virus. *J Virol* **78**, 10765-10775.

Lai, V. C., Kao, C. C., Ferrari, E., Park, J., Uss, A. S., Wright-Minogue, J., Hong, Z. & Lau, J. Y. (1999). Mutational analysis of bovine viral diarrhea virus RNA-dependent RNA polymerase. *J Virol* **73**, 10129-10136.

Lamba, J. K., Lin, Y. S., Schuetz, E. G. & Thummel, K. E. (2002). Genetic contribution to variable human CYP3A-mediated metabolism. *Adv Drug Deliv Rev* **54**, 1271-1294.

Leaman, D. W., Chawla-Sarkar, M., Vyas, K., Reheman, M., Tamai, K., Toji, S. & Borden, E. C. (2002). Identification of X-linked inhibitor of apoptosis-associated factor-1 as an interferon-stimulated gene that augments TRAIL Apo2L-induced apoptosis. *J Biol Chem* **277**, 28504-28511.

Levine, B., Huang, Q., Isaacs, J. T., Reed, J. C., Griffin, D. E. & Hardwick, J. M. (1993). Conversion of lytic to persistent alphavirus infection by the bcl-2 cellular oncogene. *Nature* **361**, 739-742.

Lewis, T. S., Shapiro, P. S. & Ahn, N. G. (1998). Signal transduction through MAP kinase cascades. *Adv Cancer Res* **74**, 49-139.

Li, K., Foy, E., Ferreon, J. C., Nakamura, M., Ferreon, A. C., Ikeda, M., Ray, S. C., Gale, M., Jr. & Lemon, S. M. (2005). Immune evasion by hepatitis C virus NS3/4A protease-mediated cleavage of the Toll-like receptor 3 adaptor protein TRIF. *Proc Natl Acad Sci U S A* **102**, 2992-2997.

Li, X. D., Sun, L., Seth, R. B., Pineda, G. & Chen, Z. J. (2005). Hepatitis C virus protease NS3/4A cleaves mitochondrial antiviral signaling protein off the mitochondria to evade innate immunity. *Proc Natl Acad Sci U S A* **102**, 17717-17722.

Liston, P., Fong, W. G., Kelly, N. L., Toji, S., Miyazaki, T., Conte, D., Tamai, K., Craig, C. G., McBurney, M. W. & Korneluk, R. G. (2001). Identification of XAF1 as an antagonist of XIAP anti-Caspase activity. *Nat Cell Biol* **3**, 128-133.

Liu, L. & Stamler, J. S. (1999). NO: an inhibitor of cell death. *Cell Death Differ* **6**, 937-942.

Loeb, K. R. & Haas, A. L. (1992). The interferon-inducible 15-kDa ubiquitin homolog

conjugates to intracellular proteins. *J Biol Chem* **267**, 7806-7813.

Maceyka, M., Sankala, H., Hait, N. C., Le Stunff, H., Liu, H., Toman, R., Collier, C., Zhang, M., Satin, L. S., Merrill, A. H., Jr., Milstien, S. & Spiegel, S. (2005). SphK1 and SphK2, sphingosine kinase isoenzymes with opposing functions in sphingolipid metabolism. *J Biol Chem* **280**, 37118-37129.

Machesky, N. J., Zhang, G., Raghavan, B., Zimmerman, P., Kelly, S. L., Merrill, A. H., Jr., Waldman, W. J., Van Brocklyn, J. R. & Trgovcich, J. (2008). Human cytomegalovirus regulates bioactive sphingolipids. *J Biol Chem*.

Magkouras, I., Matzener, P., Rumenapf, T., Peterhans, E. & Schweizer, M. (2008). RNase-dependent inhibition of extracellular, but not intracellular, dsRNA-induced interferon synthesis by Erns of pestiviruses. *J Gen Virol* **89**, 2501-2506.

Makino, A., Shimojima, M., Miyazawa, T., Kato, K., Tohya, Y. & Akashi, H. (2006). Junctional adhesion molecule 1 is a functional receptor for feline calicivirus. *J Virol* **80**, 4482-4490.

Manning, B. D. & Cantley, L. C. (2007). AKT/PKB signaling: navigating downstream. *Cell* **129**, 1261-1274.

McCubrey, J. A., Steelman, L. S., Chappell, W. H., Abrams, S. L., Wong, E. W., Chang, F., Lehmann, B., Terrian, D. M., Milella, M., Tafuri, A., Stivala, F., Libra, M., Basecke, J., Evangelisti, C., Martelli, A. M. & Franklin, R. A. (2007). Roles of the Raf/MEK/ERK pathway in cell growth, malignant transformation and drug resistance. *Biochim Biophys Acta* **1773**, 1263-1284.

Mebius, R. E. & Kraal, G. (2005). Structure and function of the spleen. *Nat Rev Immunol* **5**, 606-616.

Mendez, E., Ruggli, N., Collett, M. S. & Rice, C. M. (1998). Infectious bovine viral diarrhea virus (strain NADL) RNA from stable cDNA clones: a cellular insert determines NS3 production and viral cytopathogenicity. *J Virol* **72**, 4737-4745.

Meusel, T. R., Kehoe, K. E. & Imani, F. (2002). Protein kinase R regulates double-stranded RNA induction of TNF-alpha but not IL-1 beta mRNA in human epithelial cells. *J Immunol* **168**, 6429-6435.

Meyers, G. & Thiel, H. J. (1996). Molecular characterization of pestiviruses. *Adv Virus Res* **47**, 53-118.

Mignotte, B. & Vayssiere, J. L. (1998). Mitochondria and apoptosis. *Eur J Biochem* **252**, 1-15.

Miura, K., Taura, K., Kodama, Y., Schnabl, B. & Brenner, D. A. (2008). Hepatitis C virus-induced oxidative stress suppresses hepcidin expression through increased histone deacetylase activity. *Hepatology* **48**, 1420-1429.

Moennig, V. & Plagemann, P. G. (1992). The pestiviruses. *Adv Virus Res* **41**, 53-98.

Monick, M. M., Cameron, K., Powers, L. S., Butler, N. S., McCoy, D., Mallampalli, R. K. & Hunninghake, G. W. (2004). Sphingosine kinase mediates activation of extracellular signal-related kinase and Akt by respiratory syncytial virus. *Am J Respir Cell Mol Biol* **30**, 844-852.

Monteiro, H. P., Silva, E. F. & Stern, A. (2004). Nitric oxide: a potential inducer of adhesion-related apoptosis--anoikis. *Nitric Oxide* **10**, 1-10.

Muller-Doblies, D., Ackermann, M. & Metzler, A. (2002). In vitro and in vivo detection of Mx gene products in bovine cells following stimulation with alpha/beta interferon and viruses. *Clin Diagn Lab Immunol* **9**, 1192-1199.

Muller-Doblies, D., Arquint, A., Schaller, P., Heegaard, P. M., Hilbe, M., Albini, S., Abril, C., Tobler, K., Ehrensperger, F., Peterhans, E., Ackermann, M. & Metzler, A. (2004). Innate immune responses of calves during transient infection with a noncytopathic strain of bovine viral diarrhea virus. *Clin Diagn Lab Immunol* **11**, 302-312.

Muscoplat, C. C., Johnson, D. W. & Teuscher, E. (1973). Surface immunoglobulin of circulating lymphocytes in chronic bovine diarrhea: abnormalities in cell populations and cell function. *Am J Vet Res* **34**, 1101-1104.

Nagai, M., Sakoda, Y., Mori, M., Hayashi, M., Kida, H. & Akashi, H. (2003). Insertion of cellular sequence and RNA recombination in the structural protein coding region of cytopathogenic bovine viral diarrhoea virus. *J Gen Virol* **84**, 447-452.

Nagai, M., Hayashi, M., Sugita, S., Sakoda, Y., Mori, M., Murakami, T., Ozawa, T., Yamada, N. & Akashi, H. (2004). Phylogenetic analysis of bovine viral diarrhea viruses using five different genetic regions. *Virus Res* **99**, 103-113.

Nagai, M., Ito, T., Sugita, S., Genno, A., Takeuchi, K., Ozawa, T., Sakoda, Y., Nishimori, T., Takamura, K. & Akashi, H. (2001). Genomic and serological diversity of bovine viral diarrhea virus in Japan. *Arch Virol* **146**, 685-696.

Nakagami, H., Morishita, R., Yamamoto, K., Taniyama, Y., Aoki, M., Kim, S., Matsumoto, K., Nakamura, T., Higaki, J. & Ogihara, T. (2000). Anti-apoptotic action of hepatocyte growth factor through mitogen-activated protein kinase on human aortic endothelial cells. *J Hypertens* **18**, 1411-1420.

Nakamura, S., Shimazaki, T., Sakamoto, K., Fukusho, A., Inoue, Y. & Ogawa, N. (1995). Enhanced replication of orbiviruses in bovine testicle cells infected with bovine viral diarrhoea virus. *J Vet Med Sci* **57**, 677-681.

Neill, J. D. & Ridpath, J. F. (2008). Increase in proto-oncogene mRNA transcript levels in bovine lymphoid cells infected with a cytopathic type 2 bovine viral diarrhea virus. *Virus Res* **135**, 326-331.

Neu, B., Puschmann, A. J., Mayerhofer, A., Hutzler, P., Grossmann, J., Lippl, F., Schepp, W. & Prinz, C. (2003). TNF-alpha induces apoptosis of parietal cells. *Biochem Pharmacol* **65**, 1755-1760.

Nobes, C. D., Lauritzen, I., Mattei, M. G., Paris, S., Hall, A. & Chardin, P. (1998). A new member of the Rho family, Rnd1, promotes disassembly of actin filament structures and loss of cell adhesion. *J Cell Biol* **141**, 187-197.

Nuwaysir, E. F., Huang, W., Albert, T. J., Singh, J., Nuwaysir, K., Pitas, A., Richmond, T., Gorski, T., Berg, J. P., Ballin, J., McCormick, M., Norton, J., Pollock, T., Sumwalt, T., Butcher, L., Porter, D., Molla, M., Hall, C., Blattner, F., Sussman, M. R., Wallace, R. L., Cerrina, F. & Green, R. D. (2002). Gene expression analysis using oligonucleotide arrays produced by maskless photolithography. *Genome Res* **12**, 1749-1755.

Ohoka, N., Yoshii, S., Hattori, T., Onozaki, K. & Hayashi, H. (2005). TRB3, a novel ER stress-inducible gene, is induced via ATF4-CHOP pathway and is involved in cell death. *Embo J* **24**, 1243-1255.

Okada, T., Yoshida, H., Akazawa, R., Negishi, M. & Mori, K. (2002). Distinct roles of activating transcription factor 6 (ATF6) and double-stranded RNA-activated protein kinase-like endoplasmic reticulum kinase (PERK) in transcription during the mammalian unfolded protein response. *Biochem J* **366**, 585-594.

Olivera, A. & Spiegel, S. (1993). Sphingosine-1-phosphate as second messenger in cell proliferation induced by PDGF and FCS mitogens. *Nature* **365**, 557-560.

Olivera, A., Kohama, T., Tu, Z., Milstien, S. & Spiegel, S. (1998). Purification and characterization of rat kidney sphingosine kinase. *J Biol Chem* **273**, 12576-12583.

Olivera, A., Kohama, T., Edsall, L., Nava, V., Cuvillier, O., Poulton, S. & Spiegel, S. (1999). Sphingosine kinase expression increases intracellular sphingosine-1-phosphate and promotes cell growth and survival. *J Cell Biol* **147**, 545-558.

Paape, M. J., Rautiainen, P. M., Lilius, E. M., Malstrom, C. E. & Elsasser, T. H. (2002). Development of anti-bovine TNF-alpha mAb and ELISA for quantitating TNF-alpha in milk after intramammary injection of endotoxin. *J Dairy Sci* **85**, 765-773.

Park, B. G., Yoo, C. I., Kim, H. T., Kwon, C. H. & Kim, Y. K. (2005). Role of mitogen-activated protein kinases in hydrogen peroxide-induced cell death in osteoblastic cells. *Toxicology* **215**, 115-125.

Payne, D. M., Rossomando, A. J., Martino, P., Erickson, A. K., Her, J. H., Shabanowitz, J., Hunt, D. F., Weber, M. J. & Sturgill, T. W. (1991). Identification of the regulatory phosphorylation sites in pp42/mitogen-activated protein kinase (MAP kinase). *Embo J* **10**, 885-892.

Pestova, T. V. & Hellen, C. U. (1999). Internal initiation of translation of bovine viral diarrhea virus RNA. *Virology* **258**, 249-256.

Pitson, S. M., Moretti, P. A., Zebol, J. R., Lynn, H. E., Xia, P., Vadas, M. A. & Wattenberg, B. W. (2003). Activation of sphingosine kinase 1 by ERK1/2-mediated phosphorylation. *EMBO J* **22**, 5491-5500.

Pitson, S. M., Moretti, P. A., Zebol, J. R., Xia, P., Gamble, J. R., Vadas, M. A., D'Andrea, R. J. & Wattenberg, B. W. (2000). Expression of a catalytically inactive sphingosine kinase mutant blocks agonist-induced sphingosine kinase activation. A dominant-negative

sphingosine kinase. *J Biol Chem* **275**, 33945-33950.

Pitson, S. M., Xia, P., Leclercq, T. M., Moretti, P. A., Zebol, J. R., Lynn, H. E., Wattenberg, B. W. & Vadas, M. A. (2005). Phosphorylation-dependent translocation of sphingosine kinase to the plasma membrane drives its oncogenic signalling. *J Exp Med* **201**, 49-54.

Potgieter, L. N. (1995). Immunology of bovine viral diarrhea virus. *Vet Clin North Am Food Anim Pract* **11**, 501-520.

Prechtel, A. T. & Steinkasserer, A. (2007). CD83: an update on functions and prospects of the maturation marker of dendritic cells. *Arch Dermatol Res* **299**, 59-69.

Ramachandiran, S., Huang, Q., Dong, J., Lau, S. S. & Monks, T. J. (2002). Mitogen-activated protein kinases contribute to reactive oxygen species-induced cell death in renal proximal tubule epithelial cells. *Chem Res Toxicol* **15**, 1635-1642.

Reed, K. E., Gorbalenya, A. E. & Rice, C. M. (1998). The NS5A/NS5 proteins of viruses from three genera of the family flaviviridae are phosphorylated by associated serine/threonine kinases. *J Virol* **72**, 6199-6206.

Reiss, C. S. & Komatsu, T. (1998). Does nitric oxide play a critical role in viral infections? *J Virol* **72**, 4547-4551.

Risatti, G. R., Pomp, D. & Donis, R. O. (2003). Patterns of cellular gene expression in cells infected with cytopathic or non-cytopathic bovine viral diarrhea virus. *Anim Biotechnol* **14**, 31-49.

Robbins, D. J., Zhen, E., Owaki, H., Vanderbilt, C. A., Ebert, D., Geppert, T. D. & Cobb, M. H. (1993). Regulation and properties of extracellular signal-regulated protein kinases 1 and 2 in vitro. *J Biol Chem* **268**, 5097-5106.

Rossi, C. R. & Kiesel, G. K. (1983). Characteristics of the polyriboinosinic acid:polyribocytidylic acid assay for noncytopathogenic bovine viral diarrhea virus. *Am J Vet Res* **44**, 1916-1919.

Roulston, A., Marcellus, R. C. & Branton, P. E. (1999). Viruses and apoptosis. *Annu Rev Microbiol* **53**, 577-628.

Rumenapf, T., Unger, G., Strauss, J. H. & Thiel, H. J. (1993). Processing of the envelope glycoproteins of pestiviruses. *J Virol* **67**, 3288-3294.

Sakamoto, H., Okamoto, K., Aoki, M., Kato, H., Katsume, A., Ohta, A., Tsukuda, T., Shimma, N., Aoki, Y., Arisawa, M., Kohara, M. & Sudoh, M. (2005). Host sphingolipid biosynthesis as a target for hepatitis C virus therapy. *Nat Chem Biol* **1**, 333-337.

Samuel, C. E. (2001). Antiviral actions of interferons. *Clin Microbiol Rev* **14**, 778-809.

Saunders, L. R. & Barber, G. N. (2003). The dsRNA binding protein family: critical roles, diverse cellular functions. *Faseb J* **17**, 961-983.

Schneider, R., Unger, G., Stark, R., Schneider-Scherzer, E. & Thiel, H. J. (1993). Identification of a structural glycoprotein of an RNA virus as a ribonuclease. *Science* **261**, 1169-1171.

Schwab, S. R. & Cyster, J. G. (2007). Finding a way out: lymphocyte egress from lymphoid organs. *Nat Immunol* **8**, 1295-1301.

Schweizer, M. & Peterhans, E. (1999). Oxidative stress in cells infected with bovine viral diarrhoea virus: a crucial step in the induction of apoptosis. *J Gen Virol* **80**, 1147-1155.

Schweizer, M. & Peterhans, E. (2001). Noncytopathic bovine viral diarrhea virus inhibits double-stranded RNA-induced apoptosis and interferon synthesis. *J Virol* **75**, 4692-4698.

Shakhov, A. N., Collart, M. A., Vassalli, P., Nedospasov, S. A. & Jongeneel, C. V. (1990).

Kappa B-type enhancers are involved in lipopolysaccharide-mediated transcriptional activation of the tumor necrosis factor alpha gene in primary macrophages. *J Exp Med* **171**, 35-47.

Shaul, Y. D. & Seger, R. (2007). The MEK/ERK cascade: from signaling specificity to diverse functions. *Biochim Biophys Acta* **1773**, 1213-1226.

Shida, D., Takabe, K., Kapitonov, D., Milstien, S. & Spiegel, S. (2008). Targeting SphK1 as a new strategy against cancer. *Curr Drug Targets* **9**, 662-673.

Simon, A., Fah, J., Haller, O. & Staeheli, P. (1991). Interferon-regulated Mx genes are not responsive to interleukin-1, tumor necrosis factor, and other cytokines. *J Virol* **65**, 968-971.

Singh-Gasson, S., Green, R. D., Yue, Y., Nelson, C., Blattner, F., Sussman, M. R. & Cerrina, F. (1999). Maskless fabrication of light-directed oligonucleotide microarrays using a digital micromirror array. *Nat Biotechnol* **17**, 974-978.

Smith, K. D. & Ozinsky, A. (2002). Toll-like receptor-5 and the innate immune response to bacterial flagellin. *Curr Top Microbiol Immunol* **270**, 93-108.

Spiegel, S. & Milstien, S. (2003). Sphingosine-1-phosphate: an enigmatic signalling lipid. *Nat Rev Mol Cell Biol* **4**, 397-407.

Splichal, I., Bonneau, M. & Charley, B. (1994). Ontogeny of interferon alpha secreting cells in the porcine fetal hematopoietic organs. *Immunol Lett* **43**, 203-208.

St-Louis, M. C., Massie, B. & Archambault, D. (2005). The bovine viral diarrhea virus (BVDV) NS3 protein, when expressed alone in mammalian cells, induces apoptosis which correlates with caspase-8 and caspase-9 activation. *Vet Res* **36**, 213-227.

Sun, J., Yan, G., Ren, A., You, B. & Liao, J. K. (2006). FHL2/SLIM3 decreases cardiomyocyte survival by inhibitory interaction with sphingosine kinase-1. *Circ Res* **99**,

468-476.

Sutherland, C. M., Moretti, P. A., Hewitt, N. M., Bagley, C. J., Vadas, M. A. & Pitson, S. M. (2006). The calmodulin-binding site of sphingosine kinase and its role in agonist-dependent translocation of sphingosine kinase 1 to the plasma membrane. *J Biol Chem* **281**, 11693-11701.

Taha, T. A., Hannun, Y. A. & Obeid, L. M. (2006). Sphingosine kinase: biochemical and cellular regulation and role in disease. *J Biochem Mol Biol* **39**, 113-131.

Takizawa, T., Ohashi, K. & Nakanishi, Y. (1996). Possible involvement of double-stranded RNA-activated protein kinase in cell death by influenza virus infection. *J Virol* **70**, 8128-8132.

Tanaka, N., Sato, M., Lamphier, M. S., Nozawa, H., Oda, E., Noguchi, S., Schreiber, R. D., Tsujimoto, Y. & Taniguchi, T. (1998). Type I interferons are essential mediators of apoptotic death in virally infected cells. *Genes Cells* **3**, 29-37.

Tautz, N., Elbers, K., Stoll, D., Meyers, G. & Thiel, H. J. (1997). Serine protease of pestiviruses: determination of cleavage sites. *J Virol* **71**, 5415-5422.

Tautz, N., Harada, T., Kaiser, A., Rinck, G., Behrens, S. & Thiel, H. J. (1999). Establishment and characterization of cytopathogenic and noncytopathogenic pestivirus replicons. *J Virol* **73**, 9422-9432.

Tay, C. H. & Welsh, R. M. (1997). Distinct organ-dependent mechanisms for the control of murine cytomegalovirus infection by natural killer cells. *J Virol* **71**, 267-275.

Teichmann, U., Liebler-Tenorio, E. M. & Pohlenz, J. F. (2000). Ultrastructural changes in follicles of small-intestinal aggregated lymphoid nodules in early and advanced phases of experimentally induced mucosal diseases in calves. *Am J Vet Res* **61**, 174-182.

Thiel, H. J., Plagemann, P. G. & Moennig, V. (1996). Pestiviruses. In *Fields virology*, 3rd edn, pp. 1059-1073. Edited by B. N. Fields, D. M. Knipe & P. M. Howley. New York: Lippincott-Raven Publishers.

Thomis, D. C., Doohan, J. P. & Samuel, C. E. (1992). Mechanism of interferon action: cDNA structure, expression, and regulation of the interferon-induced, RNA-dependent P1/eIF-2 alpha protein kinase from human cells. *Virology* **188**, 33-46.

Thompson, A. J. & Locarnini, S. A. (2007). Toll-like receptors, RIG-I-like RNA helicases and the antiviral innate immune response. *Immunol Cell Biol* **85**, 435-445.

Tikoo, K., Lau, S. S. & Monks, T. J. (2001). Histone H3 phosphorylation is coupled to poly-(ADP-ribosylation) during reactive oxygen species-induced cell death in renal proximal tubular epithelial cells. *Mol Pharmacol* **60**, 394-402.

Traven, M., Alenius, S., Fossum, C. & Larsson, B. (1991). Primary bovine viral diarrhoea virus infection in calves following direct contact with a persistently viraemic calf. *Zentralbl Veterinarmed B* **38**, 453-462.

van Deventer, S. J. (2001). Transmembrane TNF-alpha, induction of apoptosis, and the efficacy of TNF-targeting therapies in Crohn's disease. *Gastroenterology* **121**, 1242-1246.

van Deventer, S. J. & Tytgat, G. N. (1998). [Drug treatment of Crohn's disease]. *Ned Tijdschr Geneeskd* **142**, 1191-1195.

Vassilev, V. B. & Donis, R. O. (2000). Bovine viral diarrhea virus induced apoptosis correlates with increased intracellular viral RNA accumulation. *Virus Res* **69**, 95-107.

Vilcek, S., Herring, A. J., Herring, J. A., Nettleton, P. F., Lowings, J. P. & Paton, D. J. (1994). Pestiviruses isolated from pigs, cattle and sheep can be allocated into at least three genogroups using polymerase chain reaction and restriction endonuclease analysis. *Arch Virol*

136, 309-323.

Wang, X., Martindale, J. L. & Holbrook, N. J. (2000). Requirement for ERK activation in cisplatin-induced apoptosis. *J Biol Chem* **275**, 39435-39443.

Ward, S. V. & Samuel, C. E. (2003). The PKR kinase promoter binds both Sp1 and Sp3, but only Sp3 functions as part of the interferon-inducible complex with ISGF-3 proteins. *Virology* **313**, 553-566.

Warrener, P. & Collett, M. S. (1995). Pestivirus NS3 (p80) protein possesses RNA helicase activity. *J Virol* **69**, 1720-1726.

Weiss, T., Grell, M., Hessabi, B., Bourteele, S., Muller, G., Scheurich, P. & Wajant, H. (1997). Enhancement of TNF receptor p60-mediated cytotoxicity by TNF receptor p80: requirement of the TNF receptor-associated factor-2 binding site. *J Immunol* **158**, 2398-2404.

Williams, B. R. (1997). Role of the double-stranded RNA-activated protein kinase (PKR) in cell regulation. *Biochem Soc Trans* **25**, 509-513.

Wiskerchen, M., Belzer, S. K. & Collett, M. S. (1991). Pestivirus gene expression: the first protein product of the bovine viral diarrhea virus large open reading frame, p20, possesses proteolytic activity. *J Virol* **65**, 4508-4514.

Xia, P., Wang, L., Gamble, J. R. & Vadas, M. A. (1999). Activation of sphingosine kinase by tumor necrosis factor-alpha inhibits apoptosis in human endothelial cells. *J Biol Chem* **274**, 34499-34505.

Xia, P., Wang, L., Moretti, P. A., Albanese, N., Chai, F., Pitson, S. M., D'Andrea, R. J., Gamble, J. R. & Vadas, M. A. (2002). Sphingosine kinase interacts with TRAF2 and dissects tumor necrosis factor-alpha signaling. *J Biol Chem* **277**, 7996-8003.

Xia, Z., Dickens, M., Raingeaud, J., Davis, R. J. & Greenberg, M. E. (1995). Opposing

effects of ERK and JNK-p38 MAP kinases on apoptosis. *Science* **270**, 1326-1331.

Xu, J., Mendez, E., Caron, P. R., Lin, C., Murcko, M. A., Collett, M. S. & Rice, C. M. (1997). Bovine viral diarrhea virus NS3 serine proteinase: polyprotein cleavage sites, cofactor requirements, and molecular model of an enzyme essential for pestivirus replication. *J Virol* **71**, 5312-5322.

Yamada, Y., Pannell, R., Forster, A. & Rabbitts, T. H. (2000). The oncogenic LIM-only transcription factor Lmo2 regulates angiogenesis but not vasculogenesis in mice. *Proc Natl Acad Sci U S A* **97**, 320-324.

Yamada, Y., Warren, A. J., Dobson, C., Forster, A., Pannell, R. & Rabbitts, T. H. (1998). The T cell leukemia LIM protein Lmo2 is necessary for adult mouse hematopoiesis. *Proc Natl Acad Sci U S A* **95**, 3890-3895.

Yeh, W. C., Hakem, R., Woo, M. & Mak, T. W. (1999). Gene targeting in the analysis of mammalian apoptosis and TNF receptor superfamily signaling. *Immunol Rev* **169**, 283-302.

Yeung, M. C., Chang, D. L., Camantigue, R. E. & Lau, A. S. (1999). Inhibitory role of the host apoptogenic gene PKR in the establishment of persistent infection by encephalomyocarditis virus in U937 cells. *Proc Natl Acad Sci U S A* **96**, 11860-11865.

Yoneyama, M., Kikuchi, M., Matsumoto, K., Imaizumi, T., Miyagishi, M., Taira, K., Foy, E., Loo, Y. M., Gale, M., Jr., Akira, S., Yonehara, S., Kato, A. & Fujita, T. (2005). Shared and unique functions of the DExD/H-box helicases RIG-I, MDA5, and LGP2 in antiviral innate immunity. *J Immunol* **175**, 2851-2858.

Yount, J. S., Moran, T. M. & Lopez, C. B. (2007). Cytokine-independent upregulation of MDA5 in viral infection. *J Virol* **81**, 7316-7319.

Yu, H., Isken, O., Grassmann, C. W. & Behrens, S. E. (2000). A stem-loop motif formed

by the immediate 5' terminus of the bovine viral diarrhea virus genome modulates translation as well as replication of the viral RNA. *J Virol* **74**, 5825-5835.

Zhang, G., Flick-Smith, H. & McCauley, J. W. (2003). Differences in membrane association and sub-cellular distribution between NS2-3 and NS3 of bovine viral diarrhoea virus. *Virus Res* **97**, 89-102.

Zhang, G., Aldridge, S., Clarke, M. C. & McCauley, J. W. (1996). Cell death induced by cytopathic bovine viral diarrhoea virus is mediated by apoptosis. *J Gen Virol* **77**, 1677-1681.

Zhao, H., Dugas, N., Mathiot, C., Delmer, A., Dugas, B., Sigaux, F. & Kolb, J. P. (1998). B-cell chronic lymphocytic leukemia cells express a functional inducible nitric oxide synthase displaying anti-apoptotic activity. *Blood* **92**, 1031-1043.

Zhong, W., Gutshall, L. L. & Del Vecchio, A. M. (1998). Identification and characterization of an RNA-dependent RNA polymerase activity within the nonstructural protein 5B region of bovine viral diarrhea virus. *J Virol* **72**, 9365-9369.

Zhuang, S. & Schnellmann, R. G. (2006). A death-promoting role for extracellular signal-regulated kinase. *J Pharmacol Exp Ther* **319**, 991-997.

LIST OF PUBLICATION

Yamane D, Nagai M, Ogawa Y, Tohya Y, Akashi H. Enhancement of apoptosis via an extrinsic factor, TNF-alpha, in cells infected with cytopathic bovine viral diarrhea virus. **Microbes Infect** 2005 7:1482-91.

Yamane D, Kato K, Tohya Y, Akashi H. The double-stranded RNA-induced apoptosis pathway is involved in the cytopathogenicity of cytopathogenic Bovine viral diarrhea virus. **J Gen Virol** 2006 87:2961-70.

Yamane D, Kato K, Tohya Y, Akashi H. The relationship between the viral RNA level and upregulation of innate immunity in spleen of cattle persistently infected with bovine viral diarrhea virus. **Vet Microbiol** 2008 129:69-79.

Yamane D, Zahoor MA, Mohamed YM, Azab W, Kato K, Tohya Y, Akashi H. Microarray analysis reveals distinct signaling pathways transcriptionally activated by infection with bovine viral diarrhea virus in different cell types. **Virus Res** (in press).

Yamane D, Zahoor MA, Mohamed YM, Azab W, Kato K, Tohya Y, Akashi H. Inhibition of sphingosine kinase by bovine viral diarrhea virus NS3 is crucial for efficient viral replication and cytopathogenesis. **J Biol Chem** (in press).

Yamane D, Mohamed YM, Zahoor MA, Azab W, Kato K, Tohya Y, Akashi H. Oxidative stress induced by bovine viral diarrhea virus infection mediates activation of extracellular signal-regulated kinase in MDBK cells. **Arch Virol** (submitted).

Zahoor MA, **Yamane D**, Kobayashi K, Kato K, Tohya Y, Akashi H. Production, characterization and application of monolconal antibodies to bovine viral diarrhea virus nonstructural protein 5A. **Virus Res** (submitted).

SUMMARY IN JAPANESE

論 文 の 内 容 の 要 旨

獣医学　専攻

平成 17 年度博士課程　入学

氏　　名　山根　大典

指導教員名　明石　博臣

論文題目　Studies on molecular biological interactions between bovine viral diarrhea virus and innate immune system

（牛ウイルス性下痢ウイルスと先天性免疫機構との分子生物学的相互作用に関する研究）

牛ウイルス性下痢ウイルス（BVDV）は、フラビウイルス科ペスチウイルス属に分類される。ペスチウイルス属には BVDV の他に、豚コレラウイルス、羊のボーダー病ウイルスが所属するが、いずれも宿主動物の病原体として非常に重要な存在である。特に BVDV はそのゲノム構造が人の病原体として重要視される C 型肝炎ウイルス（HCV）と類似しており、両者とも持続感染する特徴を持つことから、モデルウイルスとしてしばしば HCV 研究に用いられている。BVDV には細胞病原性（cp）および非細胞病原性（ncp）と生物学的性質の異なった 2 種類の生物型のウイルス株が存在する。ncp 株が胎子に持続感染を起こすと、子牛体内でやがて cp 株へと変異することによって致死的な粘膜病を引き起こすことが明らかとなっている。また、野外流行株は ncp 株であり、cp 株は持続感染を引き起こさないことが知られている。従って、BVDV の細胞病原性発現メカニズムを明らかに出来れば、牛群からの BVDV 排除法につながるばかりでなく、持続感染から粘膜病発症に至るプロセスを理解する上で有益な示唆を与えうると考えられる。

そこで、cp 株を中心にアポトーシスやインターフェロン（IFN）等の先天性免疫誘導メカニズム及びウイルス－宿主間のタンパク相互作用を解析することにより、宿主先天性免疫応答を介した細胞病原性発現メカニズムについて研究を行った。

各章の要約は以下の通りである。

第一章： 細胞病原性 BVDV 感染細胞における外因系因子 TNFαによるアポトーシス増強

BVDV の細胞病原性はアポトーシスを介していることが既に知られているが、アポトーシス誘導に至る経路については未解明である。BVDV 複製効率の良い、初代牛胎子由来筋肉(BFM)細胞における遺伝子発現誘導を網羅的な RT-PCR 法によって検出したところ、外因系因子である TNFαの過剰発現が cp 株感染細胞内において認められた。そこで、抗体や antisense 鎖を用いて TNFαを抑制したところ、アポトーシス誘導の減少が見られた。これまでアポトーシスは内因系経路が働いているとの報告があったが、これらの結果から外因系の関与も強く示唆された。同時に iNOS の誘導も RT-PCR により検出されたが、NOS 阻害剤である L-NMMA 添加によってはアポトーシス増強が見られたことから、iNOS は抗アポトーシス作用を誘導していることが示唆された。

第二章： 細胞病原性 BVDV 感染細胞における 2 本鎖 RNA 誘導性アポトーシス経路の関与

cp 株感染細胞内において TNFαや iNOS の他、IFN 誘導因子である Mx1 や PKR、OAS-1 等の抗ウイルス因子の転写誘導が認められたことから、これらの発現誘導にどのようなウイルス因子が関与しているのかを調べた。cp 株感染細胞においては、ウイルス RNA 複製量が ncp 株と比較して顕著であったことから、ウイルス RNA 複製時に複製中間体として形成される 2 本鎖 RNA がアポトーシスの引き金なのではないかと考えた。これらの mRNA は全て、2 本鎖 RNA モデル化合物である poly(IC)によって誘導されることが示され、次に 2 本鎖 RNA に結合することで活性化しアポトーシスを誘導する宿主因子である OAS-1 と PKR 双方を RNAi によりノックダウンすると、cp 株感染細胞においてアポトーシス誘導が強く抑制されたことから、2 本鎖 RNA 形成量がアポトーシス誘導及び抗ウイルス応答の引き金として重要であることが強く示唆された。

第三章： BVDV 持続感染牛の脾臓におけるウイルス RNA レベルと先天性免疫誘導との関係

BVDV 持続感染(PI)牛におけるウイルス RNA 複製と先天性免疫誘導との関係を調べるため、PI 牛より得られた脾臓内におけるウイルス RNA 量と先天性免疫因子の転写量やアポトーシス誘導レベルとの関係を回帰分析により調べた。その結果、ウイルス RNA レベルと多くの先天性免疫因子との間には有意な正の相関が認められ、ウイルス RNA レベルが高い個体ほど顕著な臨床兆候が見られたことから、*in vivo* においてもウイルス RNA 複製量が宿主の先天性免疫誘導や病態形成に重要であることが示唆された。

第四章： BVDV 感染 MDBK 細胞における酸化ストレスを介した ERK 活性化

細胞のシグナル伝達においては様々なキナーゼによるリン酸化カスケードが重要な役

割を担う。BVDV 感染細胞内においてどの様なキナーゼシグナルが働いているかを調べたところ、cp 株感染 MDBK 細胞において extracellular signal-regulated kinase（ERK）のリン酸化による活性化が認められた。また、cp 株感染細胞上清に ERK リン酸化誘導能が認められたことから、cp 株感染細胞は上清中に ERK 活性化因子を放出していることが示された。ERK リン酸化は過酸化水素の添加や血清除去によっても誘導され、一方で抗酸化物質である N-acetylcysteine やグルタチオン処理によって抑制されたことから、上清中に放出された Reactive oxygen species が ERK リン酸化を誘導していることが示された。MDBK 細胞において ERK リン酸化は生存や増殖を促進することが認められたが、ERK シグナルは NFκB を初めとする炎症シグナルを誘導することも知られていることから、ERK の異常な活性化は病態形成との関連が示唆される。

第五章： BVDV 感染により誘導される細胞型特異的シグナル経路のマイクロアレイ解析

DNA マイクロアレイを用いて MDBK 細胞及び BFM 細胞内における BVDV 感染時の遺伝子発現パターンの網羅的な解析を行った。その結果、ncp 株感染においては遺伝子発現変化が殆ど無いのに対し、cp 株感染細胞では顕著な遺伝子発現誘導が両細胞において認められた。cp 株は両細胞において同様に細胞死を誘導するが、両細胞間において大きく異なる遺伝子発現パターンが見られた。線維芽細胞である BFM 細胞においては、主に IFN 誘導因子や炎症性サイトカインの発現レベルが顕著であった。それに対し、上皮系細胞である MDBK 細胞においては小胞体ストレス関連因子の発現が特徴的である一方、IFN 応答は BFM と比較して遥かに弱いレベルであった。更に、免疫制御、アポトーシス、代謝、MAP キナーゼや転写因子等の mRNA についても、両細胞間において異なるパターンの発現誘導が見られ、細胞タイプ毎に異なる機序で細胞病原性が誘導されていることが示された。

第六章： BVDV NS3 によるスフィンゴシンキナーゼ活性抑制は細胞病原性と複製増強に関与する

BVDV の NS3 タンパク発現は cp 株でのみ顕著に認められるが、NS3 の細胞内における宿主因子との相互作用については未だ知られていない。そこで、酵母 2 ハイブリッド法を用いてスクリーニングを行い、NS3 と結合する因子としてスフィンゴシンキナーゼ 1（SphK1）を同定した。NS3 は SphK1 の酵素活性を著しく抑制することが示され、また SphK1 活性の抑制はウイルス複製を増強することが認められた。更に SphK1 の過剰発現によってアポトーシス誘導が弱まったことから、NS3 による SphK1 活性制御はウイルス複製に寄与するのみならず、細胞病原性発現にも深く関与していると考えられた。しかしながら、非開裂の NS2-3 も同様に SphK1 に結合、抑制することから、ncp 株によっても同様に

SphK1 活性が制御されていると考えられた。

本研究において、BVDV感染により誘導されるアポトーシスやストレス経路等の細胞シグナル伝達の他、ウイルスタンパクによる直接的な宿主タンパクの機能制御メカニズムを明らかとした。近縁のHCV感染によっても同様なストレスが引き起こされることが多数報告されているが、いずれの場合においても引き金となる因子については不明のままである。細胞へのストレスは細胞傷害を伴うことから病態形成への関与が強く示唆されており、これらの現象に繋がるウイルスー宿主間相互作用を見出すことは、普遍的な病態形成メカニズムの理解へと繋がると考えられる。これまでに宿主因子制御機構が判明しているウイルス因子はN^{pro}やE^{ms}に限られるが、これら 2 因子によるIFNシグナル制御のみではBVDVの持続感染成立を説明できないことが既に示されている。今後、他のウイルスタンパクについても宿主との相互作用を解明していくことが必須であると言える。BVDVは生涯を通じて持続感染する特異な性質を持つことから、未だ知られていない多様な先天性免疫制御機構を備えていると考えられる。これまでの研究はIFN経路を中心とした流れであったが、持続感染をしないA型肝炎ウイルスにおいてもHCVやBVDVと同様にIFN経路の遮断機構を備えていることが最近見出されている。このことから、IFN経路の制御は持続感染に不可欠であるというよりむしろ、ウイルスが宿主内で複製を行うために最低限必要な機能なのかもしれない。今後は、未だ多くの機能が不明なBVDVの分子間相互作用を解析することにより、新たな持続感染メカニズムを追究することで、BVDVに限らず多くのウイルスに普遍的に通じる持続感染戦略の発見へと繋がることに期待したい。